DEVELOPMENT AND EVALUATION OF NOVEL *IN SITU* DEPOT-FORMING CONTROLLED RELEASE FORMULATIONS

A DISSERTATION IN
Pharmaceutical Sciences
and
Chemistry

Presented to the Faculty of the University
of Missouri - Kansas City in partial fulfillment of
the requirements for the degree

DOCTOR OF PHILOSOPHY

by
GYAN PRAKASH MISHRA

M. Pharm., Shri G.S. Institute of Technology and Science, India, 2006

Kansas City, Missouri
2011

DEVELOPMENT AND EVALUATION OF NOVEL *IN SITU* DEPOT-FORMING CONTROLLED RELEASE FORMULATIONS

Gyan Prakash Mishra, Candidate for the Doctor of Philosophy degree

University of Missouri Kansas City, 2011

ABSTRACT

Controlled drug delivery utilizing novel biodegradable and biocompatible pentablock copolymers could be a valuable strategy for the treatment of chronic eye diseases. In attempts to achieve controlled drug release, various approaches were evaluated which eventually resulted in the development of novel polymeric material and a delivery system.

Poly (ethylene glycol)-poly (ε-caprolactone)-poly (ethylene glycol) (PEG-PCL-PEG) thermosensitive hydrogel was employed for sustained drug delivery. A polymeric additives strategy was selected based on the property to provide better packing through intra- and intermolecular interactions between the triblock polymeric chains of the hydrogel matrix. PCL was selected as a hydrophobic additive and polyvinyl alcohol (PVA) as a hydrophilic additive, respectively. The additives strategy was found to modulate the sol-gel transition and drug release kinetics from the hydrogel. The effect of PCL on the sol-gel transition was more pronounced than PVA. However, PVA played a dominant role in regulating drug release kinetics, whereas no significant difference in drug release was observed with PCL.

To accelerate the degradation rate of highly crystalline and hydrophobic PCL block we have successfully synthesized pentablock polymers based thermosensitive hydrogel by incorporating PLA block in the center of PEG-PCL-PEG. These polymers were characterized by ^{1}H NMR, GPC, and FT-IR. The effect of block composition on the sol-gel transition, crystallinity, and drug release kinetics was studied. The release kinetics of hydrophobic drug was easily modulated by altering the hydrophobic block segment. Moreover, the effect of block composition on the sol-gel transition was evaluated.

A specific combination of molecular weight and block ratio of pentablock copolymer can be utilized for nanoparticles preparation. We have also successfully polymerized PCL with PEG and faster degrading blocks such as polyglycolic acid and and polylactic acid for the preparation of nanoparticles. Nanoparticles alone demonstrate initial burst release due to surface adsorbed drug molecule. A final composite formulation based approach (nanoparticles suspended in thermosensitive gel) minimized the burst release of drug and resulted in continuous nearly zero order drug release. Pentablock copolymers also resulted in a negligible release of inflammatory mediators in different cell lines. Therefore, we have successfully developed a novel biomaterial for controlled drug delivery.

APPROVAL PAGE

The faculty listed below, appointed by the Dean of the School of Graduate Studies have examined a dissertation titled "Development and Evaluation of Novel *In Situ* Depot-Forming Controlled Release Formulations" presented by Gyan Prakash Mishra, candidate for the Doctor of Philosophy degree, and certify that in their opinion it is worthy of acceptance.

Supervisory Committee

Ashim K. Mitra, Ph.D., Committee Chair
Department of Pharmaceutical Sciences

Chi Lee, Ph.D.
Department of Pharmaceutical Sciences

Kun Cheng, Ph.D.
Department of Pharmaceutical Sciences

J. David Van Horn, Ph.D.
Department of Chemistry

Andrew Holder, Ph.D.
Department of Chemistry

CONTENTS

ILLUSTRATIONS

TABLES

Table Page

ACKNOWLEDGEMENTS

Finally the day arrived where I have to express my sincere regards to everyone contributed in the successful completion of my research work. I am extremely thankful to my advisor Dr. Ashim K. Mitra for his constant motivation, exceptional guidance and support to pursue research on novel block copolymers. His guidance was extremely helpful in successfully solving many scientific challenges encountered during synthesis and characterization of pentablock copolymers for ocular drug delivery. I am thankful to Drs. Chi Lee, Kun Cheng, J. David Van Horn and Andrew Holder for their valuable contributions as my dissertation supervisory committee members. I am also thankful to Drs. Dhananjay Pal, Swapan Samanta and Subramanian Natesan for valuable scientific discussions in the field of cell culture, chemistry and formulations. These discussions helped me to solve many challenging difficulties in the area of polymeric drug delivery. I would also express my regards to Mrs. Ranjana Mitra for constant support throughout my stay at UMKC. I am also thankful to Viral Tamboli for constant discussions and helping me in carrying out almost every single experiment performed during my graduate study. I am also thankful to Sulabh Patel for helping in all the cell culture work. I am privileged to have the company of these brilliant labmates in my research group. I am also thankful to the other faculty members especially Dr. Thomas Johnston for improving my understanding about basic concepts of drug delivery.

I am also thankful to numerous researchers from UMKC and other institutions for not only allowing me to use their equipments but also helping me to understand the basics of the equipment in their lab. In this regard, I am thankful to Dr. Richard Hopkins and Dr. Gabriel

L. Converse from The Children's Mercy Hospital for helping in the DSC studies. I would also express my sincere thanks to Dr. James B. Murowchick (School of Geological Sciences) and Dr. Vladimir M. Dusevich (School of Dentistry) for helping in XRD and SEM studies respectively. I am thankful to Joyce Johnson and Sharon Self for assistance in administrative work. I appreciate Connie Mahone and Nancy Hoover from School of Graduate Studies for their help. I am also thankful to National Institute of Health for constant funding for performing this work. Last, but the most important, I thank my parents for immense faith in me throughout my studies.

CHAPTER 1

LITERATURE REVIEW

Ocular Anatomy and Physiology

Ocular drug delivery is challenging in terms of achieving optimum drug concentration due to the unique protective mechanisms of the eye. Development of a drug delivery system for attaining therapeutic concentration at the target site requires a comprehensive understanding of the static and dynamic barriers of the eye. The eye is divided into two chambers – commonly known as the anterior chamber and the posterior chamber (Fig. 1.1). The anterior chamber is mainly comprised of cornea, conjunctiva, iris, ciliary body, and lens. The posterior chamber includes sclera, choroid, vitreous humor, and retina. The common routes of drug administration for the treatment of eye disorders are topical, systemic, periocular, and intravitreal. Topical administration is the most preferred route because of highest patient compliance and its least invasive nature. Upon topical instillation, absorption of drugs takes place either through a corneal route (cornea, aqueous humor, intraocular tissues) or noncorneal route (conjunctiva, sclera, choroid/RPE). The cornea can be mainly divided into the epithelium, stroma and endothelium, where each layer offers a different polarity and a potential rate-limiting structure for drug permeation. The non-corneal route involves absorption across the sclera and conjunctiva into the intraocular tissues. However, a small fraction of the topically applied drug, generally less than 5%, reaches the intraocular tissues. Factors responsible for poor ocular bioavailability following topical instillation are precorneal drainage and the lipoidal nature of the corneal epithelium. In addition, a major fraction of drug reaches the systemic circulation through conjunctival

vessels and nasolacrimal duct, which leads to severe adverse effects. Consequently, topical routes have met with limited success in attaining therapeutic drug concentrations in the posterior segment. Systemic administration can provide therapeutic levels in the posterior segment, but administration of high doses is necessary, which often leads to severe side effects. The Blood-aqueous barrier and blood-retinal barrier are the two major barriers for anterior segment and posterior segment ocular drug delivery, respectively, after systemic administration. The tight junctional complexes located in the two discrete cell layers, the endothelium of the iris/ciliary blood vessels, and the nonpigmented ciliary epithelium offer blood-aqueous barrier which prevents the entry of solutes into the aqueous humor. The Blood retinal barrier is composed of two types of cells, that is, retinal capillary endothelial cells and retinal pigment epithelium (RPE) cells which prevent the entry of solute into the retina. Intravitreal administration requires frequent administration which may lead to high susceptibility for vitreous hemorrhage, retinal detachment and endophthalmitis. These side effects can be minimized by developing delivery systems which provide controlled and targeted drug delivery for prolonged periods (Geroski and Edelhauser, 2000; Mitra, 2009; Urtti, 2006). Conventional ophthalmic formulations such as solutions and suspensions exhibit poor bioavailability. Over the last decade, numerous drug delivery systems have been explored to overcome the limitation of conventional dosage forms. Novel formulations such as nanoparticles, liposomes, dendrimers, and niosomes were developed to enhance drug bioavailability and to minimize adverse effects (Kaur and Kanwar, 2002; Mishra et al., 2011; Wadhwa et al., 2009). Among them polymeric formulations were widely explored in the last decade for drug delivery applications.

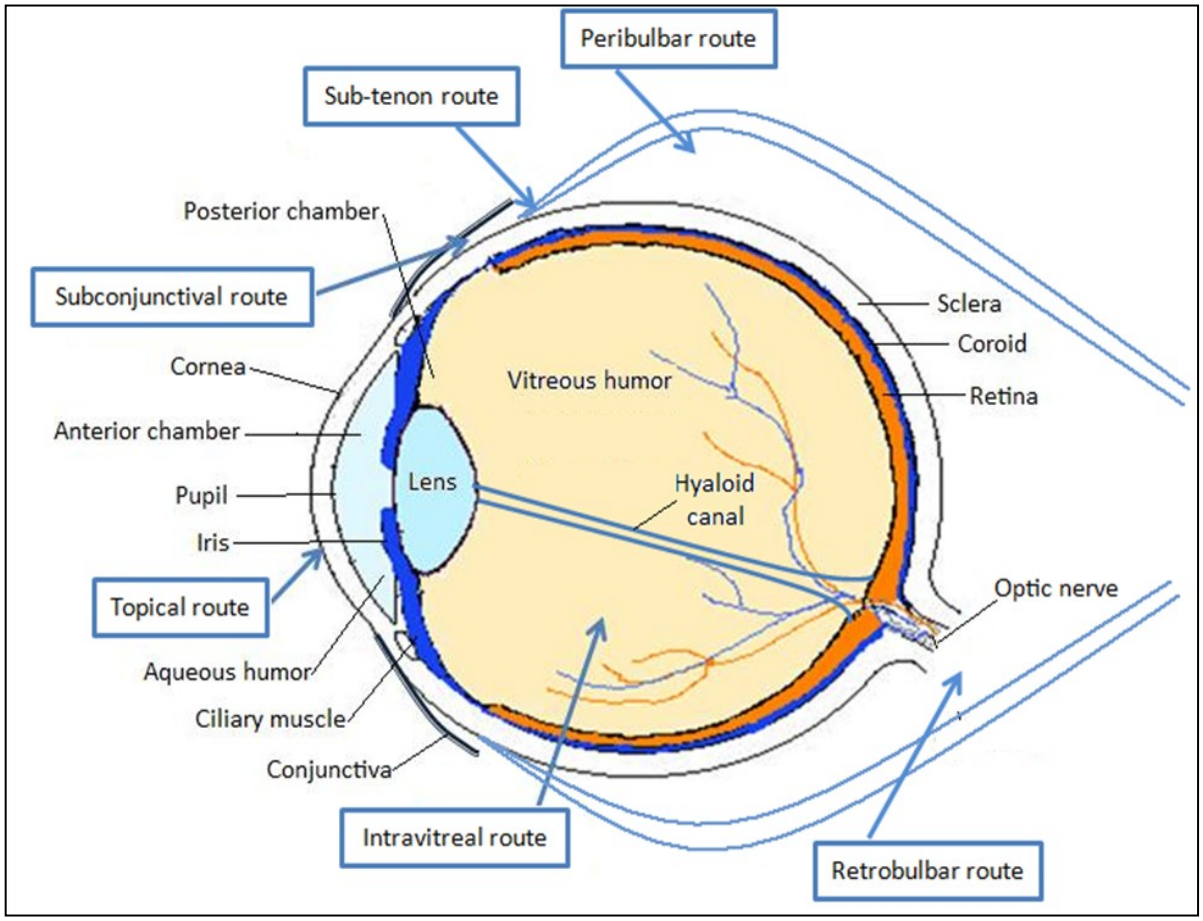

Figure 1.1 Structure and schematic representation of various routes of ocular drug delivery [adapted with permission from ref (Mishra et al., 2010)]

Anterior Chamber

(i) Cornea

The Cornea is the outermost transparent membrane of the eye. It is avascular in nature and receives nourishment from the aqueous humor and capillaries originating in limbal area. The Human cornea is about 0.5 mm thick and composed of five layers – corneal epithelium, Bowman's membrane, stroma, Descemet's membrane, and endothelium (in this sequence from the outermost to the innermost). The epithelial layer consists of five to six layers of columnar cells. The outermost layer is composed of non-keratinized squamous cells with tight junctions between adjacent cells. The innermost layer is columnar in shape and commonly known as the germinal layer. Bowman's membrane is mainly formed from collagen fibrils. Stroma, also known as substantia propria, is composed primarily of collagen fibrils. Descemet's membrane is a thick basal lamina between the stroma and the endothelium. The endothelium is composed of single layer of squamous cells (Klyce and Beuerman, 1988).

(ii) Iris

The iris is composed of pigmented epithelial cells and the constrictor iridial sphincter muscles (circular muscle of the iris). These muscles are innervated by cholinergic nerves which upon contraction cause miosis, (constriction of the pupil). Iris also contains the dilator muscles, oriented radially, which mediate mediate mydriasis (dilation of the pupil) upon sympathetic stimulation (Stjernschantz and Astin, 1993).

(iii) Ciliary Body

The ciliary body is formed from ciliary muscles and ciliary processes. Ciliary muscle is a smooth muscle comprised of fibrous bundles which are vascularized with folding that

extends into the posterior chamber. Its non-pigmented epithelial cells form the blood-aqueous barrier, which restricts the movement of proteins and colloids into the aqueous humor (Stjernschantz and Astin, 1993).

(iv) Conjunctiva

The conjunctiva consists of a clear mucous membrane, consisting of three parts - palpebral, fornical, and bulbar, and an underlying basement membrane. The membrane covers the inner part of the eyelid as well as the visible part of sclera (white part of the eye). It is composed of non-keratinized stratified columnar epithelial cells (Stjernschantz and Astin, 1993). It helps to lubricate the eye by producing mucus and some tears.

(iv) Aqueous Humor

Aqueous humor is the nutritive and protective fluid between the lens and the cornea. It is composed of 99% water and proteins, glucose, ascorbates, amino acids, and ions such as bicarbonate, chloride, sodium, potassium, calcium and phosphate. It is secreted from the ciliary body (2-3 µl/ min) and circulates from the posterior to the anterior chambers before most of it is drained through the trabecular meshwork, to the canal of Schlemm. A minor route of aqueous outflow is through the uveoscleral pathway. Impaired outflow of aqueous humor causes elevated intraocular pressure which leads to permanent damage of the optic nerve and consequential visual field loss which can progress to blindness (Hazin et al., 2009).

Posterior Chamber

(i) Retina

Retina is a light sensitive tissue comprised of two major layers – retinal pigmented epithelium (RPE) and neural retina. RPE is the outermost layer which is directly in the contact with the rods and cones (the light sensing neural cells). These photoreceptors are

linked to bipolar cells and ganglionic cells. The optic nerve is directly in contact with the ganglionic cells, which are coupled through amacrine cells. The primary function of RPE is to provide nutrients to the retina from the choroid. RPE forms a tight junction between the choroid and the retina. These cells also aid in the removal of shredded photoreceptors through phagocytosis. The innermost retina primarily receives blood supply from the retinal artery, whereas the outermost retina receives oxygen and nutrients from choriocapillaries (Sharma and Ehinger, 2003).

(ii) Vitreous Humor

The vitreous humor is comprised of a hydrogel matrix localized between the retina and the lens. This matrix is separated from the anterior chamber by anterior hyaloids membrane and is linked to the retina through ligaments. The vitreous is primarily composed of hyaluronic acid and collagen fibrils. However, the cortical region contains dispersed hyalocytes. The volume of vitreous humor is around 4 ml with a water content of 98 to 99.7% and pH around 7.5 (Andersen and Sander, 2003).

(iii) Choroid

Choroid is situated between retina and sclera. It is a highly vascularized tissue which can be divided into vessel layer, choriocapillaries, and Bruch's membrane. The vessel layer is comprised of arteries and veins, whereas choriocapillaries consist of a dense network of capillaries. Bruch's membrane is located between the choroid and the RPE. It is composed of basal lamellae of RPE and the endothelial cells of choroid (Cour, 2003; Sharma and Ehinger, 2003).

(iv) Sclera

The sclera is an external layer above choroid, which primarily protects the inner organs of the eye. It is about 0.5 to 1 mm thick and mainly composed of collagen bundles with some dispersed melanocytes and elastic fibers (Edelhauser and Ubels, 2003).

Barriers to Ocular Drug Delivery

The barriers to ocular drug delivery exist at both the molecular and tissue level, as classified in Fig. 1.2.

Precorneal Tear Clearance

Precorneal tear clearance is a major rate limiting factor in ocular drug absorption of topically administered drugs because the instilled drug is eliminated from the corneal surface by lacrimal fluid drainage. An applied dose can also be eliminated by systemic absorption through the conjunctival sac and/or the nasolacrimal duct (Urtti et al., 1984). All these factors limit ocular bioavailability of topically administered drugs to less than 5 % (Urtti and Salminen, 1993).

Corneal and Conjunctival Barriers

The corneal epithelial cells limit the permeation of hydrophilic drug molecules across the cornea due to the presence of tight junctions and the lipid-rich epithelial membrane (Fig 1.3). Tight junctions act as a seal around the epithelium, which restricts the entry of polar drug molecules into the cornea. These tight junctions are formed around the epithelial cell membranes, which are bound by cell adhesion proteins such as occludin, zonula occludens-1 (ZO-1) and ZO-2 (Yi et al., 2000). The tight junctions hinder paracellular transport of polar drugs across cornea, whereas lipophilic drugs can permeate through lipid bilayer by passive diffusion.

Permeation enhancers, such as L-arginine, can improve the permeability of polar molecules (e.g., fluorescein isothiocyanate (FITC)-dextran), across the cornea by modulating tight junctions (Nemoto et al., 2006). Ionization can also decrease the transcellular permeability, whereas molecular size does not have any significant effect on corneal permeability. Therefore, the pH of topical ocular formulations is an important factor in optimizing the ocular bioavailability of ionizable compounds (Brechue and Maren, 1993).

The stroma, which lies beneath the corneal epithelium, constitutes a major barrier to lipophilic drug absorption. This layer is composed of 90% water. Therefore, lipophilic drugs cannot readily partition into the stroma. Thus, it may act as a depot for hydrophobic drug molecules (Prausnitz and Noonan, 1998).

The Bowman's and Descemet's membranes do not provide any significant resistance to drug permeation, whereas the single layer of endothelial cells presents a weak lipophilic barrier for drug molecules. The conjunctival epithelium is leakier and has approximately twenty times more area, two times larger pore size, sixteen times higher pore density, and two hundred thirty times more paracellular space relative to cornea. As a result, it allows easy permeation of hydrophilic macromolecules and serves as a potential route for the delivery of macromolecules (Watsky et al., 1988). The apical conjunctival epithelial cells are attached by desmosomes, which connect the intracellular spaces and thus restrict the movement of proteins and peptides (Pfister, 1975).

Conjuctival permeability of peptides and proteins such as insulin (molecular weight 5800) and *p*-aminoclonidine (molecular weight 245.7) is higher than corneal permeability (Chien et al., 1991). Studies by Urtti et al. showed that the permeability of polyethylene glycols (PEGs) across the cornea was fifteen to twenty times less than the sclera or

conjunctiva. However, permeability across sclera is about half the conjunctival permeability, but it is ten times more than the cornea (Hamalainen et al., 1997).

Blood-Ocular Barriers

(i) Blood-Retinal Barrier (BRB)

BRB is similar in function to blood-brain barrier (BBB) and has similar capillary endothelial cell permeability to mannitol and sucrose (Cunha-Vaz et al.). However, interendothelial junctions of the BRB are slightly different than the BBB. The retinal capillary endothelium constitutes the inner blood-retinal barrier (i-BRB). These endothelial cells are sealed with zonulae occludens, which acts as a barrier to hydrophilic molecules, such as trypan blue and fluorescein (Cunha-Vaz et al.). The BRB also acts as a barrier to small protein tracers (such as microperoxidase, MW ~1.9 kDa and a hydrodynamic radius of 2 nm) and large protein tracers (such as horseradish peroxidase, MW ~40 kDa and a hydrodynamic radius 5 nm) (Smith and Rudt, 1975).

The i-BRB restricts bidirectional drug transport from both luminal and abluminal sides (Peyman and Bok, 1972). It primarily prevents the entry of drug molecules into the posterior segment of the eye (Fig. 1.4). This barrier is formed by the retinal pigmented epithelium (RPE) and the retinal endothelium. The RPE forms the outer BRB between the choroid and the neural retina. It regulates the transport of molecules from choriocapillaries into retina. Blood flow through choroid and BRB allows only a limited percentage of orally administered drug molecules to reach the retina. The apical junctional complex of RPE is formed of tight junctions and adherent junctions. The tight junctions are formed with actin filaments, which encircle each cell at the apical end to form junctional complexes. Studies

with trypan blue and fluorescein showed the localization of these dyes at the RPE, which confirmed the presence of tight junctions. A few studies also correlated an increase in the tight junction-associated protein ZO-1 content with decreased permeability across the RPE (Stevenson et al., 1988).

Development of these barrier properties was studied with chick RPE, where the barrier starts developing in the embryo state at day 7 and becomes fully functional within day 15 to 19 (Ban and Rizzolo, 1997). Permeability across the RPE depends upon the pore radius. It was characterized by permeation studies of solutes with different shapes, charges, molecular weight, and lipophilicity. Studies by Vargus et al. suggested that compounds with large molecular radii (such as insulin, 14 Å, and sucrose, 5.3 Å) cannot permeate into vitreous humor; where as smaller molecules (such as glycerol, 3 Å) permeate very slowly (Saha et al., 1998). The permeability of molecules of different sizes and polarity is summarized in Tables 1.1 and 1.2 (Hughes et al., 2005; Pitkanen et al., 2005).

(ii) Blood-Aqueous Barrier (BAB)

The BAB, also known as the anterior chamber barrier, primarily prevents the entry of exogenous compounds into the aqueous humor. It is formed from the endothelial cells of uvea, the middle vascular layer of the eye, and is comprised of three parts: the iris, ciliary body and choroid. The BAB restricts the movement of drug molecules from the plasma into the anterior chamber (Cunha-Vaz, 2004; Davson et al., 1949).

The BAB is not as effective as the BRB due to the leaky nature of the non-pigmented epithelium. After intravenous administration, higher concentrations of test substances, particularly proteins, urea, inorganic salts (sodium, potassium, chloride), and antibiotics are found in the anterior part of vitreous humor (Davson et al., 1949).

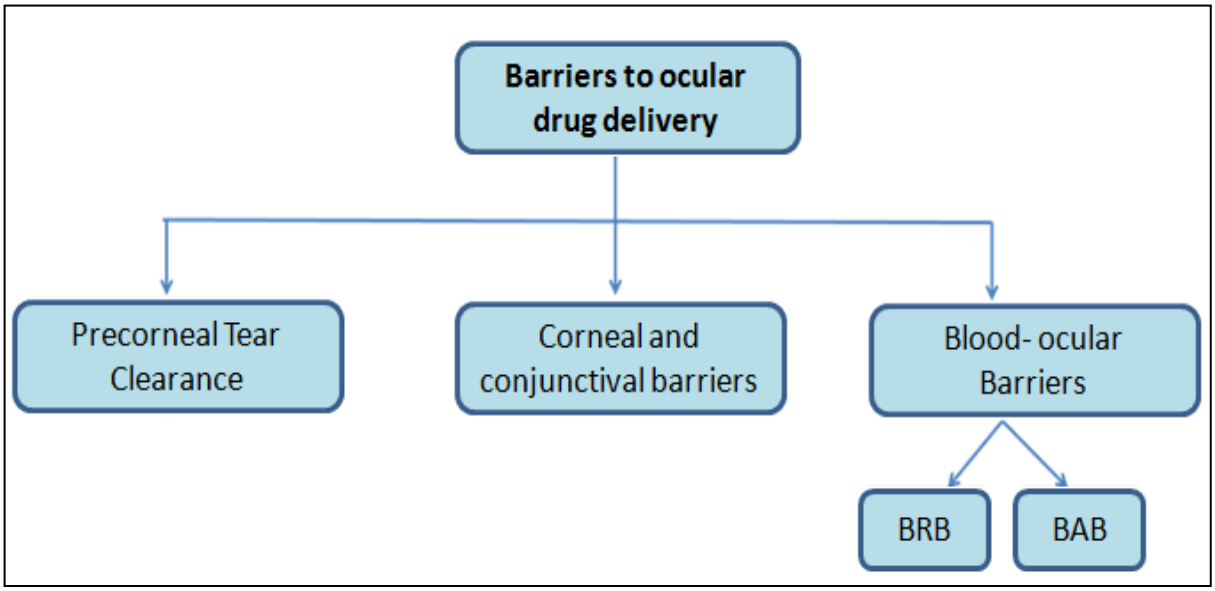

Figure 1.2 Classification of major barriers to ocular drug delivery. BRB: Blood- Retinal Barrier; BAB: Blood- Ocular Barrier [adapted with permission from ref (Mishra et al., 2010)]

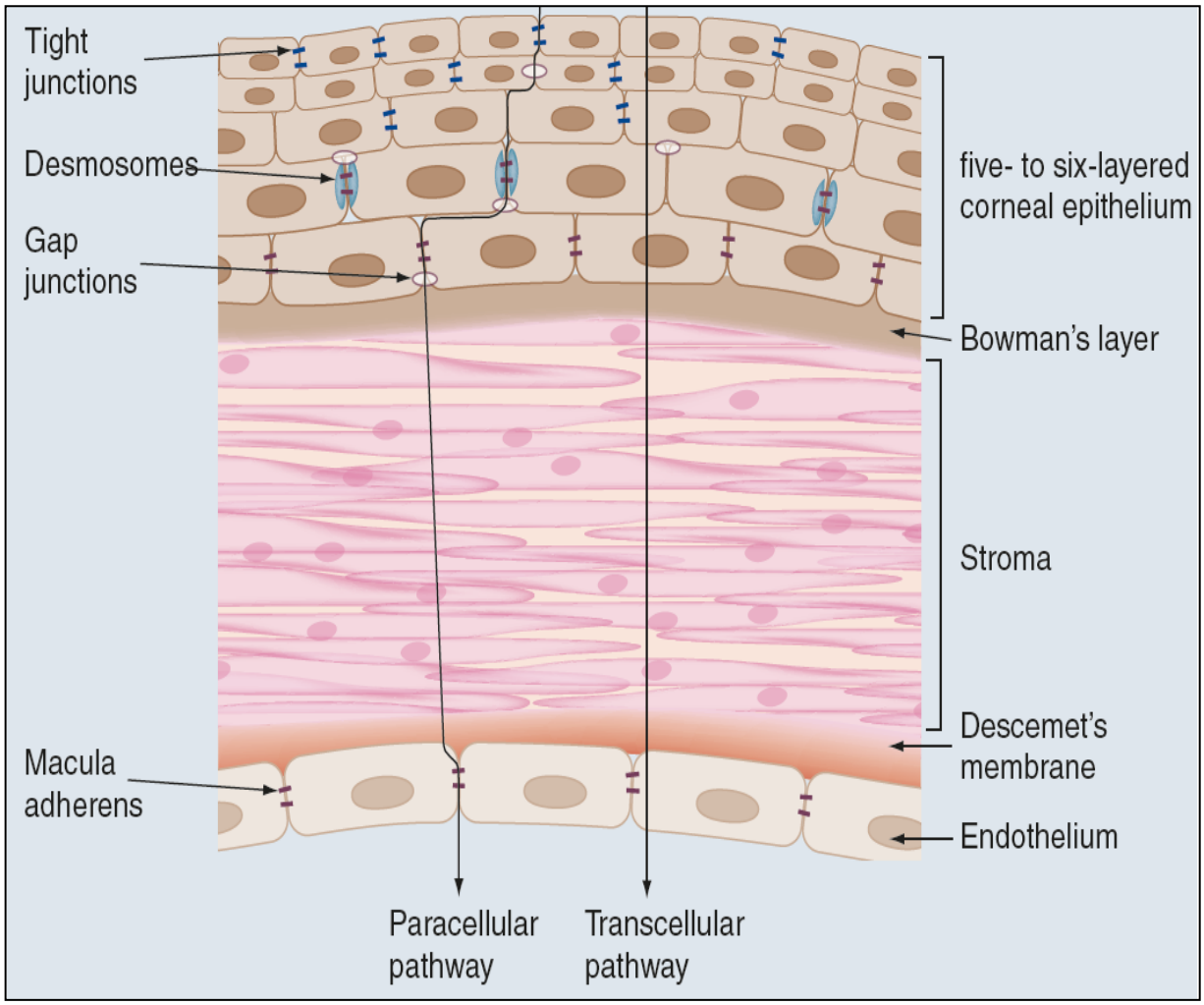

Figure 1.3 Corneal barriers [adapted with permission from ref (Tamboli et al., 2011)]

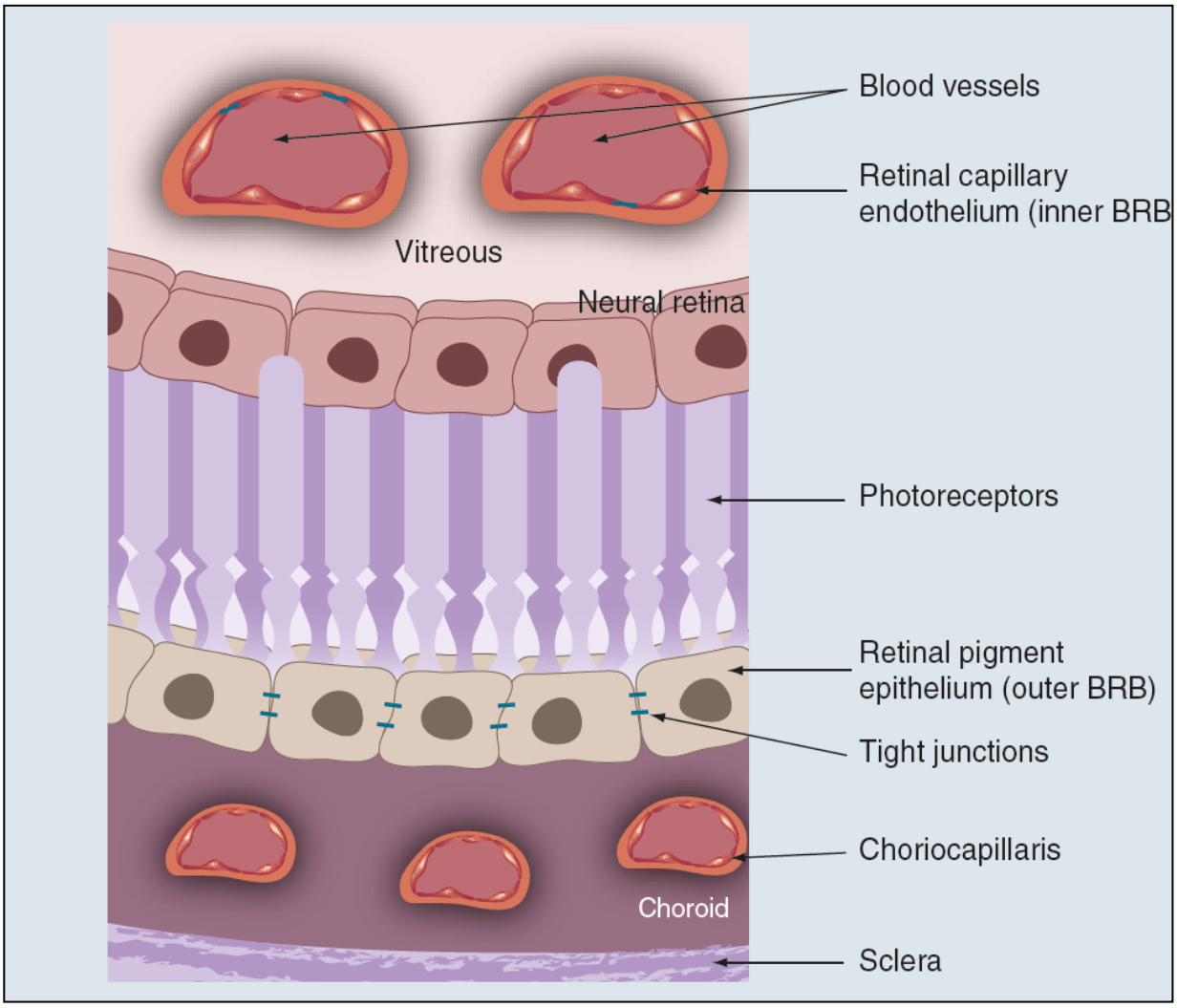

Figure 1.4 The blood retinal barrier [adapted with permission from ref (Tamboli et al., 2011)]

Table 1.1 The permeability of various molecular weight fluorescent probes across rabbit RPE-Choroid [adapted with permission from ref (Mishra et al., 2010)]

Probe	Molecular Weight (Da)	Molecular Radius (nm)	Diffusion Direction*	Permeability Coefficient ($\times 10^{-7}$ cm/sec)
Carboxyfluorescein	376	0.5	Inward outward	9.56 ± 3.87 23.3 ± 10.6
FITC-dextran 4 kDa	4,400	1.3	Inward	2.36 ± 1.56
FITC-dextran 10 kDa	9,300	2.2	Inward outward	2.14 ±1.02 2.04 ±1.03
FITC-dextran 20 kDa	21,200	3.2	Inward	1.34 ± 1.80
FITC-dextran 40 kDa	38,200	4.5	Inward	0.46 ± 0.29
FITC-dextran 80 kDa	77,000	6.4	Inward	0.27 ± 0.32

*Inward is the choroid-to-retina direction; outward is the retina-to-choroid direction

Table 1.2 The permeability of molecules with different lipophilicity across the rabbit RPE-choroid [adapted with permission from ref (Mishra et al., 2010)]

Solute	Molecular weight	Log p	Diffusion Direction*	Permeability Coefficient ($\times 10^{-6}$ cm/sec)
Atenolol	266	0.16	Inward outward	2.21 ± 0.50 2.00 ± 0.47
Nadolol	309	0.93	Inward outward	2.24 ± 0.54 2.03 ± 0.46
Pindolol	248	1.75	Inward outward	5.62 ± 1.87 3.48 ± 1.69
Metoprolol	267	1.88	Inward outward	18.8 ± 4.34 10.6 ± 3.19
Timolol	316	1.91	Inward outward	14.5 ± 3.48 8.41 ± 2.67
Betaxolol	307	3.44	Inward outward	16.7 ± 4.48 10.3 ± 3.65

* Inward is the choroid-to-retina direction; outward is the retina-to-choroid direction

Administration Routes for Ocular Drug Delivery

The selection of the appropriate route of drug administration plays a critical role in targeted drug delivery to the eye. Both local and systemic routes are used for ocular drug delivery. Local routes include topical, intravitreal and periocular administration as mentioned in (Fig. 1). The barriers for drug delivery through various routes and strategies to overcome these barriers are summarized in Table 1.3.

Topical Route

A topical route is commonly utilized for the treatment of anterior segment diseases. Various constraints such as precorneal tear clearance and conjunctival absorption limit ocular bioavailability (sometimes to even less than 1%). Also, drug metabolism in the iris-ciliary body and elimination through the canal of Schlemm (a scleral-venous sinus that collects aqueous humor from the anterior chamber and delivers it to the bloodstream) results in further loss from the anterior segment.

Application of this route for posterior segment diseases is limited. Therapeutic drug concentrations in the posterior segment usually may not be attained as the drug would need to permeate through cornea, aqueous humor, and the lens (Urtti and Salminen, 1993). However, some reports suggest that therapeutic levels of some drugs, like verapamil and brominidine, are attainable in the posterior segment following topical instillation into the rabbit eye (Kent et al., 2006). Earlier, it was believed that overall drug concentration in posterior segment depends upon the physiochemical properties of the drug itself. Drugs like nepafenac, a non-steroidal anti-inflammatory drug (NSAID), are used as a prescription eye drop (e.g., a 0.1 % solution) to treat pain and inflammation associated with cataract surgery.

Table 1.3 Overview of various routes of ocular drug delivery [adapted with permission from ref (Mishra et al., 2010)]

Routes of drug administrations	Advantages	Disadvantages	Major Barriers	Strategies to overcome these barriers
Topical route	Ease of administration	Low ocular bioavailability	Precorneal tear clearance, conjunctival absorption, drug metabolism by iris-ciliary body, elimination through the canal of schlemn	Gel systems, prodrugs, viscosity and penetration enhancers
Intravitreal route	Circumvents BRB	Repeated injections required that cause retinal detachment	Toxicity and Patient non-compliance	Prodrugs, micro and nanoparticles, liposomes
Periocular routes Examples: Retrobulbar Peribulbar Subtenon Sub-conjunctival	Lower risk of injury, least invasive route, provide large surface area, easy accessibility, high permeability across sclera	Ocular haemorrhage, artery occlusion and globe perforation	Loss of drug by choriocapillaries and through conjunctival and lymph circulation	Implants, insitu-gelling systems, micro/nanoparticles

Nepafenac reaches the posterior segment on topical application and inhibits choroidal and retinal neovascularization by lowering the production of vascular endothelial growth factors (Lindstrom and Kim, 2006). Other studies have indicated that even macromolecules like insulin can reach therapeutic concentrations in the retina.[30] Some of these topically applied drugs cause systemic toxicity. For example, phenylephrine causes tachycardia and hypertension, whereas timolol can cause bradycardia and congestive heart failure (Koevary, 2003). Thus, even though topical drug delivery has some limitations, this route can be used for targeted drug delivery to both anterior and posterior segment of the eye (Rait, 1999).

Systemic Route

The systemic route is not frequently used for ocular drug delivery. However systemic administration of acetazolamide is preferred for severe glaucoma as higher intraocular pressures reduce the absorption of drug from topically administered eye drops (Rosenberg et al., 1998). Treatments of ocular conditions utilizing systemic administration include human cytomegalovirus (HCMV) retinitis, however, the drug concentration achieved at the targeted ocular tissues is only 1-2 % of the plasma concentration (Macha and Mitra, 2001). Following systemic administration, drug penetration from blood into the ocular fluid is less in the vitreous humor compared to the aqueous humor. This is due to the presence of the BOB. Studies by Macha et al. have shown that only 1-2 % of the plasma concentration can be detected in the vitreous humor. Therefore, the maintenance of the minimum therapeutic concentration in the eye may require frequent systemic drug administration, which may cause adverse effects in other tissues. Therefore, systemic administration may not be considered a desired route for the treatment of ocular pathologies (Macha and Mitra, 2001).

Intravitreal (IVT) Administration

IVT injection is mainly utilized for the treatment of posterior segment diseases such as diabetic retinopathy, using drugs such as bevacizumab (Avastin®), triamcinolone (Kanalog®), and pegaptanib sodium (Macugen®). Also, viral infections like HCMV retinitis and endophthalmitis have been treated by intravitreal administration of antivirals like ganciclovir, cidofovir, and foscarnet (Cheng et al., 2004). This route circumvents the blood-retinal barrier (BRB). Thus, it is more efficient than either topical or systemic routes.

IVT administration is limited by patient non-compliance due to repeated administration which may cause retinal detachment followed by vision loss (Baum et al., 1982). Various strategies have been developed to reduce the frequency of administration by prolonging drug residence time in the vitreous humor by using prodrugs, microparticles, nanoparticles, and liposomes (Lopez-Cortes et al., 2001). Reports from our laboratory have indicated that administration of ganciclovir (GCV) monoester prodrug provides a sustained GCV level in the vitreous humor compared to the parent drug (Macha and Mitra, 2002). However, toxicity and non-compliance associated with this route restrict applicability in the treatment of ocular pathologies.

Periocular Administration

This is one of the least invasive routes of drug administration for the back of the eye. This route provides direct access to the sclera and transscleral delivery can provide therapeutic drug concentrations both in the anterior and posterior segments. This route can be further classified into retrobulbar, peribulbar, subtenon, and subconjunctival depending upon the site of injection.

(i) Retrobulbar Injection

This injection is given directly into retrobulbar space. It is generally utilized for drug delivery into the macular region (highly pigmented yellow spot near the center of retina, rich in ganglion cells and responsible for central vision). Hyndiuk et al. showed that steroids get localized near the macular region after retrobulbar injection (Hyndiuk and Reagan, 1968). Generally, a special type of 23 gauge needle with a 10° bend is utilized for this injection. A major disadvantage of this technique is damage to the blood vessels around the site of injection.

(ii) Peribulbar Injection

This route possesses the advantage of lower risk of injury to the ocular structure in comparison to the retrobulbar injection. The injection can be performed with a 26 gauge needle (Ebner et al., 2004). Based on the site of administration it can be classified into circumocular, periocular, periconal, and apical (van den Berg, 2004). This route is generally useful for the administration of analgesics, but it may cause complications including ocular haemorrhage, artery occlusion, and globe perforation.

(iii) Subtenon Injection

The subtenon route is mostly used for drug delivery to the posterior segment. It involves drug administration into the tenon space, which is formed by the void between the tenon's capsule and sclera. The major limitation of this route is rapid clearance by choriocapillaries and drug diffusion across the sclera (Mather and Kirkpatrick, 2003).

(iv) Subconjunctival Injection

This method is one of the least invasive routes among all periocular routes for drug administration. The subconjunctival space can accommodate up to 500 µl of drug solution

and injection can be made through a 30 gauge needle (Kim et al., 2002). This route can be utilized for the treatment of both anterior and posterior segment diseases. It provides large surface area, easy accessibility, and high permeability across the sclera. This mode of administration can be utilized for sustained drug delivery in various chronic diseases, including glaucoma and age-related macular degeneration. A higher dexamethasone concentration could be achieved in the retina following subconjunctival injection relative to peribulbar injection or oral administration (Weijtens et al., 2000).

Ambati et al. reported that large hydrophilic molecules, such as proteins and peptides, can be successfully delivered through this route (Ambati et al., 2000). Similarly, Kim et al. reported higher concentrations of gadolinium (III) - diethyltriaminepentaacetic acid (Gd-DTPA) in the iris ciliary body following subconjunctival injection compared to other parts of the eye. This route can also be utilized for the administration of intra-ocular pressure-lowering drugs, such as mitomycin-C and 5-fluorouracil, both used to treat glaucoma. The main limitation of this delivery route is the loss of drug, mainly through conjunctival blood and lymph circulation (Kim et al., 2004a).

Biodegradable polymers

Biodegradable polymers have numerous applications in the field of ocular drug delivery and can be classified as natural or synthetic. Applications of polyglycolide (PGA) as suture material in the late 1960 provided an impetus for the design and development of novel synthetic biodegradable polymers. Synthetic biodegradable polymers (Fig. 1.5) can be tailored in various compositions and molecular weights. The molecular weight or composition regulates the degradation of polymer where the main weight loss takes place due to chain cleavage. Biodegradable polymers generally undergo homogenous or heterogeneous

erosion. Homogenous erosion, commonly referred as bulk erosion, involves hydrolytic cleavage of the complete cross-section of polymer matrix. In case of bulk erosion, hydrolytic degradation is slower than diffusion of water inside the polymer matrix in contrast to faster hydrolysis rates in heterogeneous or surface erosion. The degradation rate of bulk eroding polymers is slower and may vary from several weeks to years. Polymers of poly (α-hydroxyl esters) usually undergo bulk erosion and follow first order degradation kinetics. Polyesters show complex patterns of no significant degradation in the initial phase followed by rapid mass loss (Lee et al., 2003; Pulapura and Kohn, 1992). The hydrolytic degradation rate of polyesters depends on their molecular weight and crystallinity. Low molecular weight poly-(lactic-co-glycolic acid) (PLGA) degrades faster than high molecular weight PLGA (Lu et al., 2000). Drug release from a bulk eroding polymer matrix depends upon swelling, diffusion, and hydrolytic degradation in contrast to surface eroding polymers, where it primarily depends on hydrolytic degradation. Surface erosion commonly occurs in faster degrading polymers such as polyanhydrides and poly-(ortho esters) (Jain et al., 2008).

Polyesters

Polyesters are biodegradable polymers having short aliphatic ester linked backbone. These classes of polymers are generally produced by either ring opening or condensation polymerization. Ring opening polymerization (ROP) is preferred over condensation reactions to produce high molecular weight polyesters. Homo- or co-polymers of cyclic lactones and anhydrides having narrow molecular weight distribution can be polymerized via ROP. In ROP, hydroxyl group containing polymers such as polyethylene glycol are commonly employed as an initiator whereas compounds such as stannous octoate and 2-ethylhexanoic acid are utilized as catalyst. The molecular weight of final polymer can be controlled by

varying the ratio of monomers. The molecular weight of the polyesters regulates the hydrolytic cleavage that follows bulk erosion kinetics to produce metabolic products which are eliminated through normal metabolic pathways (Middleton and Tipton, 2000). The hydrolytic degradation rate can be altered by varying the crystallinity and structure of the polymeric chain. These tailor-made degradation properties make them appropriate for biomedical applications. Among polyesters, poly-α-hydroxy esters are the most broadly investigated class of polymers for ocular drug delivery applications. This mainly includes poly (glycolic acid) (PGA), poly (lactic acid) (PLA) and their copolymers.

(i) Polyglycolide (PGA)

PGA is a relatively hydrophilic polymer with high crystallinity and low solubility in organic solvents. The low solubility in organic solvent is attributed to its higher tensile modulus. It has a high a melting point of 225 °C and glass transition temperature of 36 °C. High molecular weight polyglycolide is synthesized by ring opening polymerization. It has a comparatively higher degradation rate than other polyesters and generates glycine upon degradation, which eventually eliminates through the citric acid cycle. Major losses in the mechanical strength of PGA usually take place in one to two months whereas it completely degrades within six to twelve months. PGA was initially explored for developing sutures because of their fiber-forming properties and excellent mechanical strength. However, it has limited role in ocular drug delivery due to faster degradation rate and higher crystallinity. PGA implants can be easily fabricated by widely applicable processing techniques such as solvent casting, compression and extrusion techniques. Processing technique utilized for the production of implant regulate the degradation properties of implant (Jain et al., 1998).

(ii) Polylactide (PLA)

PLA is comparatively more hydrophobic than PGA due to the presence of the additional methyl group. It is chiral in nature because of the structure of lactic acid and commonly exists in three isomeric forms the D (-), L (+) and racemic (D, L) lactide. The crystalline nature of PLA depends upon the isomeric forms and molecular weight. Poly-L-lactide (PLLA) is hydrolyzed through normal metabolic pathway due to presence of naturally occurring isomer (L-lactide). It has a melting point of 175 °C and glass transition temperature of 60–65 °C. It also possesses a good tensile strength of 50–70 MPa and high modulus of 4.8 GPa. The degradation rate of PLLA is slower than PGA and usually takes around two to six years for complete elimination from the body. On the other hand, poly-DL-lactide (PDLLA) is amorphous in nature due to presence of racemic mixture. It has glass transition temperature of 55-60 °C and comparatively faster degradation rate than PLLA. Its faster degradation kinetic property was utilized for drug delivery applications. All isomeric forms of PLA follow bulk erosion kinetics and generate lactic acid upon hydrolytic cleavage (Hyon et al., 1997). Researchers have often utilized PLA for ocular drug delivery applications. In a recent studies performed by Cui et al., it was observed that subconjunctival administration of 5-FU loaded PLA disc can provide sustained release for 91 days. Corneal endothelial toxicity was not observed due to controlled release of 5-FU below its toxic limit. In addition, conjunctival biopsy revealed that the PLA-based discs are biocompatible for SC administration.

(iii) Poly (lactide-co-glycolide)

Poly-lactide-co-glycolide commonly known as PLGA is obtained by the copolymerization of lactide and glycolide. This copolymer is hydrolytically less stable than the monomers, PLA or PGA. Extensive research on the full range of these copolymers

suggests their implication in drug delivery. These copolymers are divided into two main compositions, comprised of L or (D, L) lactide. It was observed that compositions having 25-75% of L-lactide and up to 70% (D, L) lactide are amorphous in nature. As the ratio of glycolide in copolymer decreases hydrolytic degradation rate increases. The intermediate PLGA i.e. 50:50 hydrolyses faster in comparison to PLGA 75:25 and PLGA 85:15. PLGA follows bulk erosion kinetics and its degradation depends on molecular weight and lactide to glycolide ratio. It is FDA approved for human applications because of the excellent biocompatibility and controlled degradation profiles (Lu et al., 2009).

PLGA has negative charge and thus has non-mucoadhesive nature. Studies by Gupta et al. on sparfloxacin loaded PLGA nanoparticles suggest that smaller size of nanoparticles improve the spreading coefficient and retention time of the formulation (Gupta et al.). PLGA was also utilized for the production of a drug eluting contact lens. Ciolino et al. investigated the role of pHEMA (poly [hydroxyethyl methacrylate]) coated PLGA films for the delivery of ciprofloxacin in the treatment of staphylococcus aureus associated ocular infections. They reported zero-order release kinetics for a period of 4 weeks and concluded that PLGA derived contact lens could serve as platform for ocular drug delivery (Ciolino et al., 2009). Other studies by Eperon et al. showed that PLGA based drug delivery system (DDS) has better patient compliance due to biodegradable nature of PLGA which avoids surgical procedure for implant removal. In addition, they observed a significant reduction in post-operative inflammation and rise of intraocular pressure following application of triamcinolone loaded drug delivery systems (Eperon et al., 2008).

(iv) Polycaprolactone (PCL)

PCL is a semicyrstalline polymer synthesized by ring opening polymerization of ε-caprolactone. It has a glass transition temperature of -60 °C and a melting temperature in the range of 59-64 °C. PCL was investigated for long term delivery due to higher permeability to many drugs, excellent biocompatibility and extremely slow hydrolytic cleavage of polyester backbone. The PCL based Capronor® implant was developed for controlled delivery of levonorgestrel. It has a low tensile strength of 23 MPa and an extremely high elongation more than 700%. Numerous investigations were attempted to modulate the slower degradation of PCL which generally shows a degradation time of two to three years. Copolymers of ε-caprolactone with D,L lactide or glycolide exhibits remarkably better degradation profile. Yenice et al. evaluated the ocular bioavailability of cyclosporine A (Cy A) loaded PCL nanoparticles alone and coated with hyaluronic acid (HA). They observed significantly higher Cy A levels in the rabbit corneal tissue. In PCL alone they observed Cy A concentration of 5.9 – 15.5 ng/mg tissues and in HA-coated PCL nanoparticles 11.4-23.0 ng/mg tissue. These levels were observed higher than the conventional eye drops and showed promising approach for the treatment of immune mediated corneal diseases (Yenice et al., 2008). Beeley et al. designed a triamcinolone acetonide loaded polycaprolactone implant for the treatment of retinal diseases. PCL implant was well tolerated in the sub-retinal space of rabbit eyes. Authors observed TA release for a period of four weeks (Beeley et al., 2005).

(v) Poly (Alkyl Cyanoacrylates)

PACA belongs to class of acrylate polymers synthesized from alkyl cyanoacrylic monomers through anionic polymerization. PACA faster degradation rate was attributed to its unique instability of carbon-carbon sigma bond and presence of electron withdrawing neighboring groups. It has shown remarkable applicability as surgical glue and skin adhesive. PACA was also explored for the development of nanoparticles. PACA degradation rate depends on the length of alkyl side chain. It varies from hours to days. For example PACA having shorter alkyl chain length such as poly-methyl cyanoacrlates degrades in few hours whereas higher alkyl chain length derivatives such as octyl and isobutylcyanoacrylates degrade slowly. Nanoparticles composed of PACA are advantageous over other nanoparticles in terms of fabrication and application in drug delivery (Arias et al., 2008a; Arias et al., 2008b).

Fresta et al. investigated ocular tolerability and in vivo ocular bioavailability of PEG and HP B-CD coated polyethyl-2-cyanoacrylate nanospheres loaded with ACV. They observed that PEG has decreased the zeta potential of nanospheres from -25.9 mV to -12.2 mV. However, HPB-CD did not change the zeta potential. PEG coated nanospheres are well tolerated by ocular structures and investigators observed 25-fold increments in ocular bioavailability in comparision to drug alone (Fresta et al., 2001). In another study Desai et al. fabricated pilocarpine loaded polyisobutyl cyanoacrylate (PIBCA) nanocapsules. The authors reported drug loading of 13.5 % and size in the range of 370 to 460 nm. They observed that incorporation of 1.1 % pilocarpine nanocapsules in pluronic F127 gel increased the mitotic response in albino rabbit eyes compared to the nanocapsules alone (Desai and Blanchard, 2000).

(vi) Polyanhydrides

Numerous investigations have studied the role of polyanhydrides **(**POA) in ocular drug delivery applications. These polymers exhibit faster degradation and limited mechanical strength, which make them an ideal candidate for fabrication of sustained release devices. Low molecular weight polyanhydrides were synthesized through dehydrative coupling and dehydrochorination, whereas melts polycondensation polymerization was employed for the synthesis of high molecular weight polymers. The degradation rate of polyanhydrides can be easily modulated by changing the polymer composition and the rate also depends on the crystallinity and hydrophilicity of the polymer. These polymers undergo surface erosion and generate monomeric non-toxic acid nature. Homo polyanhydrides have limited application in controlled drug delivery due to their crystalline nature. In contrast, copolymers such as poly [(carboxyphenoxy)propane–sebacic acid (PCPP-SA) demonstrate a controlled degradation rate (Tamargo et al., 1989).

This polymer was approved by the US FDA for human applications for the delivery of BCNU in the treatment of brain cancer (Brem, 1990). Other approaches based on aromatic co-monomers composed of hydrophobic aliphatic linear fatty acids were also investigated for drug delivery applications (Kumar et al., 2002).

(vii) Poly (ortho esters)

Poly-ortho-esters (POE) is a hydrophobic polymer composed of a hydrolytically unstable polyester linkage. However, it undergoes slower degradation due to surface erosion. This degradation characteristic is useful in designing sustained release devices. Polymer degradation profile can be easily adjusted by employing different diols for polymerization (Tang et al., 2009). POE is hydrolytically unstable in acidic conditions and required basic

additives to inhibit autocatalysis. The first generation of POE was developed by ALZA Corporation. It was synthesized by transesterification reaction of diol with diethoxytetrahydrofuran (Heller et al., 2002). The degradation profile of POE II can be easily altered by incorporation of acidic additives such as adipic acid. POE III upon hydrolysis generates diol and pentaerythriol dipropionate, which subsequently generate proponic acid and pentaerythriol. This class of polymers is biocompatible and follows pH dependent degradation behavior. It does not require organic solvent for the incorporation of drug due to its semisolid nature. However, difficulties in scale up process limit its application for drug delivery. Modification of second generation polyester (POE II) with smaller chain of lactic or glycolic acid leads to the development of POE-IV. This polymer, upon hydrolysis, liberates acids which further promote polymer degradation. The physical form and degradation rate of the polymer can be easily varied by changing diols or acid segment, respectively. POE IV demonstrated good biocompatibility for controlled delivery applications (Einmahl et al., 2001b; Heller, 2005; Heller et al., 2000).

In a recent studies by Polak et al. controlled delivery of 5-flurouracil and 5-chlorouracil was attempted utilizing POEs in the treatment of glaucoma filtration surgery. The authors observed IOP and bulb persistence after injecting the POE formulation into the subconjunctival space. In addition, histological analysis revealed functioning of bulb and no damage to the conjunctival epithelium. Investigators concluded that POE formulation is effective in the patients of glaucoma filtration surgery (Polak et al., 2008). Einmahl et al. evaluated POE IV biocompatibility after intraocular administration through various routes including subconjunctival, intracameral and intravitreal injections (Einmahl et al., 2001a; Einmahl et al., 2003).

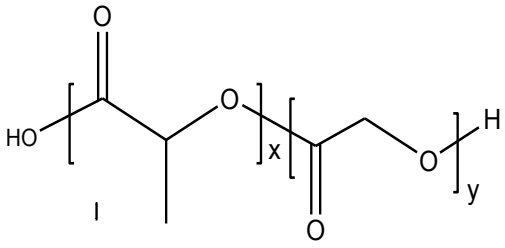

PLGA

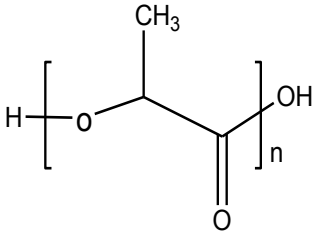

PLA

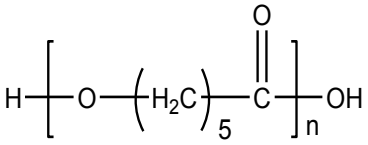

Polycaprolactone

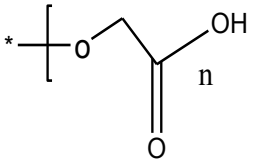

PGA

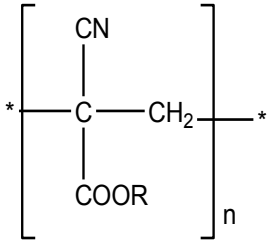

Poly(cyanoacrylates)

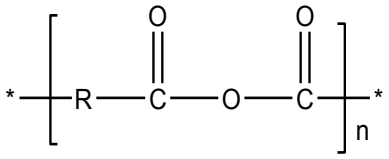

Poly(anhydrides)

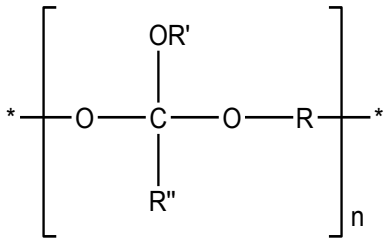

Poly(ortho esters)

Figure 1.5 Structures of biodegradable polymers

CHAPTER 2

INTRODUCTION

Overview

A PCL-based triblock polymer, i.e. poly (ethylene glycol)-poly-(ε-caprolactone)-poly (ethylene glycol) (PEG-PCL-PEG) remains in solution at room temperature (25 °C) but forms a transparent gel at body temperature (37 °C). This change in physical state is rapid and reversible, which makes thermosensitive hydrogels an attractive means for drug delivery. This unique thermoreversible property could be utilized for sustained delivery of timolol maleate (TM) in the treatment of ocular hypertension or glaucoma. Currently, the only non-invasive mode of treating glaucoma requires once or twice daily topical administration. PCL based hydrogel formulation of TM could eliminate daily dosing, thereby improving therapy and patient compliance.

Drug release from a PEG-PCL-PEG hydrogel depends primarily on the diffusion mechanism due to the extremely slow degradation rate of PCL. It also exhibit burst release due to a porous matrix. Such an initial burst release can provide high drug levels causing systemic or local toxicities. In attempts to achieve sustained release and a lower burst release of TM from the hydrogel we will utilize a novel polymeric additive strategy. It has been observed that hydrogel applications in therapeutic delivery are limited by burst release due to porous structure and frontal diffusion processes.

Hydrogel polymeric matrix is porous in nature and TM molecules can diffuse through the pores of polymeric chains. Polymeric additives can easily fit into the spaces of a hydrogel

matrix and modify drug release rates. PCL will be selected as a hydrophobic additive and polyvinyl alcohol (PVA) as a hydrophilic additive. These polymeric additives are already approved by FDA for application in humans. The rationale behind selecting PCL and PVA as additives depends on their molecular property to provide better packing of the hydrogel matrix through intra- and intermolecular interactions between the triblock polymeric chains.

PEG-PCL-PEG degrades slowly and posses higher crystallinity. Considering this in our second approach we have incorporated a PLA block in the center of PEG-PCL-PEG, in an attempt to accelerate the degradation rate of the highly crystalline and hydrophobic PCL block. We hypothesize that incorporation of PLA will promote degradation-mediated drug release. Therefore, we will develop novel pentablock copolymers by introducing faster degrading polymeric block.

The major challenge for controlled delivery of therapeutic molecules is to maintain drug concentration for prolonged periods. A specific combination of molecular weight and block ratio can generate polymeric nanoparticles. Pentablock copolymers will be comprised of multi-polymer blocks such as polyethylene glycol (PEG), PCL and small fraction of PGA or PLA, which are FDA approved for human use. In comparison to PLGA, pentablock polymers would generate very small amounts of either glycolic acid or lactic acid upon degradation due to low molecular weight blocks of PGA or PLA. Pentablock polymers should result in negligible cytotoxicity and release of inflammatory mediators.

Nanoparticles alone demonstrate initial burst release due to surface adsorbed drug molecules. The dual approach of nanoparticles suspended in a thermosensitive gel is

expected to minimize the burst release of drugs due to longer diffusion pathway of drug molecules from the system.

Statement of the problem

Noncompliance plays a major role leading to blindness in glaucoma patients. There is a need for a better delivery strategy which can sustain and release constant levels of drug over long periods of time. To maintain the therapeutic concentration, frequent administrations are required that may not be practical. The objective of my study is to develop novel controlled drug delivery system for glaucoma therapy.

The most commonly used polymer for controlled drug delivery is PLGA. PLGA upon degradation produces a high molar mass of lactic acid and glycolic acid, which may cause tissue irritation and toxicity by decreasing pH. PLGA particles allow rapid release (40-50%) of payload within one to two days. Therefore, we proposed to introduce novel engineered biodegradable pentablock copolymers. The rationale behind developing novel biodegradable and biocompatible pentablock polymer is to achieve controlled release over prolonged period of time. These polymers are comprised of multi-polymer blocks such as PEG, PCL and small amount of PGA. In comparison to PLGA, pentablock polymers will release less glycolic acid upon *in vivo* degradation due to low molecular weight of the PGA block. This results in negligible tissue irritability and toxicity. Existing PGA based diblock or triblock polymers have burst release from nanoparticles or thermosensitive gel due to faster degradation. On the other hand PCL or PLA based block polymers have primarily diffusion mediated drug release due to extremely slow degradation. This approach may lead to development of novel polymers with optimum degradation rates to achieve zero-order drug release via both

diffusion and degradation mediated pathways. PB could be utilized for the preparation of nanoparticles and thermosensitive gel. However nanoparticles and thermosensitive gels alone demonstrate initial burst release due to surface-adsorbed drug molecules. The dual approach of nanoparticles suspended in a thermosensitive gel could minimize the burst release of drugs due to longer diffusion pathway of drug molecules from the system. Such novel technology upon subconjunctival administration will result in a prolonged duration of action and thereby eliminate the need for repeated administration.

Therefore the broad objective of this research was to develop novel pentablock polymer based drug delivery systems to provide controlled release of drugs.

Objectives

1. To delineate the effects of polymeric additives with hydrophilic and hydrophobic properties on the gelling behavior and release profiles of TM from a PCL-based triblock polymer. In addition, the effects of parameters such as drug loading and molecular weight of polymer on the release profile of TM will be investigated.
2. To optimize the ratio of PCL and PLA in the novel pentablock (PEG-PCL-PLA-PCL-PLA) copolymer; (ii) to determine molecular weight distribution, rheological behavior, degradation kinetics and biocompatibility; (iii) to investigate the effect of molecular weight and PCL/PLA block length ratio on the sol-gel transition and *in vitro* release kinetics of different molecules of varying size and polarity.
3. to synthesize novel tailor-made pentablock polymers of different molecular weight and block ratio for the preparation of nanoparticles; (ii) to characterize pentablock polymers for molecular weight distribution and cytocompatibility.

4. To optimize *in-vitro* drug release from nanoparticles suspended in thermosensitive gel by evaluating various compositions of pentablock polymers; (ii) to evaluate biocompatibility of composite formulation.

CHAPTER 3

EFFECT OF HYDROPHOBIC AND HYDROPHILIC ADDITIVES ON SOL-GEL TRANSITION AND RELEASE BEHAVIOR OF TIMOLOL MALEATE FROM POLYCAPROLACTONE BASED HYDROGELS

Rationale

Hydrogels composed of biodegradable polymers such as PLA, PLGA or PCL have wide application in the field of drug delivery due to the excellent biocompatibility of these polymers with living tissues (Garripelli et al., 2010; Huynh et al., 2008; Klouda and Mikos, 2008). These systems provide controlled drug release via diffusion as well as through degradation mechanisms (Soares and Zunino, 2010; Wu and Chu, 2008; Zhang et al., 2010). Several articles have reported the development of thermoreversible hydrogels composed of PEG as a hydrophilic block and PLA, PLGA or PCL as hydrophobic blocks (Chen et al., 2005; Jeong et al., 2000; Kan et al., 2005; Kang et al.; Kim et al., 2004b; Li et al., 2007; Qiao et al., 2005; Wei et al., 2009).

PCL is a biodegradable and biocompatible polymer approved by FDA for application in drug delivery systems and medical devices (Mohan and Nair, 2008; Rohner et al., 2003). Recent studies have explored the applications of PCL based hydrogels in sustained release formulations (Huynh et al., 2008; Jiang et al., 2008; Jones et al., 2005; Lee et al., 2001; Zhao et al., 2010). A PCL based triblock polymer, i.e. PEG-PCL-PEG, remains in solution state at room temperature (25 °C) and forms a transparent gel at body temperature (37 °C). This change in physical state is rapid and reversible, which makes thermosenstive hydrogel an attractive means for drug delivery (Hwang et al., 2005). This unique thermoreversible

property could be utilized for sustained delivery of TM in the treatment of ocular hypertension or glaucoma.

Currently, the only non-invasive mode of treating glaucoma requires once or twice daily topical administrations of eye drops. A PCL based hydrogel formulation of TM could eliminate daily dosing, thereby improving therapy and patient compliance. Topical beta-blockers, particularly TM, are major drugs for treating glaucoma and ocular hypertension because of their excellent intra-ocular pressure (IOP)-lowering efficacy. TM is a selective β-adrenergic blocker and is widely indicated in the treatment of glaucoma (Peeters et al.; Zimmerman and Kaufman, 1977a, b). Typically drug release from a hydrogel depends initially on diffusion. At later time points it depends upon a combination of diffusion and degradation mechanisms (Wu and Chu, 2008). In this case, drug release from PEG-PCL-PEG hydrogel depends primarily on the diffusion mechanism due to the extremely slow degradation rate of PCL. It also has the limitation of burst release due to a porous matrix. Such initial burst release can provide high drug levels causing systemic and local toxicities (Cheong et al., 2008; Munroe et al., 1985). In attempts to achieve sustain release and lower burst release of TM from the hydrogel; we have utilized a novel polymeric additive strategy.

Earlier studies focused on synthesis and release of hydrophilic and hydrophobic model drugs from PEG-PCL-PEG thermosenstive hydrogel (Gong et al., 2009b). However, it has been observed that hydrogel applications in therapeutic delivery are limited by burst release due to its porous structure and frontal diffusion processes. In this study an attempt has been made to study the effects of additives the on sol-gel transition and drug release from hydrogels with the addition of hydrophilic and hydrophobic polymers. The hydrogel

polymeric matrix is porous in nature and TM molecules can diffuse through the pores of polymeric chains. Polymeric additives can easily fit into the spaces of a hydrogel matrix and modify drug release rates.

Hence, the objective of this study was to delineate the effects of polymeric additives with hydrophilic and hydrophobic properties on the gelling behavior and release profiles of TM from PCL based triblock polymer. In addition, the effects of parameters such as drug loading and molecular weight of polymer on the release profile of TM were also investigated.

Material and Methods

Timolol maleate, monomethoxy poly (ethylene glycol) (MW = 550 and 750), ε-caprolactone, stannous octoate, polyvinyl alcohol and polycaprolactone diol (PCL) were obtained from Sigma chemical company (St. Louis, MO). Hexamethylene diisocyanate (HMDI) (Aldrich) was procured from Acros Organics (Morris Plains, NJ). All chemicals were used without further purification.

Synthesis of Triblock Polymer PEG-PCL-PEG

PEG-PCL diblock polymers were synthesized by ring opening polymerization of ε-caprolactone utilizing either monomethoxy poly (ethylene glycol) (mPEG) 750 or 550 as an initiator and stannous octoate as the catalyst. The diblock polymer was further coupled using HMDI to synthesize the triblock polymer PEG-PCL-PEG. The resulting polymer was purified by dissolving in methylene chloride followed by precipitation from diethyl ether. Briefly, the synthesis of PEG-PCL-PEG (Fig. 3.1) was carried out as follows; the mPEG was dried under vacuum for 3 h before copolymerization. Calculated amounts of mPEG (0.01

mol), ε-Caprolactone (0.1 mol) and stannous octoate (0.5 wt %) were added to the reaction mixture. The reaction was left for 24 h at 130 °C. The coupling of the diblock polymer was allowed to proceed by adding HMDI (0.01 mol) and the reaction was continued for 6 h at 60 °C. The final product was dissolved in 20 ml of methylene chloride and purified by fractional precipitation with petroleum ether. The purified polymer product was vacuum dried for 48 h to remove residual solvent.

Characterization of Polymeric Material

(i) NMR

^{1}H NMR spectroscopy was performed to characterize the composition of polymer. Spectra were recorded by dissolving polymeric material in $CDCl_3$ and then analyzing the proton NMR spectra recorded using Varian-400 NMR instrument.

(ii) Gel Permeation Chromatography (GPC) Analysis

GPC analysis was performed with the refractive index detector (Waters 410) to determine molecular weight and its distribution. Polymeric material (2mg/ml) was dissolved in Tetrahydrofuran (THF). Analysis was performed with THF as eluting solvent at a flow rate of 1 ml/min utilizing Styragel HR-3 column maintained at 35 °C. Polystyrenes with narrow molecular weight distribution were used as standards for GPC analysis.

(iii) Fourier Transform Infrared Spectroscopy (FT-IR)

The FT-IR spectra were recorded with a Nicolet-100 infrared spectrophotometer at a resolution of 4 sec^{-1}. Polymer was dissolved in methylene chloride and casted on KBr plates.

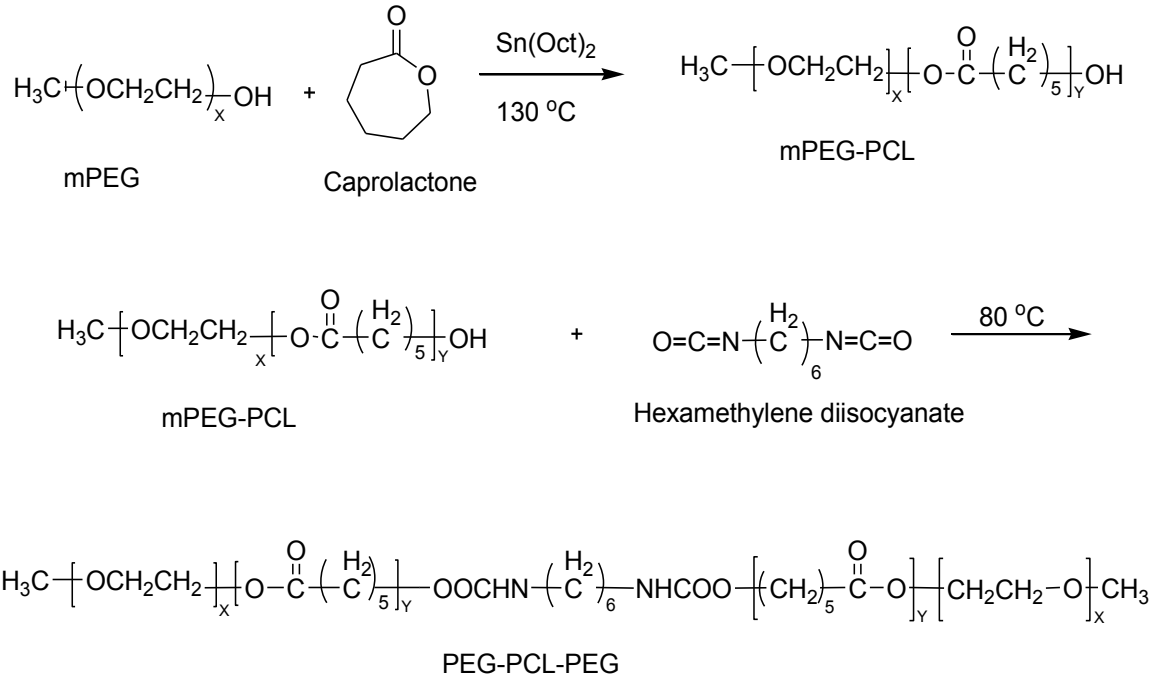

Figure 3.1 Synthetic scheme of PEG-PCL-PEG

Characterization of Thermosensitive Gel

(i) Sol-Gel Transition

Sol-gel transition studies were performed by test tube inversion method. First, the polymer was solubilized in PBS by storing overnight at 4 °C. Then 0.5 ml of polymer solution in 4 ml tube was placed in water bath and temperature was increased from 20 to 60 °C with 1 °C increment at each step. The gel formation was characterized visually by inverting the tube. A physical state of flow was characterized as sol phase, whereas a state of no flow was characterized as gel phase. Similar studies were performed by incorporating PCL or PVA (5 wt. %) as an additive to the hydrogel matrix. Viscosities of hydrogel alone and in the presence of additives were determined by cone and plate viscometer at 750 rpm and 37 °C.

(ii) Scanning Electron Microscopy (SEM)

Aqueous polymeric solutions of PCEC II alone and with additives were allowed to gel at 37 °C and then lyophilized for 48 h. The lyophilized hydrogels were sputtered with gold/palladium at 0.6 kV. The samples were examined by FEG ESEM XL 30 electron microscope.

In Vitro Release

TM dissolved in PEG-PCL-PEG triblock polymeric aqueous solution (0.4 ml) was injected into 10 ml vial with 12 mm internal diameter. Vials were kept in shaker bath at 37 °C with a stroke rate of 30 rpm. The polymeric solution was allowed to gel for 2 min. Then 5 ml of the release medium containing phosphate buffer (pH 7.4) and sodium azide (0.02 wt.

%) were added in order to prevent microbial contamination during a release study. The entire release medium was replaced with fresh buffer at predetermined intervals to mimic the sink condition. Samples were stored at -20 °C until further analysis. The release samples were analyzed by high performance liquid chromatography (HPLC) with a phenomex C_{18} column at a flow rate of 1 ml/min. The mobile phase was composed of 20 mM phosphate buffer with pH adjusted to 2.5. The analyte was measured at 294 nm. All experiments were conducted in triplicate.

(i) Effect of Molecular weight

mPEG of two different molecular weights i.e. m-PEG 550 and 750 were utilized to delineate the effect of molecular weight on release kinetics of TM from the gel matrix. Release study was performed with 25 wt. % of hydrogel with 1.0 wt% drug loading.

(ii) Effect of Drug Loading

The effect of drug loading on the release behavior was evaluated with two different concentrations of TM (0.5 and 1 wt. %) in the 25 wt. % hydrogel. A method as described previously was followed for release study.

(iii) Effect of PVA as Additive

PVA was used as a hydrophilic additive (Mw = 30,000-70,000) to modulate TM release rate. It was incorporated along with drug and polymer during hydrogel preparation. Incorporation of PVA up to 5 wt% concentration in hydrogel matrix retained reversible sol-gel transition. Therefore, optimized concentration (5 wt. %) of additive was incorporated in 20 wt% hydrogel with 1 % drug loading.

(iv) Effect of PCL as additive

PCL of low molecular weight (Mw = 550) was utilized as a hydrophobic additive. PCL was selected to explore the role of hydrophobic interactions. In order to compare the effect of hydrophobic and hydrophilic additives on sol-gel transition and release profile of TM, similar methods followed for PVA were utilized for the hydrogel preparation and release study.

Drug Release Mechanisms

Drug release parameters were computed by three different methods utilizing First order, Higuchi and Korsmeyer equations. Release data were fitted into the model equations in order to determine release mechanism.

First order Equation:

It is applicable for modeling release of water soluble drug molecules from porous matrix.

$LnM_t = kt$

M_t represents the cumulative amount of drug released at time t, k is the release rate constant obtained by plotting LnM_t against time

Higuchi equation:

It is applicable for modeling drug release from matrix based system. It was initially developed for planer system but later extended to other systems.

$M_t = K_H t^{1/2}$

K_H denotes the higuchi release rate constant obtained by plotting cumulative percent drug released against the square root of time.

Korsmeyer-peppas equation:

$M_t / M_\infty = kt^n$

M_t and M_∞ represent the cumulative amount of drug released at a time t and at the equilibrium, respectively. The constant k is the kinetic constant and n is the release exponent that indicates the drug release mechanism. Values of $n < 0.5$ indicate Fickian (ideal) diffusion mechanism and values of $0.5 < n < 1.0$ suggest non-Fickian diffusion. When value of n is greater than 1.0, it represents case II transport or zero order release kinetics. Drug release data is employed to obtain the release exponent for $M_t / M_\infty \leq 0.6$. Release constant is computed by plotting log cumulative percentage drug release against log of time.

Cytotoxicity Studies

Cell viability studies were performed utilizing MTS assays in which novel tetrazolium compound, 3-(4, 5-dimethylthiazole-2-yl)-5- (3-carboxymethoxyphenyl)-2-(4-sulfophenyl)-2H-tetrazolium (MTS) was reduced into a colored formazan product by live cells. Rabbit primary corneal epithelial culture cells (rPCEC) were grown in the culture media comprising MEM, 10% FBS, HEPES, sodium bicarbonate, penicillin, and streptomycin sulfate. Cells were maintained under a humidified atmosphere of 5% CO_2 at 37°C and then sub cultured and seeded in 96-well culture plates at a density of 10,000 cells/well. After 24 h incubation, fresh media containing hydrogels of different concentrations ranging from 0.5 mg/ml to 20 mg/ml were added alone and with 5 wt% (PVA or PCL) polymeric additives. Triton X-100 (0.1%) was used as positive control while the blank (without treatment) was considered as negative control. Following 24 h incubation,

100 µL serum free medium containing 20 µL of MTS solution was added to the 96 well plates and were incubated at 37 °C and 5% CO_2 for 4 h. After incubation, the absorbance of each well was measured at 450 nm by an ELISA plate reader. Absorbance was directly proportional to viability of cells which was calculated by following equation.

$$\% \text{ cell viability} = \frac{(\text{Abs. of sample}) - (\text{Abs. of negative control}) * 100}{(\text{Abs. of positive control}) - (\text{Abs. of negative control})}$$

Statistical Analysis

All release experiments were conducted in triplicates and the results were reported as mean ± standard deviation. Statistical analysis of the effect of additives, molecular weight and drug loading on release rates were compared by one-way ANOVA. Statistical package for social science (SPSS) version 11 was used to compare mean of each group. A level of $p < 0.05$ was considered statistically significant in all cases.

Result and Discussion

Synthesis and Characterization of PEG-PCL-PEG

PEG-PCL-PEG was synthesized by ring opening polymerization reaction utilizing stannous octoate as the catalyst. ^{1}H NMR spectra (Fig. 3.2) shows two main peaks at 3.60 (-O***CH2CH2***-) and *4.06* (-O***CH2***CH2CH2CH2CH2CH2CO-) that corresponds to mPEG and PCL respectively, confirmed the formation of triblock polymer. Gel permeation chromatography analysis (Fig. 3.3) also points to (Table 3.1) narrow polydispersity between 1.41-1.47 and molecular weight between 5000-7000.

FT-IR spectrum (Fig. 3.4) indicated appearance of absorption band at 1526 cm^{-1} characteristic of –NH group and at 1732 cm^{-1} characteristic of C=O group, confirms the formation of triblock polymer. Absence of absorption band at 2270-2285 cm^{-1} due to –NCO stretching confirms complete conjugation of HMDI.

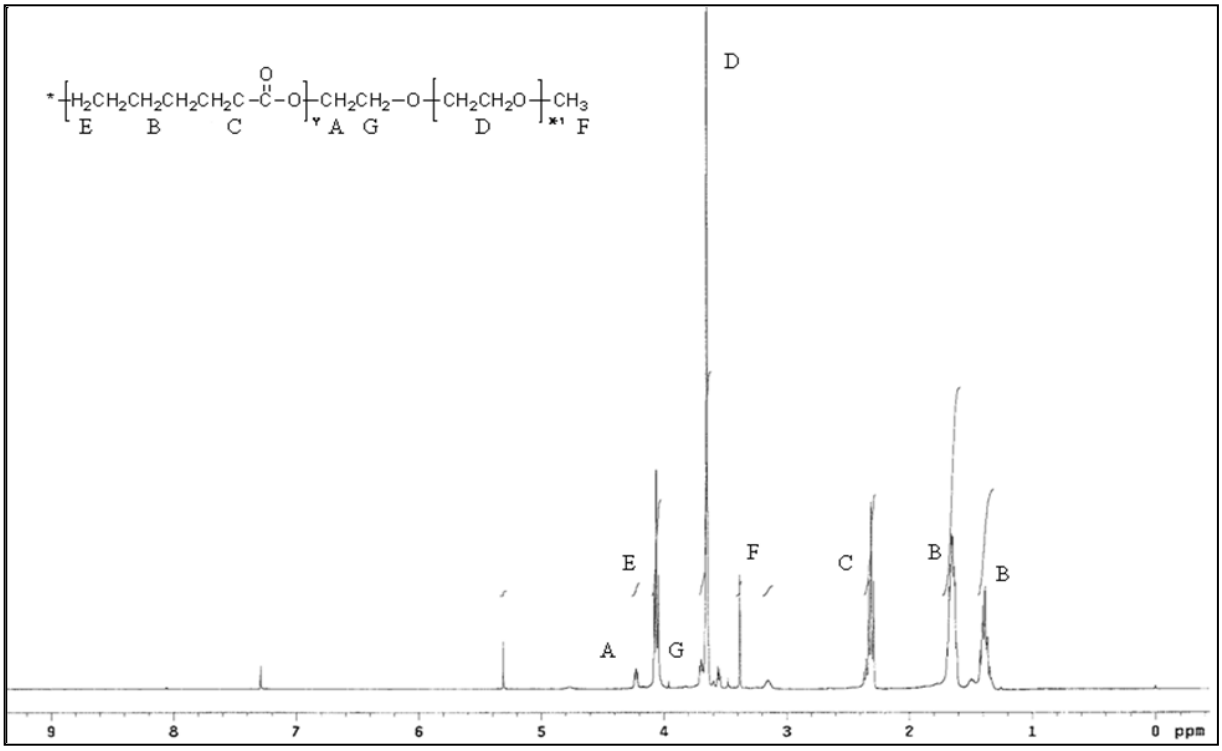

Figure 3.2 ^{1}H-NMR spectra of PECE copolymer in $CDCl_3$

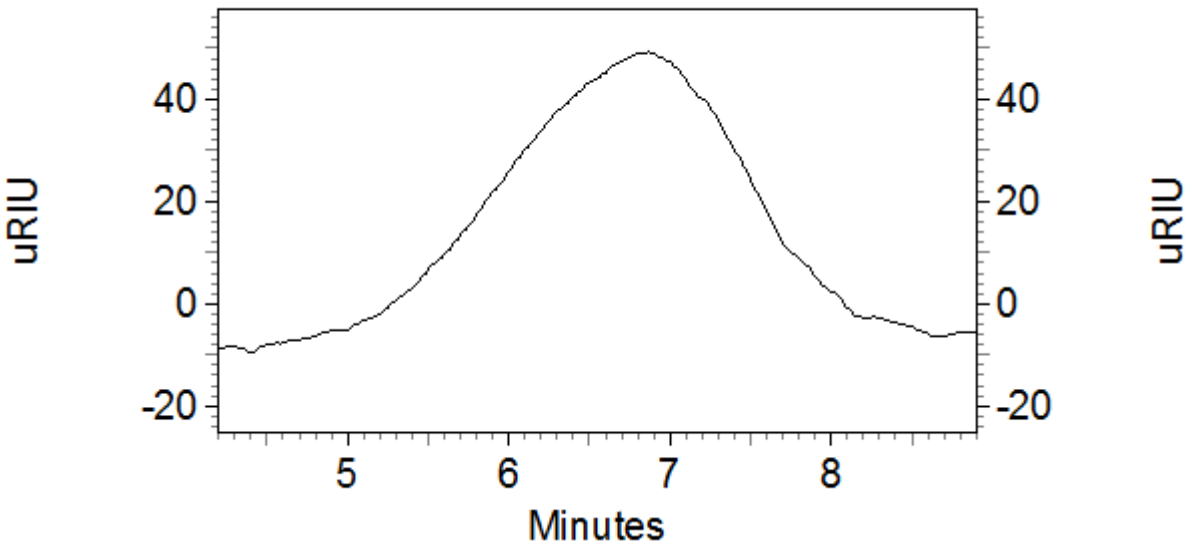

Figure 3.3 Gel permeation chromatogram of PCEC II

Table 3.1 Molecular weight distribution

Polymer	Total Mn (Theoretical)	Mn	Mw	Polydispersity
PEG_{750}-PCL_{3750}-PEG_{750}	5250	4568	6754	1.47
PEG_{550}-PCL_{2420}-PEG_{550}	3500	3995	5640	1.41

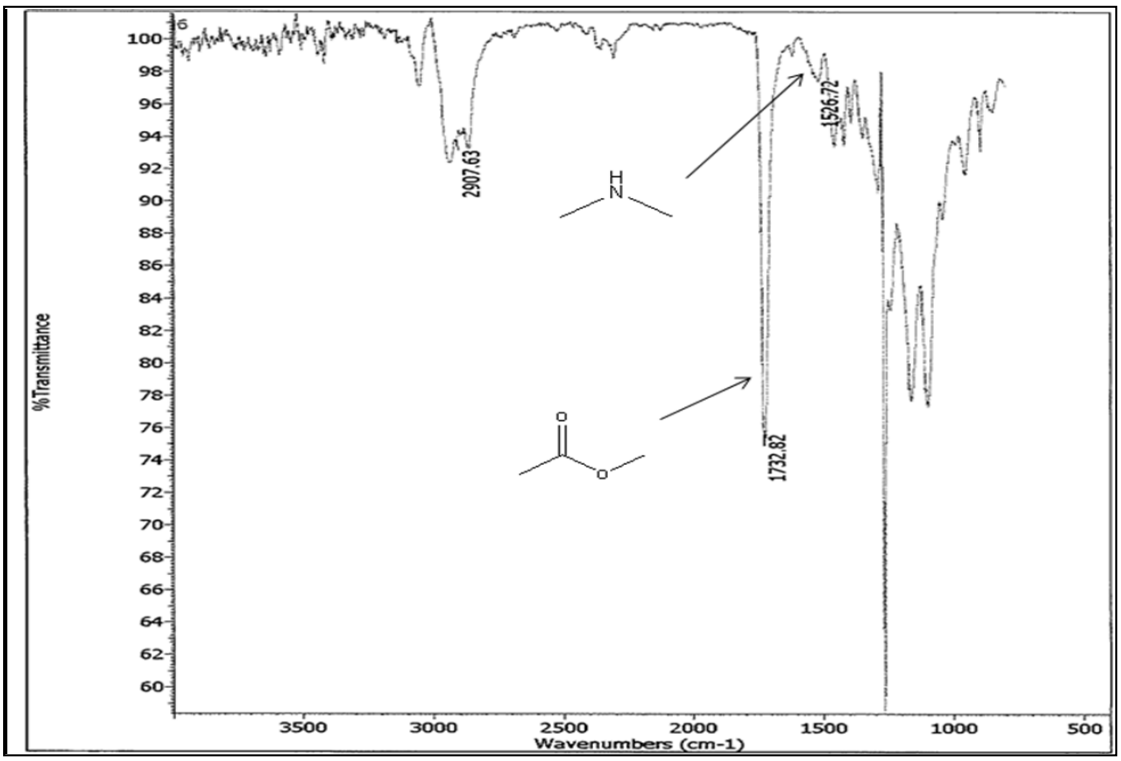

Figure 3.4 FTIR spectrum of PCEC II

Sol-Gel Transition Studies

Sol-gel transition studies revealed that PEG_{550}–PCL_{2420}–PEG_{550} (PCEC I) has 20 wt% critical gelling concentration (CGC) whereas PEG_{750}–PCL_{3750}–PEG_{750} (PCEC II) has CGC of 25 wt%. Such difference in CGC can be attributed to a difference in the hydrophilicity-hydrophobicity ratio between the two polymers. This observation is in agreement with findings of other investigators (Hwang et al., 2005). In this study, we evaluated the role of both hydrophilic and hydrophobic polymeric additives on sol-gel transition studies. Addition of PVA and PCL increased the viscosity of hydrogel and improved the gelling efficiency possibly by providing better packing of the gel matrix. We have observed that viscosity of 25 wt% PCEC II hydrogel alone was 0.51 ± 0.03 poise whereas incorporation of 5 wt% PCL and PVA in 20 wt% PCEC II has increased the viscosity of hydrogels to 0.83 ± 0.02 and 2.59 ± 0.04 poise, respectively. As shown in Figs. 3.5 and 3.6 both hydrophilic and hydrophobic additives have lowered the CGC of PCEC II. Addition of PVA (Fig. 3.5) in PCEC II decreased CGC from 25 wt% to 22 wt%. Previous studies reported that incorporation of PEG in the PCL based hydrogel lowers the CGC (Gong et al., 2009b). However, addition of PCL (Fig. 3.6) decreased CGC to 18 wt%. We observed more pronounced effect of PCL on sol-gel transition in comparison to PVA on PCEC II because PCL is a hydrophobic polymer and promotes better micellar aggregation for the formation of gel. However, addition of PVA or PCL in PCEC I did not produce any significant change in the sol-gel transition phenomenon. PCEC I was relatively more hydrophobic gel due to lower molecular weight of PEG block in comparison to PCEC II and have higher micellar aggregation tendency. Therefore, incorporation of additives did not further alter hydrophobic aggregation, which is the primary mechanism responsible for sol-gel transition.

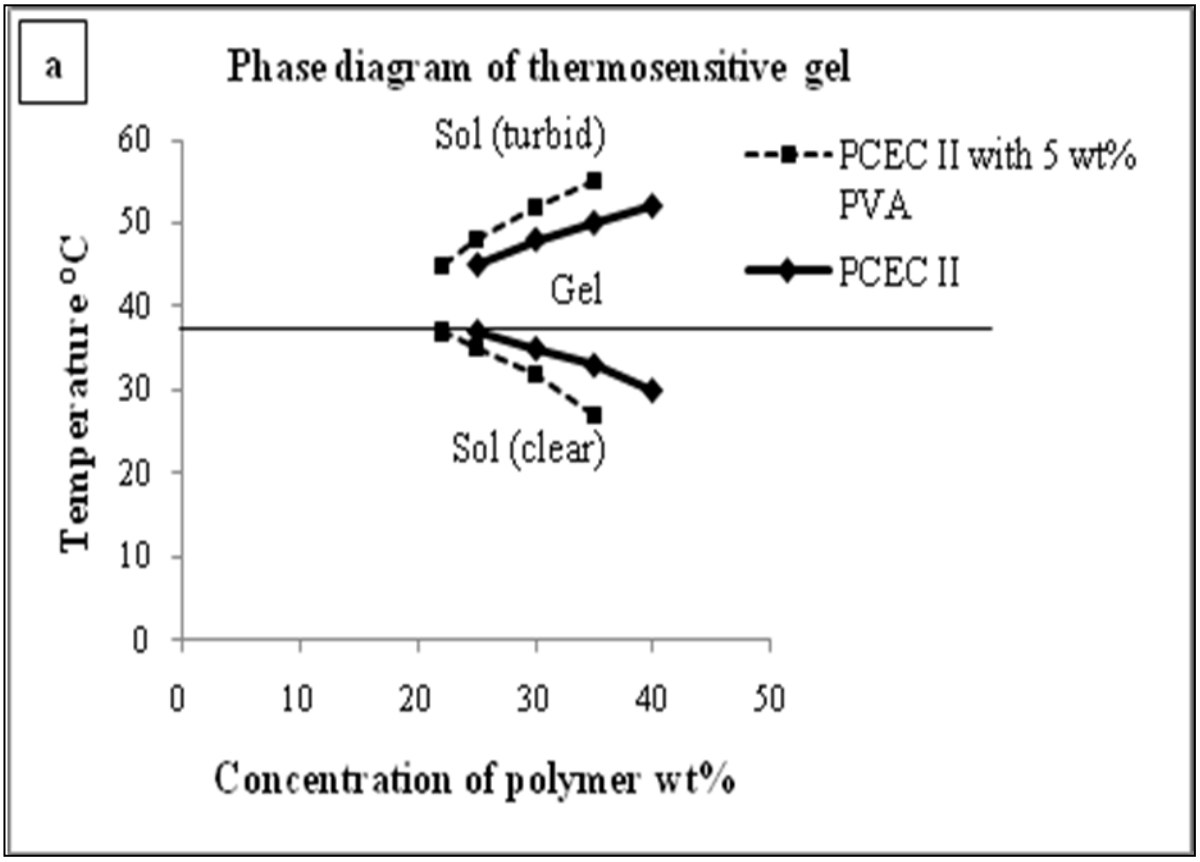

Figure 3.5 Sol-gel transition phase diagram PCEC II triblock copolymer aqueous solutions alone and with 5 wt. % PVA

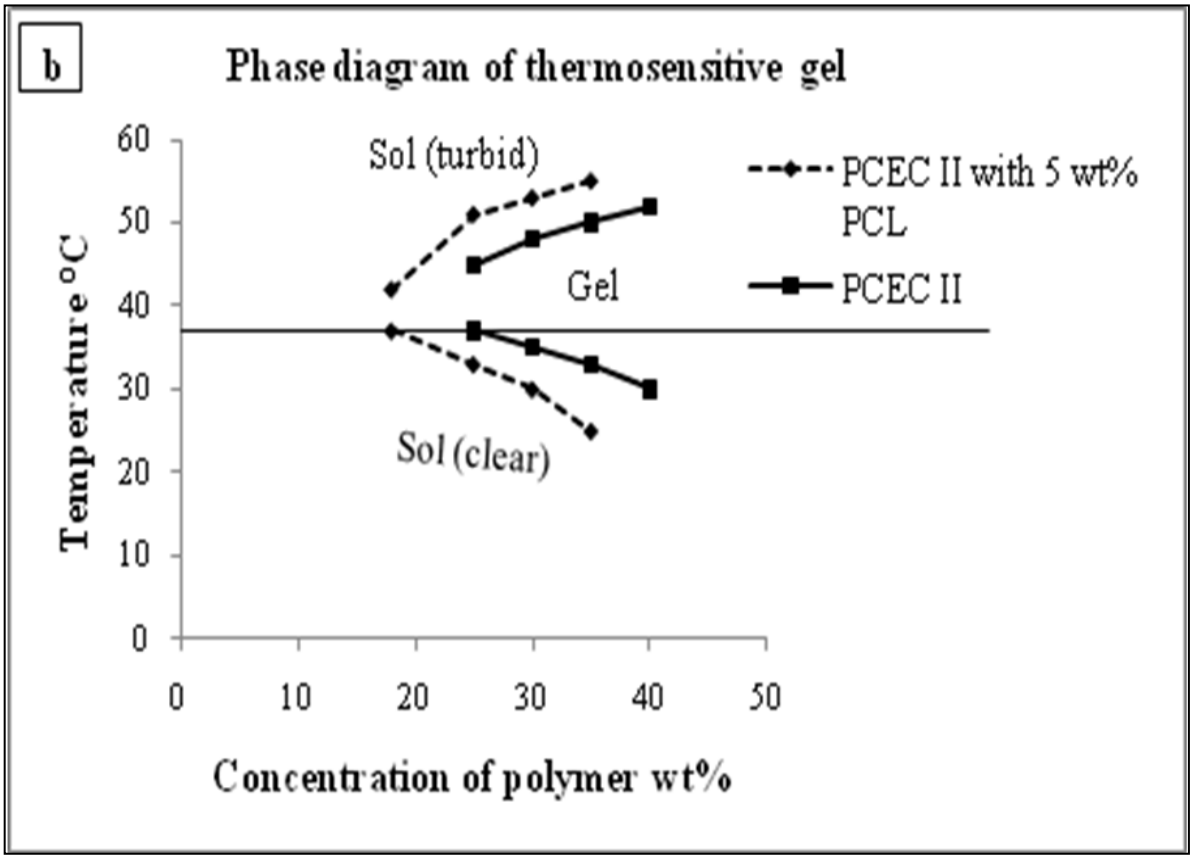

Figure 3.6 Sol-gel transition phase diagram PCEC II triblock copolymer aqueous solutions alone and with 5 wt. % PCL

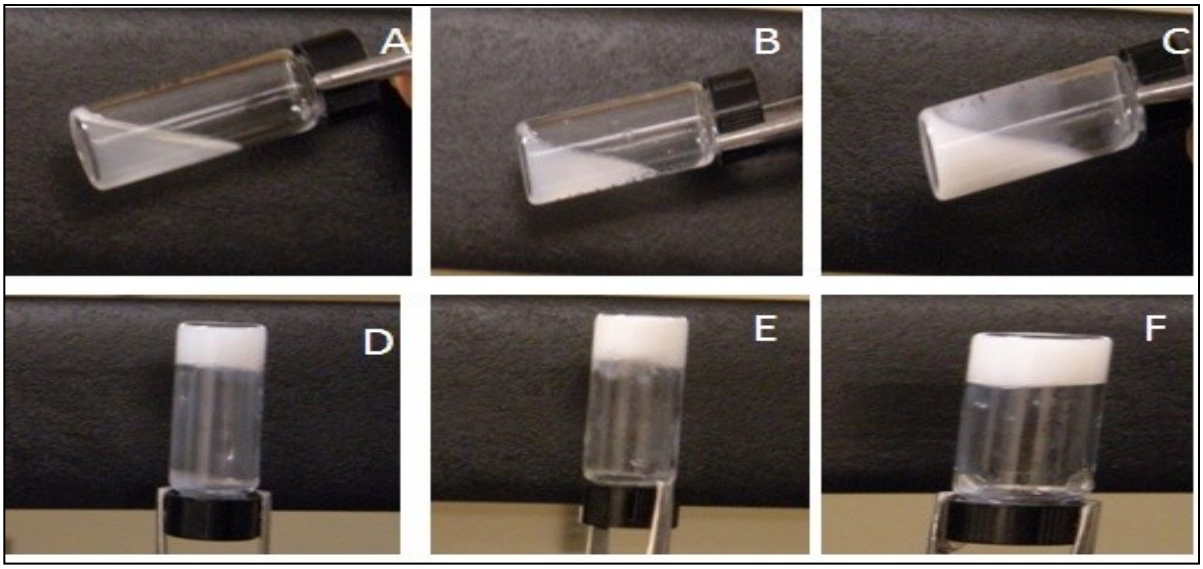

Figure 3.7 Photograph of PCEC-II at 25 °C (A) alone (B) with 5 wt. % PVA (C) with 5 wt. % PCL and at 37 °C (D) alone (E) with 5 wt. % PVA (F) with 5 wt. % PCL

Images in Fig. 3.7 illustrate that additives also reduced the transparency of the gel, which confirmed the formation of a denser gel matrix.

Fig. 3.8 shows the SEM of PCEC II alone and with PCL or PVA as additives. Fig. 3.8a represents the porous matrix of hydrogel alone at 37 °C. Addition of PVA provided less porous surface morphology (Fig. 3.8c) than PCEC II alone. We speculate that high molecular weight PVA uniformly cover the porous matrix of hydrogel and thereby may reduce the diffusion of drug molecules from the hydrogel matrix. However, addition of PCL promoted the aggregation of polymeric chains at 37 °C but did not alter the porosity of the hydrogel matrix (Fig. 3.8b) due to its low molecular weight.

In Vitro Release Studies

We investigated the effect of different parameters such as molecular weight, drug loading, hydrogel concentration and polymeric additives on the release profile of TM form the hydrogel matrix.

(i) Effect of molecular weight

Release of TM from the hydrogel matrix depended on the molecular weight of polymer ($p < 0.05$) as shown in Fig. 3.9. Release rate of TM was slower with PCEC II (MW = 5250) than PCEC I (MW = 3500). For instance, in the first 48 h cumulative percentage drug release from PCEC I was 78.0 ± 2.8% whereas in PCEC II it was 41.3 ± 2.3%. The reason for this behavior can be attributed to higher molecular weight of PCEC II with relatively longer PCL block length that may have restricted the permeation of water molecules across the polymeric matrix. Hence, slower hydration of gel resulted in decreased diffusion coefficient of the drug across the hydrogel matrix. These results suggest that the release rate

of TM may have been affected by two major factors i.e. hydrophilic/hydrophobic balance and total molecular weight of the polymer. TM (pK_a 9.2) exists predominantly in ionized from at pH 7.4. We have observed that addition of PVA or PCL did not change the pH (7.4) of aqueous polymeric solution and pH of release medium was constant due to extremely slow degradation of PCL.

(ii) Effect of drug loading and hydrogel concentration

Fig. 3.10 suggested that no statistically significant difference in release rate of TM was observed with two different concentrations i.e. 0.5 to 1.0 wt% in 25 wt% PCEC II hydrogel, due to higher aqueous solubility of TM. Other studies also reported minor change in release rates of hydrophilic molecules with higher drug content in the hydrogel (Huynh et al., 2009; Zhang et al.). It was reported that physicochemical property of the active drug such as charge, hydrophilicity and molecular size also affects the release rate (Henke et al., 2010; Kim et al., 1992; Makino et al., 2001). Hydrophilic drug molecules tend to partition in the PEG domain of the hydrogel whereas hydrophobic drug molecules partition into PCL core. Therefore, TM disperses in PEG domain and easily diffused out in the release medium irrespective of drug

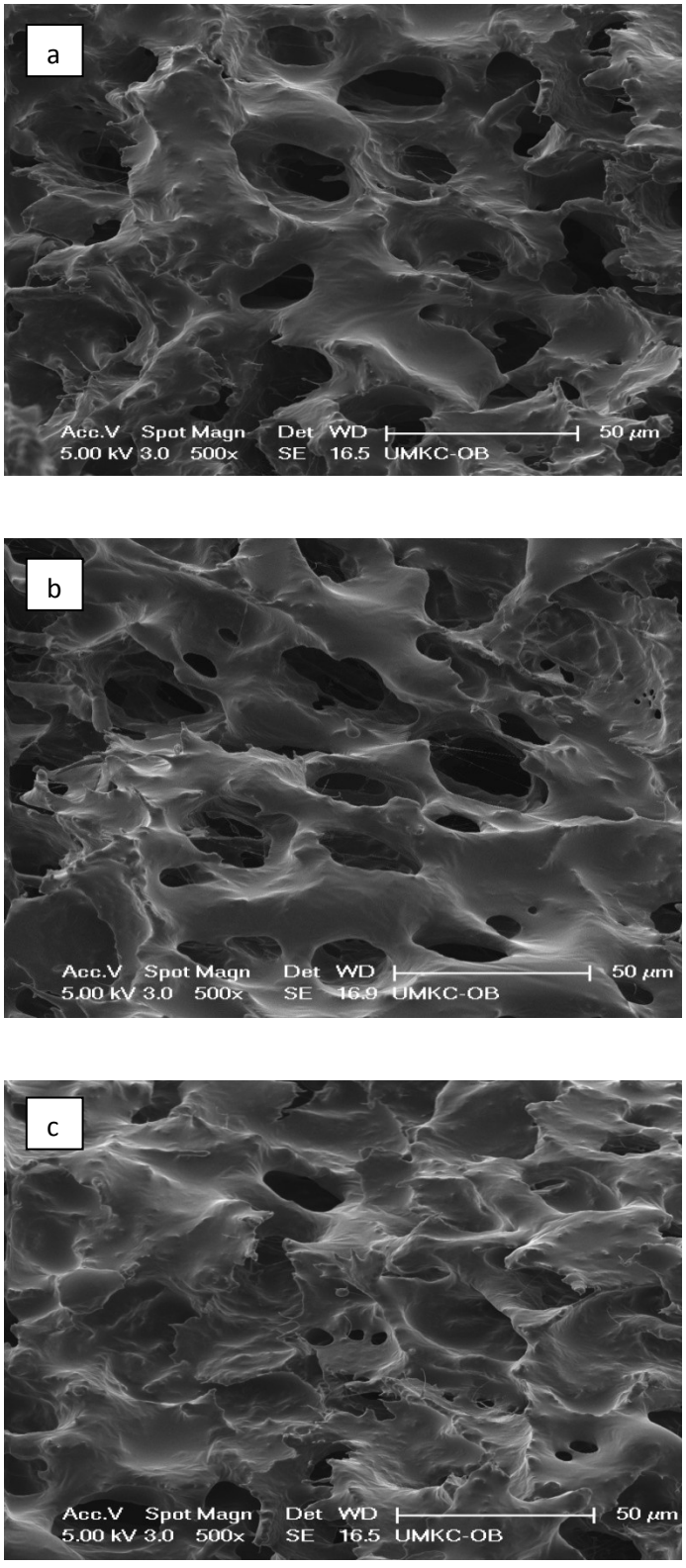

Figure 3.8 SEM of PCEC-II (a) alone (b) with 5 wt. % PCL (c) with 5 wt. % PVA

loading. Hydrogel concentration played a significant role in TM release. Release of TM from 25 wt% polymer is slower than 20 wt% due to volume effect of gel (data not shown). Since 25 wt% hydrogel forms a dense matrix, 20 wt% was selected for the incorporation of different polymeric additives to observe the effect of polymeric additives on the diffusion process.

(iii) Effect of Polyvinyl alcohol as additive

PVA is a long chain synthetic polymer incorporated in ophthalmic formulations as additive. It acts as a wetting agent and reduces surface and interfacial tension (Reddy Ik et al., 1996). Moreover, addition of PVA is advantageous due to its biocompatibility with ocular tissues. Addition of PVA may reduce the burst release by promoting hydrophobic aggregation of the polymer chains in the gel matrix. Therefore, we have selected PVA as an additive. Fig. 3.11 illustrates that release of TM was altered by PVA ($p < 0.05$). Incorporation of PVA in the hydrogel matrix lowered TM release from 86.4 ± 0.8% to 73.7 ± 1.8% in 316 h. Moreover, it was observed that burst release in initial 24 h significantly minimized to 22.3 ± 1.9% from 44.9 ± 0.4% in presence of PVA. The effect of different percentage of PVA on release profile of TM was also evaluated. In case of 1 wt% PVA any significant difference was not noticed in release profile (data not shown). However, as shown in Fig. 3.11, 5 wt% PVA caused drug release rate from hydrogel to be significantly reduced in the initial phase. Slower drug release from 5 wt% PVA added hydrogel may be accounted by restricted diffusion of TM than hydrogel alone.

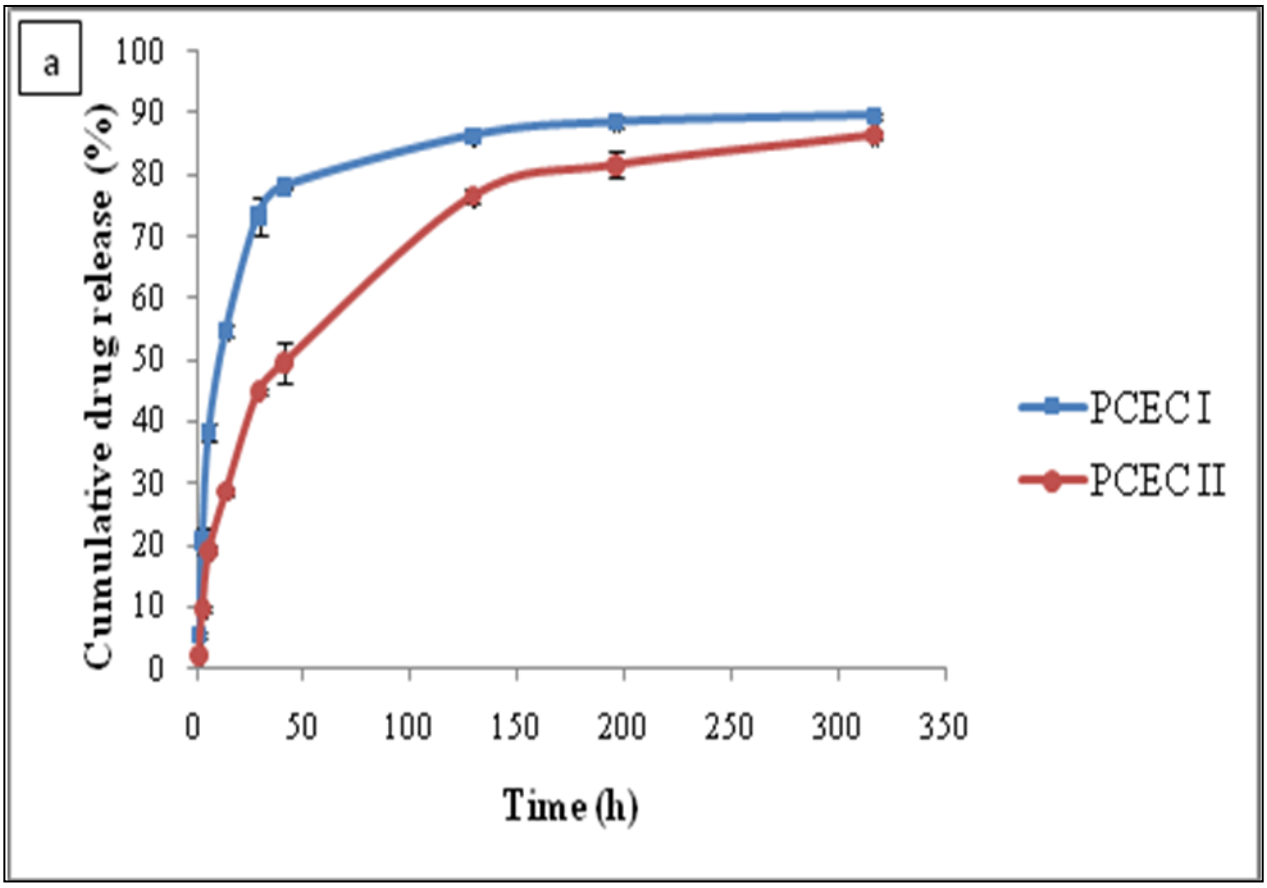

Figure 3.9 *In vitro* release of TM from PCEC I and PCEC IIbtriblock copolymer (25 wt. %) hydrogel in PBS buffer (pH 7.4) at 37 °C. The values are represented as mean ± standard deviation of n=3

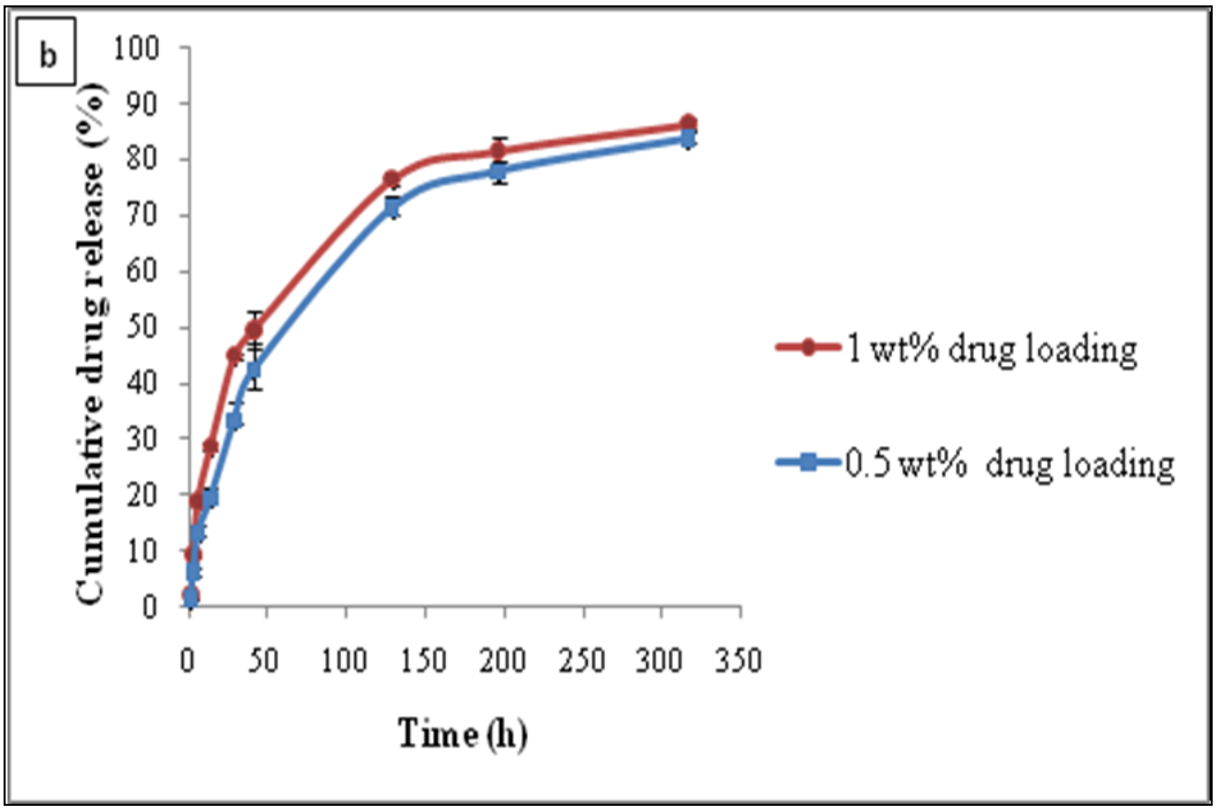

Figure 3.10 *In vitro* release of TM 0.5 wt. % and 1.0 wt. % from PCEC II triblock copolymer (25 wt%) hydrogel in PBS buffer (pH 7.4) at 37 °C. The values are represented as mean ± standard deviation of n = 3

This mechanism of aggregation was also evaluated previously. A study reported that PVA as additive promoted the gelling of methylcellulose based hydrogel. This study suggested the role of PVA as a cosolute, which was dominant over pseudo-surfactancy effect of other additives (Kundu P, 2003). Therefore, in this study, long chain PVA molecules had successfully modulated the drug release profile.

(iv) Effect of Polycaprolactone as additive

Release of TM from hydrogel depends on diffusion and degradation mediated processes. However, degradation of PCL based hydrogel is extremely slow (Jiang et al., 2009). In order to modulate diffusion mediated release by hydrophobic additive, low molecular weight PCL (Mw = 550), was incorporated in the hydrogel matrix. In this study, first we tried to incorporate the high molecular weight PCL but due to more hydrophobicity it was not soluble in the hydrogel polymeric matrix. Therefore, we utilized low molecular weight PCL, which can be easily solubilized in the hydrogel solution. To elucidate the role of PCL and compare the TM release profile with PVA added hydrogel, 5 wt% PCL was selected as additive for the release study. As shown in Fig. 3.12, release rate was not affected by the addition of PCL and no statistically significant difference was observed with 5 wt% PCL. We presume that PCL being a hydrophobic polymer tends to partition with hydrophobic block of hydrogel. However as we discussed earlier majority of TM disperses in the hydrophilic block therefore addition of PCL did not significantly modulate the release of TM. Other attempts of dissolving higher percentage of PCL remain unsuccessful due to excessive hydrophobic interactions.

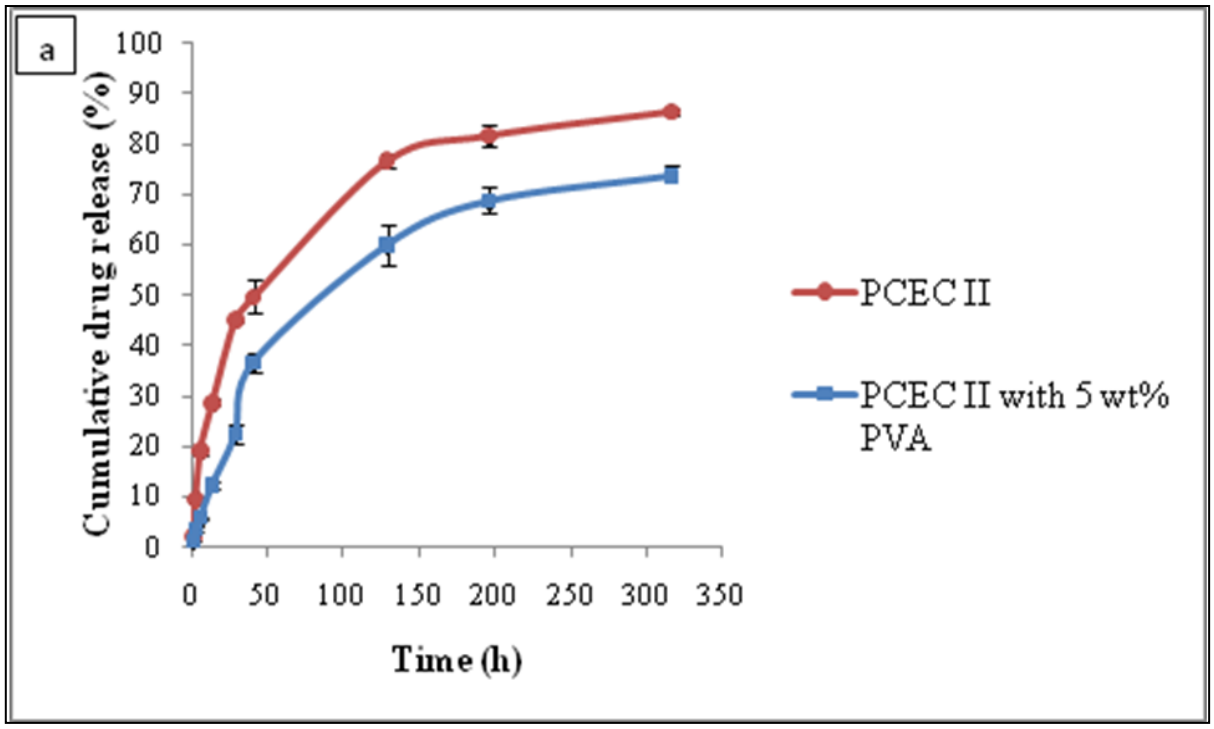

Figure 3.11 *In vitro* release of TM from PCEC II (25 wt. %) and PCEC II (20 wt. %) with 5 wt. % PVA hydrogel in PBS buffer (pH 7.4) at 37 °C. The values are represented as mean ± standard deviation of n = 3

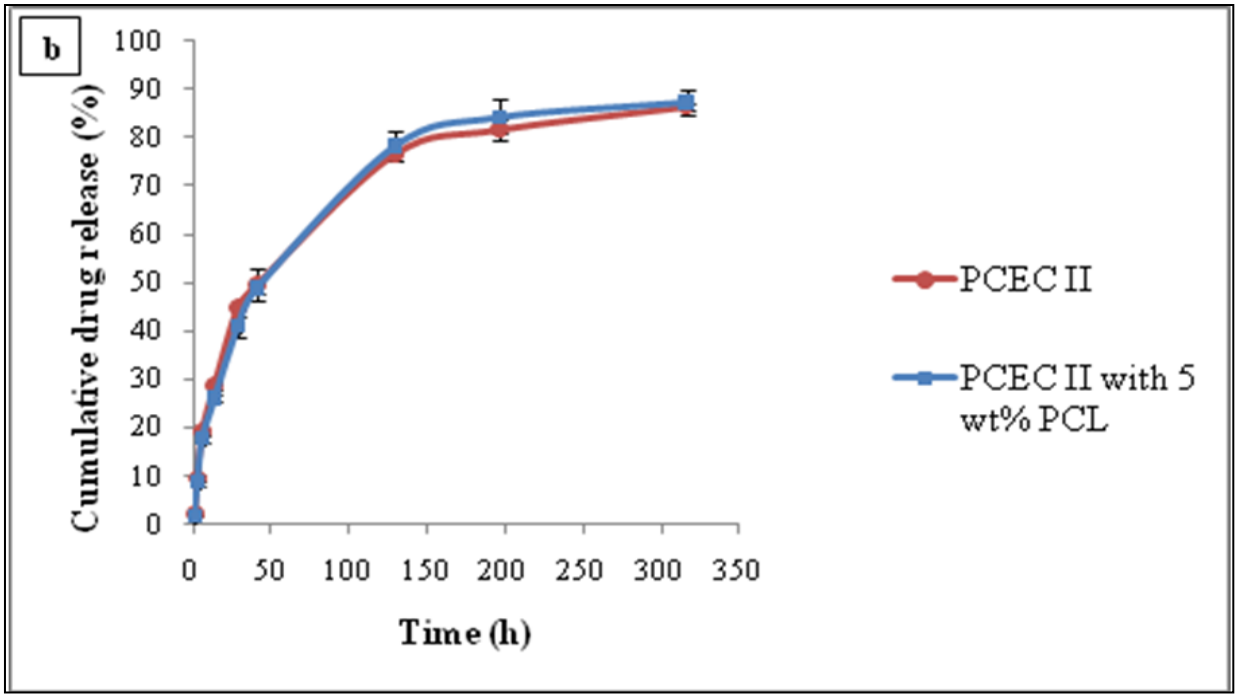

Figure 3.12 *In vitro* release of TM from PCEC II (25 wt. %) and PCEC II (20 wt. %) with 5 wt. % PCL hydrogel in PBS buffer (pH 7.4) at 37 °C. The values are represented as mean ± standard deviation of n = 3

Drug Release Kinetics

Drug release from hydrogel generally follows diffusion/degradation or a combination (Wu and Chu, 2008). Analysis of drug release kinetics, as shown in Table 3.2, correlated well with Higuchi and Korsmeyer models. This observation suggests that drug release depended primarily on diffusion from the hydrogel matrix rather than on bulk erosion process of the polymer (first order). In addition, analysis of first 60% release data, according to Korsmeyer model suggested that addition of polymeric additives (PVA or PCL) can significantly lower the release rate constant. However, the effect of PVA on release kinetics was more pronounced than PCL. In hydrogel alone K_{KP} value was 3.03 whereas with PVA, K_{KP} was found to be 1.368 and for PCL it was 2.455. A diffusion exponent $0.685 < n < 0.869$ suggest anomalous diffusion mechanism from all the matrixes.

Cytotoxicity Studies

Cell viability response showed that PCEC-II alone and in presence of 5% additives is not toxic to rPCEC cells. Fig. 3.13 and 3.14 suggested that cytotoxicity of hydrogel was concentration dependent. However, at low concentrations no statistically significant difference from control was observed. Cell viability studies suggest that polycaprolactone based hydrogels alone and with polymeric additives are biocompatible with the corneal epithelial cells. Similar results were reported with human lens epithelial cells (HLECs) (Yin et al., 2010).

Table 3.2 Kinetic parameters

Polymer	First order		Higuchi		Korsmeyer-Peppas		
	r^2	k_o (h^{-1})	r^2	k_H ($h^{-1/2}$)	r^2	K_{KP} (h^{-n})	n
PCCE-I	0.298	0.0046	0.702	4.433	0.923	7.889	0.685
PCEC- II	0.425	0.0071	0.923	5.154	0.941	3.033	0.819
PCEC- II + PCL	0.428	0.0078	0.933	5.382	0.933	2.455	0.869
PCEC -II + PVA	0.560	0.0092	0.961	4.811	0.995	1.368	0.852

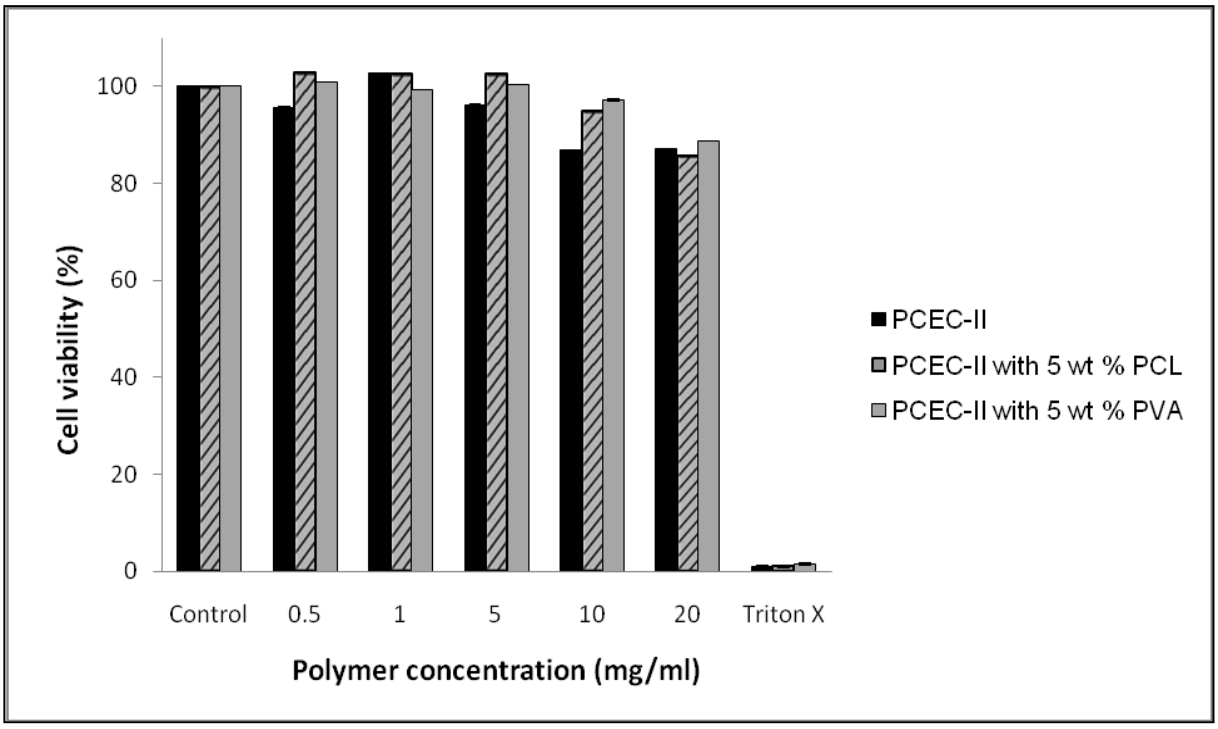

Figure 3.13 Rabbit primary corneal epithelial culture cell (rPCEC) viability study. Cell survival decreased with increase of concentration of PECE hydrogel. The values are represented as mean ± standard deviation of n = 6

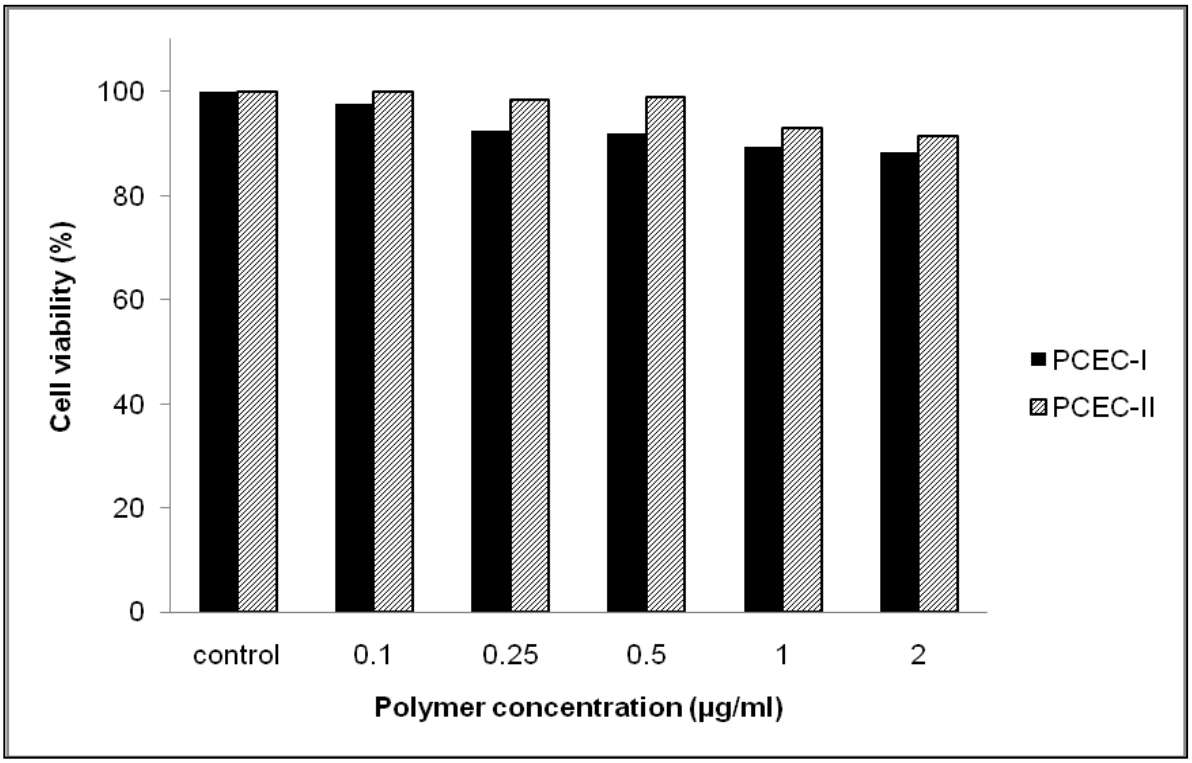

Figure 3.14 Rabbit primary corneal epithelial culture cell (rPCEC) viability study performed on two different compositions. Cell survival decreased with increase of concentration of PECE hydrogel. The values are represented as mean ± standard deviation of n = 6

Conclusions

PEG-PCL-PEG of different compositions was synthesized. The additives strategy was applicable to modulate the sol-gel transition and TM release kinetics from hydrogel. Effect of PCL on the CGC was more pronounced than PVA. Release of TM was sustained longer in case of high molecular weight PCEC II. PVA as additive played a dominant role in regulating drug release kinetics whereas no significant difference in release was observed with PCL. Cell viability studies confirmed that hydrogel alone or in presence of polymeric additives was biocompatible to corneal epithelial cells. Therefore additive based drug delivery may be a promising strategy for optimizing sustained drug delivery systems in the treatment of ocular hypertension and glaucoma.

CHAPTER 4

SYNTHESIS AND CHARACTERIZATION OF NOVEL THERMOSENSITIVE PENTABLOCK HYDROGELS FOR CONTROLLED DRUG DELIVERY

Rationale

In past decade bioresponsive hydrogels have gained significant momentum in drug delivery and tissue engineering. In particular, temperature responsive drug delivery systems have been explored widely for drug delivery applications. Thermogelling polymers exhibit unique reversible sol-gel transition behavior which can be utilized for *in situ* depot formation. Polymeric aqueous solution remains in solution state below body temperature and form a gel depot *in situ* at body temperature (He et al., 2008; Klouda and Mikos, 2008). Thermosenstive hydrogels demonstrate unique properties such as ease of application, high drug loading and controlled drug delivery (Nguyen and Lee et al., 2010).

In recent years considerable attention has been focused on developing a block copolymer of amphiphillic character composed of hydrophobic and hydrophilic constituents. Thermoresponsive hydrogel composed of hydrophilic PEG and hydrophobic polyesters have shown potential for pharmaceutical and clinical applicable because of their biocompatible and bioresorbable nature (He et al., 2008; Yu and Ding, 2008).

Block copolymers of ABA or BAB type, where A and B represents hydrophobic and hydrophilic block respectively, have been reported to demonstrate temperature sensitive phase transition. Triblock polymers of ABA type includes PLGA–PEG–PLGA and PCL–PEG–PCL (Duvvuri et al., 2005; Gong et al., 2009c; Qiao et al., 2005).

Subsequently the next generation of triblock polymers of BAB type such as polyethylene PEG-PLLA-PEG and PEG-PCL-PEG were reported (Gou et al.; Hwang et al., 2010; Hwang et al., 2005; Li et al., 2007; Yin et al.).

More recently pentablock polymers having dual-stimuli responsive behavior have been evaluated for drug delivery. Polymers such as poly(β-amino ester)–poly(ε-caprolactone)–poly(ethylene glycol)–poly(ε-caprolactone)–poly(β-amino ester) and poly(2-diethylaminoethylmethyl-methacrylate)–poly(ethylene oxide)–poly(propylene oxide)–poly(ethylene oxide)–poly(2-diethylaminoethyl-methyl methacrylate) were reported to show pH sensitive thermogelling properties (Huynh et al., 2009; Huynh et al., 2008).

PCL or PLA based block copolymers have primarily diffusion mediated drug release due to extremely slow degradation. So we have developed novel pentablock copolymers with optimum degradation rate and achieved zero order drug release via both diffusion and degradation mediated pathway. These copolymers are amphiphilic in nature which assist in optimizing the release profile of therapeutic molecules by varying the molecular weight of hydrophilic and hydrophobic blocks. Moreover, we can control the hydrolytic degradation of pentablock copolymers that will preserve the drug molecules.

PCL is a biodegradable and biocompatible polymer approved by FDA for application in drug delivery systems and medical device. Recent studies have explored the applications of PCL based hydrogel in sustained release formulations. PCL based triblock polymer i.e. PEG-PCL-PEG remains in solution state at room temperature (25 °C) and forms a transparent gel at body temperature (37 °C). However, PCL degrades slowly and posses higher crystallinity. Considering this we have incorporated PLA block in the center of PEG-PCL-PEG, in an attempt to accelerate degradation rate of highly crystalline and hydrophobic

PCL block. We hypothesized that incorporation of PLA will promote degradation mediated drug release. Therefore, we have developed novel pentablock copolymers by introducing faster degrading polymeric block.

We have optimized the ratio of PCL and PLA in the novel pentablock (PEG-PCL-PLA-PCL-PLA) copolymer. We have investigated the effect of molecular weight and PCL/PLA block length ratio on the sol-gel transition and *in vitro* release kinetics of different molecules of varying size and polarity. We have synthesized several compositions of different molecular weight and block length ratio. Two composition PGPCPL-1 (PEG_{550}-PCL_{550}-PLA_{550}-PCL_{550}-PEG_{550}) and PGPCPL-2 (PEG_{550}-PCL_{825}-PLA_{550}-PCL_{825}-PEG_{550}) have demonstrated sol-gel transition in the physiological temperature range. Other compositions with different hydrophobic /hydrophilic block length ratio did not demonstrate the desired sol-gel transition in the physiological temperature range. Therefore we have selected these two compositions for further studies.

Materials and Methods

Monomethoxy polyethylene glycol (mPEG) (M_w=550), ε-caprolactone, L-Lactide (L-Lactide) stannous octoate, ofloxacin and prednisolone were received from Sigma-Aldrich. Hexamethylene diisocyanate (HMDI) were obtained from Acros Organics. All other reagents utilized for the study are of analytical grade.

Synthesis of PEG-PCL-PLA-PCL-PEG

mPEG-PCL diblock polymer was synthesized by ring opening polymerization of ε-caprolactone utilizing mPEG 550 as initiator and stannous octoate as catalyst. The diblock polymer was further reacted with L-lactide to from triblock polymer PEG-PCL-PLA. The

triblock polymer was further coupled using hexamethylene diisocyanate (HMDI) as a coupling agent, and the reaction was performed for 8 hours to synthesize final pentablock polymer (Fig. 4.1) PEG-PCL-PLA-PCL-PEG. The resulting final polymer was purified by dissolving in methylene chloride followed by precipitation in petroleum ether.

Briefly for the synthesis of PEG-PCL-PLA-PCL-PEG, the mPEG was dried under vacuum for 3 h before copolymerization. Then calculated amount of mPEG (0.01 mol), ε-caprolactone (0.06 mol) and stannous octoate (0.5 w/w % of monomer concentration) were added to the reaction mixtures in a round bottom flask. The reaction was performed for 24 h at 130 °C. Then polymer was dissolved in methylene chloride and purified by fractional precipitation with petroleum ether. The purified product was vacuum dried for 48 hrs to remove residual solvent. For the synthesis of triblock copolymer, the diblock copolymer was taken in a round bottom flask and L-lactide (0.01 mol) was added to it. Reaction was performed for 24 hours at 130 °C. Then coupling of triblock polymer was performed by adding HDMI (0.01 mol) and reaction was continued for 6 hours at 60 °C. The final polymer was dissolved in 20 ml of methylene chloride and purified by precipitation with petroleum ether. The purified product was vacuum dried for 48 h to remove residual solvent.

Characterization of Polymeric Material

(i) ^{1}H NMR Spectroscopy

The copolymer compositions and structures were characterized by ^{1}H NMR spectroscopy. $CDCl_3$ was utilized as solvent and TMS as internal standard for obtaining NMR spectra using Varian 400-MHz NMR spectrophotometer.

(ii) FT-IR Spectroscopy

The IR spectrum was obtained using Nicolet-100 Infrared Spectrophotometer at a resolution of 4 sec^{-1} with 16 scans. The copolymer samples were dissolved in methylene chloride and casted on KBr Plates.

(iii) GPC

Molecular weights and molecular weight distributions of pentablock copolymer were determined by GPC utilizing Shimadzu RID-10A detector. Styragel® HR 3 column at 40 °C was utilized for analysis. Tetrahydrofuran was utilized as an eluting solvent at a flow rate of 1 ml/min. GPC system was calibrated with polystyrenes standards.

Phase transition studies

The phase transition behavior of aqueous co-polymeric solution was investigated from 10 to 55 ^{o}C by test tube inverting method with an increment temperature of 2 ^{o}C. The copolymer was dissolved in PBS (pH 7.4) and then incubated for 12 h at 4 ^{o}C. The glass vials with an inner diameter of 12 mm was immersed in the water bath for 20 min followed by inversion. Gel state was regarded as condition of no flow within 30 sec of inversion. The transition temperature was an average of three subsequent measurements.

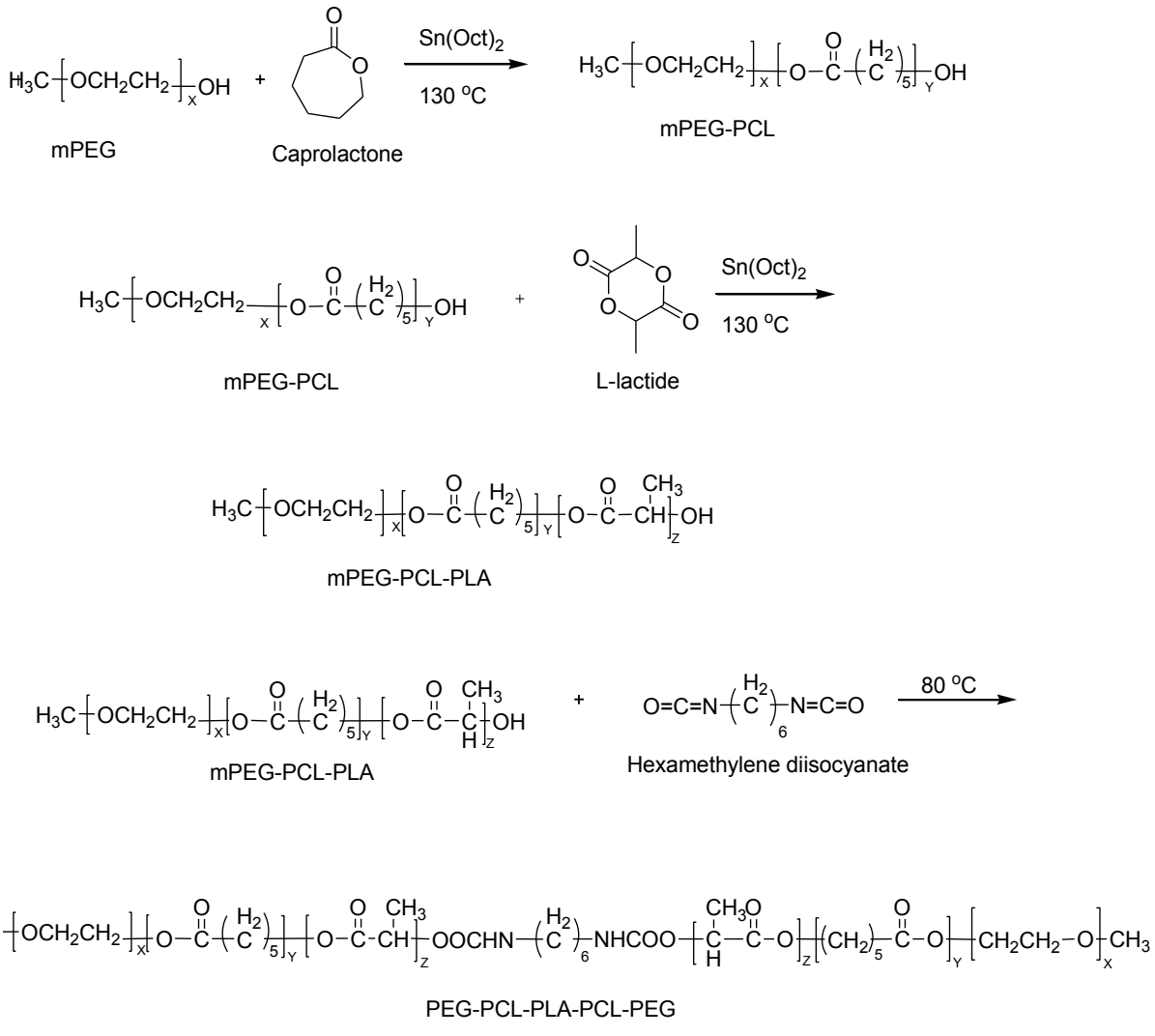

Figure 4.1 Synthetic scheme of PEG-PCL-PLA-PCL-PEG

Determination of critical micelle concentration (CMC)

Dye solubilization method was employed to study the CMC of two different compositions. DPH (1,6-Diphenyl -1,3,5-hexatriene) (0.4 mM) was solubilized in methanol. Then dye was added in to copolymer solutions in the concentration range of 0.0001 - 0.5 wt. % followed by equilibration for 8 h at 25 °C. UV spectra were recorded in the 330-430 nm range. CMC was determined by plotting the difference in absorbance at 378 nm and 400 nm against logarithmic concentration of copolymers.

Morphology of Hydrogels

Scanning electron microscopy (SEM) studies were performed to characterize the surface morphology of hydrogel. The copolymer aqueous solution after gel formation was frozen at -80 ^{o}C for 2 hrs and freeze dried under vacuum at -42 °C for 48 h. The lyophilized sample was mounted on the metal stubs utilizing double adhesive carbon taps and then sputtered with gold palladium at 0.6 kV. The sample was analyzed by FEG ESEM electron microscope at a resolution of 4,000 X.

In vitro release studies

Prednisolone acetate and ofloxacin was utilized as model drugs of varying lipophilicity for *in vitro* release studies. Similar protocols for release study were followed for both drugs. 10 mg of drug (1% w/w) was added into 2 ml of 25% w/w aqueous polymeric solution at room temperature and vortexed thoroughly to ensure uniform mixing of drug into the polymeric solution. Then 500 µl of polymeric solution was injected into the glass vial of 12 mm internal diameter. The polymeric solution was incubated for at 37 °C to form clear gel matrix. After 10 min, 5 ml of the release medium containing 0.01 M phosphate buffer (PBS) pH 7.4 was added to each vial. The vials were kept at 37 °C with a stroke rate of 20 rpm. At

designated interval 4 ml of release medium was removed and replaced with similar volume of fresh release medium to ensure maintenance of sink condition during the entire release duration. The samples were analyzed by high performance liquid chromatography (HPLC) method as mentioned below. All studies were performed in triplicates.

HPLC Method of Analysis

Prednisolone acetate samples were analyzed by HPLC (Shimadzu, Japan) with a phenomex C_{18} column at a flow rate of 1 ml/min. The mobile phase was composed of 0.1 % trifluoroacetic acid and 40% acetonitrile with pH adjusted to 2.5. PA was measured at 254 nm. All experiments were conducted in triplicate. For the analysis of Ofloxacin, mobile phase composed of 20 mM potassium dihydrogen phosphate and 40% acetonitrile with 0.1 % glacial acetic acid was utilized. Analysis was performed at 318 nm and a flow rate of 1ml/min using phenomex C_{18} column. All observations were recorded in triplicates.

Differential Scanning Calorimetry Analysis

Thermal properties of two different compositions of pentablock copolymer, PGPCPL-1and 2 were evaluated by DSC (TA instruments). Analysis was performed in the temperature range of 10-60 °C. Both the samples were analyzed at the heating and cooling rate of 5 °C/min.

X-Ray Diffraction Analysis

Crystallinity of both the polymeric compositions were evaluated by MiniFlex automated X-ray diffractometer (Rigaku, The Woodlands, Texas). Radiation was Ni-filtered and generated through Cu-kα at 30 kV and 15 mA. The analysis was performed at room temperature. Samples were scanned from 10-60° at a scan rate of 5°/min.

Cell viability studies

Cell viability studies were determined by MTS assay. Cell proliferation assay measures the conversion of 3-(4,5-dimethylthiazol-2-yl)-5-(3-carboxymethoxyphenyl)-2-(4-sulphophenyl)-2H-tetrazolium compound to colored formazen product by dehydrogenase enzyme in the metabolically active living cells. rPCEC and ARPE 19 were grown in the culture media comprising MEM, 10% FBS, HEPES, sodium bicarbonate, penicillin, and streptomycin sulfate. Cells were maintained under a humidified atmosphere of 5% CO_2 at 37°C. Cells were sub cultured and seeded in 96-well culture plates at a density of 10,000 cells/well. After 24 h of incubation, fresh medium containing hydrogel of different concentrations ranging from 0.5 mg/ml to 20 mg/ml were added. Following 24 h incubation, 100 µL of serum free medium containing 20 µL of MTS solution was added to the 96 well plates and these plates were incubated at 37 °C and 5% CO_2 for 4 h. After incubation, the absorbance of each well was measured at 450 nm by the ELISA plate reader.

Result and Discussion

Synthesis and Characterization of Polymer

Pentablock polymers were synthesized successfully. The ^{1}H NMR spectra (Fig. 4.2) confirmed the composition of final polymer. The ratio of mPEG, ε-caprolactone and L-lactide were computed through proton integration ratio of methylene proton at 3.65, 4.13 and 5.10 respectively.

GPC analysis revealed molecular weight and molecular weight distribution were in the range of 5260-6925 and 1.3-1.7 respectively. The unimodal GPC distribution of copolymer suggested successful coupling of mPEG-PCL-PLA by HDMI. Table 4.1 illustrates the molecular weight of pentablock copolymers employed for the study.

FT-IR analysis (Fig. 4.3) confirmed the structure of pentablock polymer. A weak C=O stretching at 1736 cm^{-1} confirms the formation of ester bond and absence of absorbance at 2270-2285 cm^{-1} indicates the complete reaction of –NCO group in HDMI. Further, N-H bending vibration at 1540 cm^{-1} confirms the formation of urethane group in pentablock copolymer.

Phase Transition Studies

Aqueous solution of pentablock copolymers exhibited sol-gel transition response upon increasing the temperature in a concentration range of 10-30 wt%. The phase diagram (Fig. 4.4) revealed that the critical gel concentration (CGC) showed solution to gel state conversion at 37 °C.

Sol-gel transition of two different copolymers of varying ε-caprolactone and L-lactide ratios suggested that upon increasing the block length of PCL, CGC decreased from 20 to 18 wt%. These results suggested that increasing ε-caprolactone to the L-lactide ratio with similar block length of mPEG resulted in lowering the CGC and increasing the stability of gel at higher temperature. The decrease in CGC was attributed to better micellar packing of copolymer with higher content of ε-caprolactone. The change in absorbance of DPH with polymer concentration suggested micelle formation as shown in Fig. 4.7. It was reported that PCL chains are more hydrophobic than PLA and thus, polymer PGPCPL-2 with higher block length of PCL exhibited lower CMC value as shown in Fig. 4.8 and 4.9. A decrease in CMC value from 0.038 wt. % to 0.016 wt. % of PGPCPL-1 and PGPCPL-2 respectively corresponds well with the lower CGC of copolymer PGPCPL-2. Similar results were observed in case of PCL-PEG-PCL and in case of PEG-PCL-PEG of different compositions. The phase transition behavior of the pentablock polymer aqueous solution was similar to

other triblock polymers. The clear aqueous solution of polymer was observed due to self assembly of polymeric chains into micellar structure which showed aggregation upon increasing the temperature and resulted in the formation of gel. However, upper gel-sol conversion was due to increased molecular motion of hydrophobic chain of PCL and PLA. Further, increase in temperature results in the dehydration of mPEG chains that leads to the syneresis. SEM analysis revealed that hydrogel matrix is porous in nature (data not shown).

Earlier compositions of PEG-PCL-PEG exhibited lowered CGC than the polymer synthesized in this study due to the fact that incorporation of PLA lowers the hydrophobicity of central block. Sol-gel transition studies also showed wider gelation window for PGPCPL-2 than PGPCPL-1 for polymeric aqueous solution. This observation was supported by the fact that PEG-PLGA-PEG exhibited higher CGC and wider gelation than PEG-PCL-PEG because of higher hydrophobicity of PCL block. Therefore, phase transition of thermosenstive pentablock hydrogel depends on the block length and hydrophobic nature of the central block.

DSC Analysis

DSC results of pentablock copolymers (PGPCPL-1 and PGPCPL-2) are shown in Fig. 4.6. It was observed that PGPCPL-1 with PEG of molecular weight 550 did not showed any crystalline peak for PCL block whereas characteristic melting transition for PGPCPL-2 was observed at 23.7 °C and 33.2 °C. These two characteristic transitions for PCL were observed due to melting of PCL and recrystallized PCL.

X-Ray Diffraction Analysis

X-ray diffraction patterns of two different compositions were reported in Fig. 4.5. We have not observed any characteristic peak for PEG in both the copolymers i.e., PGPCPL-1 and PGPCPL-2. However, for PGPCPL-2 we have observed two characteristic diffraction peaks at $2\theta = 10.6°$ and 11.8°, which suggest that PCL exist in crystalline form in the case of PGPCPL-2. On the other hand, absence of diffraction peak for PCL in PGPCPL-2 suggests that PCL block is too short to exhibit crystalline nature. Our observations are consistent with the DSC results. Moreover, similar pattern of diffraction was reported for different block copolymers of ε-caprolactone and PEG.

In Vitro Hydrolytic Degradation

We have evaluated the hydrolytic degradation of PGPCPL-1 and 2 in PBS buffer at pH 7.4 utilizing GPC. It was found that molecular weight of PGPCPL-1 decreased (Fig. 4.10) from initial 3800 to 1200 after 15 days whereas for PGPCPL-2 decrease in molecular weight from 4000 to 3100 takes place in similar time duration. These results suggest that decrease in molecular weight was depended on the copolymer compositions. We have observed faster degradation in the case of PGPCPL-1 due to its amorphous nature. On the other hand, PGPCPL-2 demonstrated slower degradation rate due to crystalline nature. Moreover, we have also monitored the change in crystallinity following degradation at different time points. As shown in Fig. 4.11, crystallinity of PCL was gradually increased due to scission of PLA chains as evident from the change in diffractogram of peaks of PCL. In order to confirm our findings we have also performed the NMR analysis of degradation samples at 1, 15 and 30 days. . We observed change in peak ratio due to PEG, PCL and PLA component at 3.6, 4.6

and 5.1 ppm at different time point. ^{1}H NMR spectra (Fig. 4.12) shows that peak due to PLA component completely disappeared at the end of 30 days. In addition, we found change in peak intensity due to PCL component. These results support our finding that due to faster degradation of PLA, crystallinity of copolymer increases at the end of 30 days.

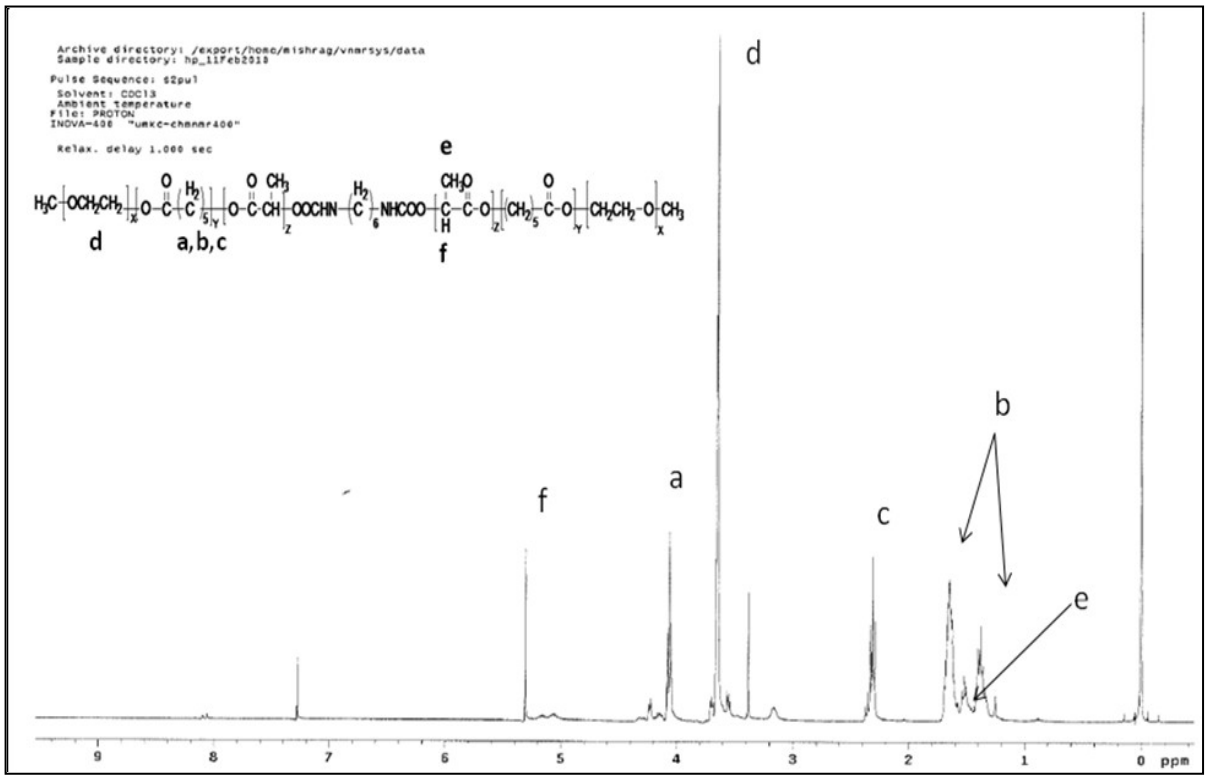

Figure 4.2 ^{1}H-NMR spectra of PEG-PCL-PLA-PCL-PEG copolymer in $CDCl_3$

Table 4.1 Molecular weight distribution

Polymer	Mn	Mw	Poly-dispersity	Nomenclature
PEG_{550}-PCL_{550}-PLA_{1100}-PCL_{550}-PEG_{550}	3872	5260	1.35	PGPCPL-1
PEG_{550}-PCL_{825}-PLA_{550}-PCL_{825}-PEG_{550}	4031	6925	1.71	PGPCPL-2

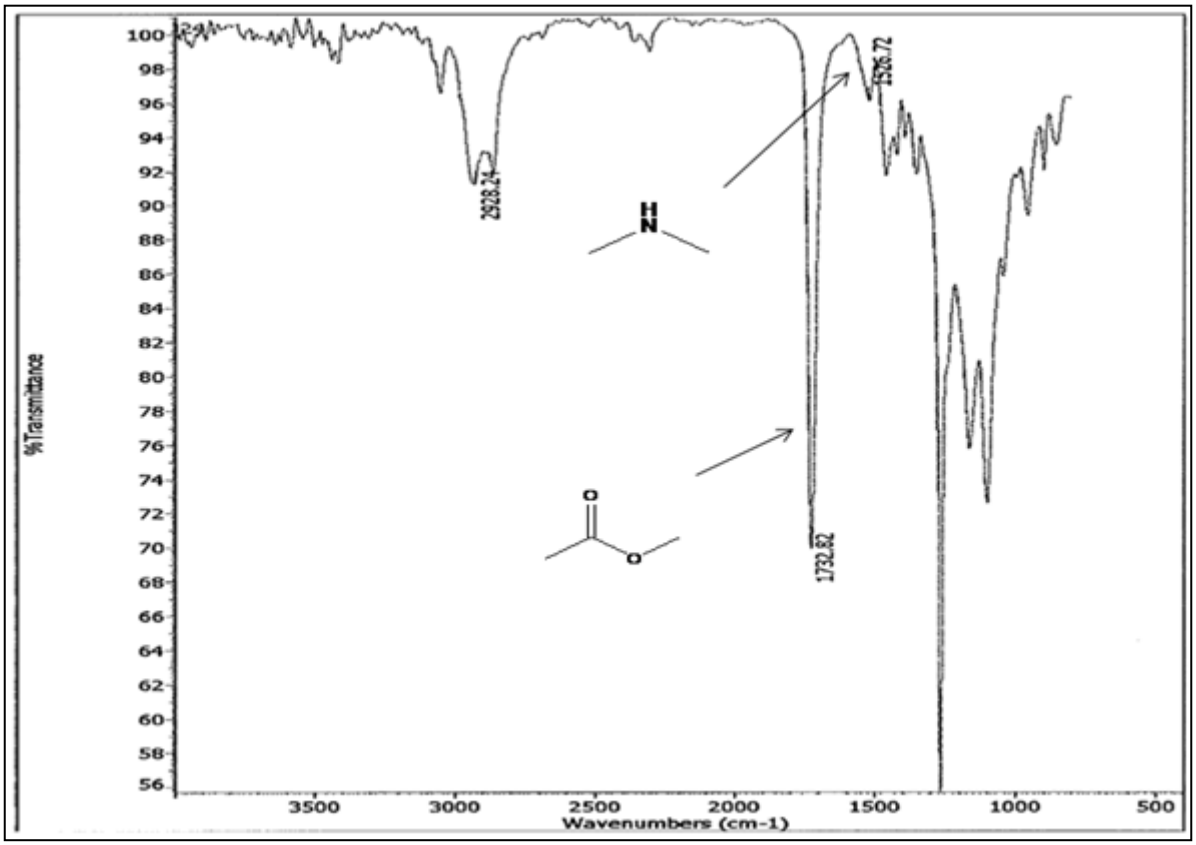

Figure 4.3 FTIR spectrum of PEG-PCL-PLA-PCL-PEG

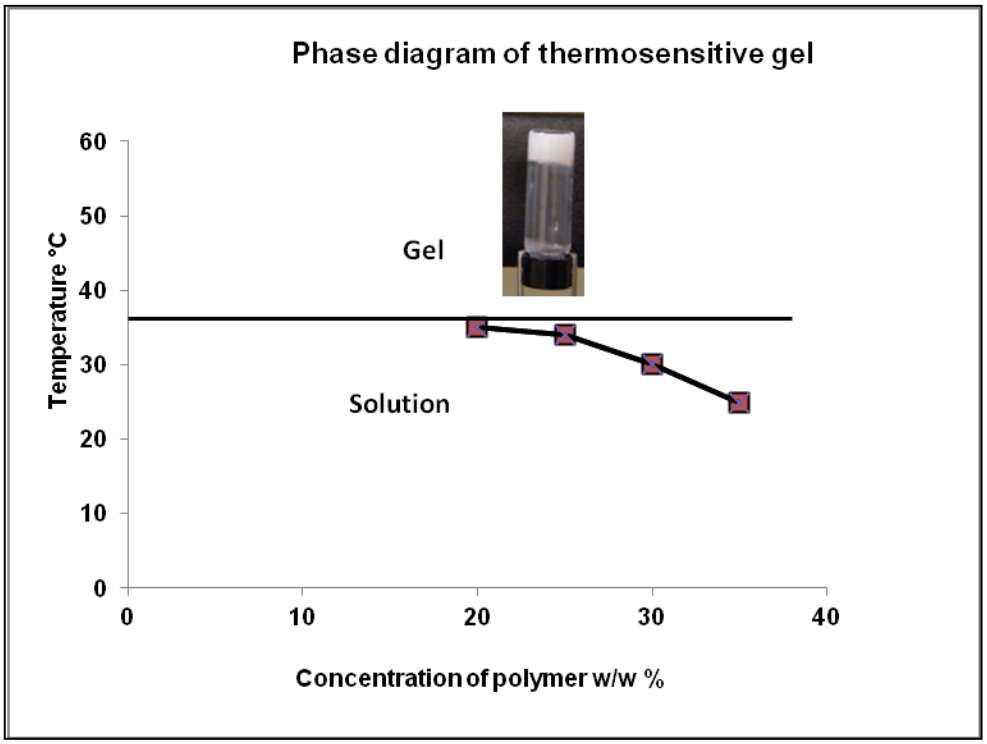

Figure 4.4 Sol-gel transition phase diagram

In Vitro Release Studies

Ofloxacin and Prednisolone acetate were utilized as model compounds of varying hydrophobicity to examine the potential of pentablock based thermosensitive hydrogel for controlled ocular drug delivery. Ofloxacin has a logP of -0.45 and water solubility of 4 mg/ml whereas Prednisolone is relatively hydrophobic with a logP of 1.9 and water solubility of 123 μg/ml. Fig. 4.13 shows the release profile of ofloxacin from two different composition of pentablock polymer. Release of ofloxacin was not significantly different from both the polymeric compositions. Fig. 4.14 i*n vitro* release studies showed that in 145 h 73.67 ± 7.6 % and 58.01 ± 5.3 % of prednisolone acetate was released from PGPCPL-2 and 1 respectively. These results suggest that the release rate of prednisolone acetate was affected by hydrophilic/hydrophobic balance of the polymer. In addition, relatively longer PCL block length of PGPCPL-2 may have restricted the permeation of water molecules across the polymeric matrix. Hence, slower hydration of gel resulted in decreased diffusion coefficient of the drug across the hydrogel matrix.

Release profile of ofloxacin was not significantly different from both the compositions. ofloxacin being a hydrophilic drug molecule tend to partition in the PEG domain of the hydrogel whereas hydrophobic drug molecule partition into PCL core. Therefore, ofloxacin dispersed in PEG domain was easily diffused out in the release medium irrespective of polymer composition whereas change in hydrophobic component altered the release profile of prednisolone acetate by altering the micellar aggregation which influenced the porosity of hydrogel matrix.

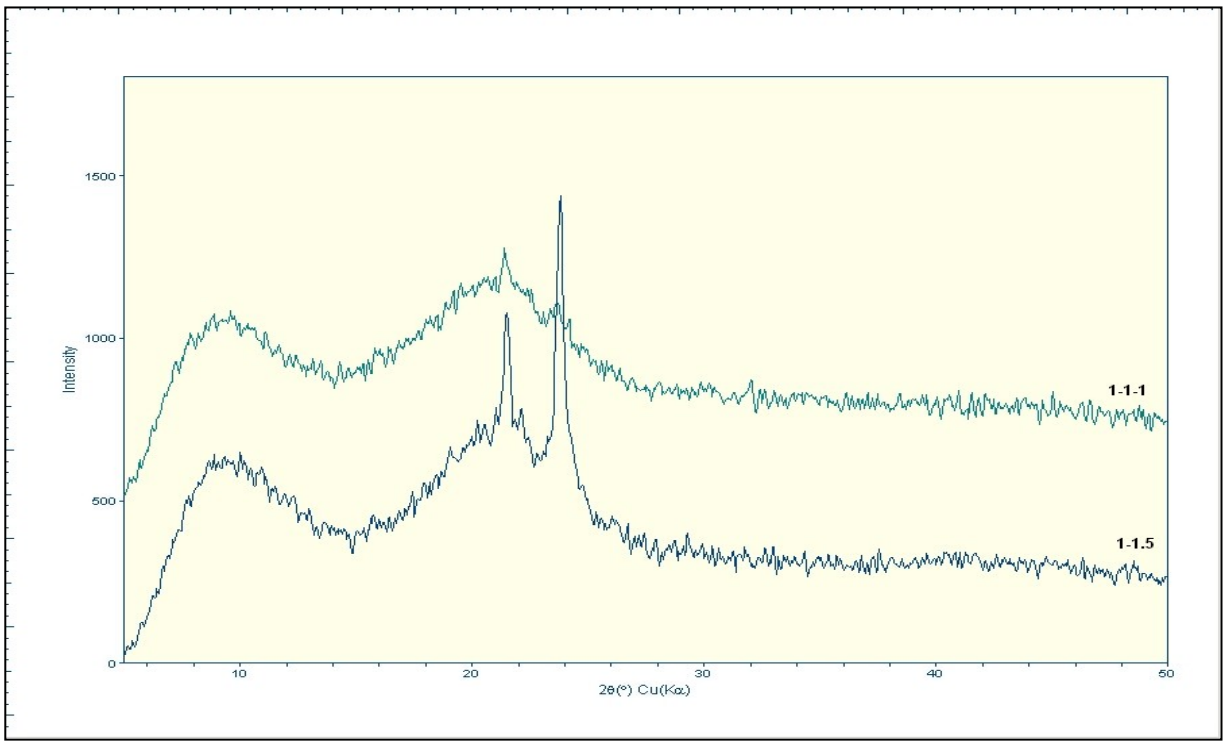

Figure 4.5 X-ray diffractogram of PGPCPL-1(green line) and PGPCPL-2(blue line)

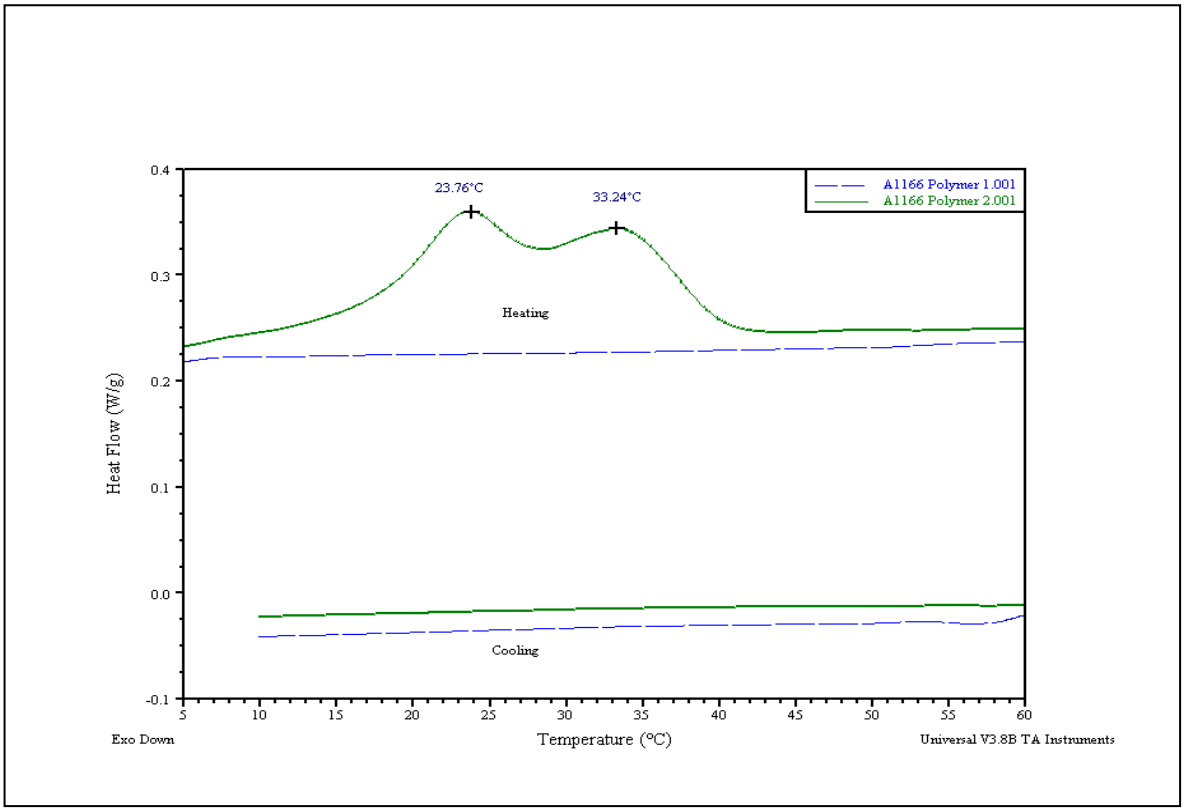

Figure 4.6 DSC thermogram of PGPCPL-1(green) and PGPCPL-2 (blue)

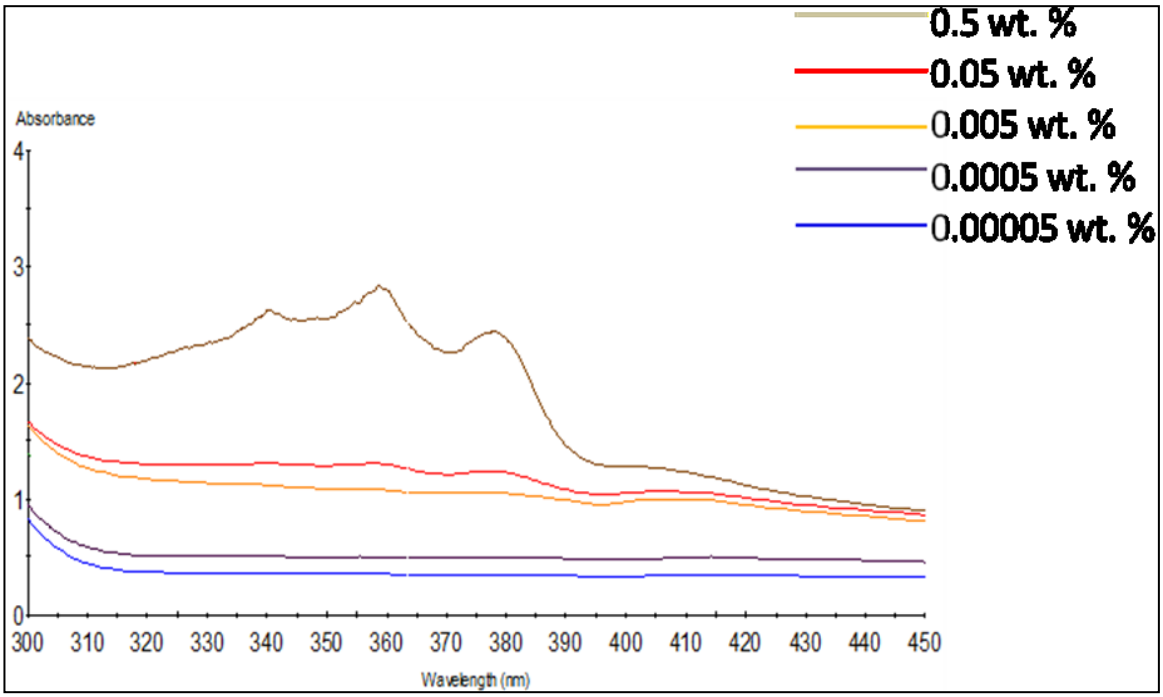

Figure 4.7 UV-Visible spectra of hydrophobic dye (1,6-Diphenyl-1,3,5-hexatriene) in different concentrations of PGPCPL-1

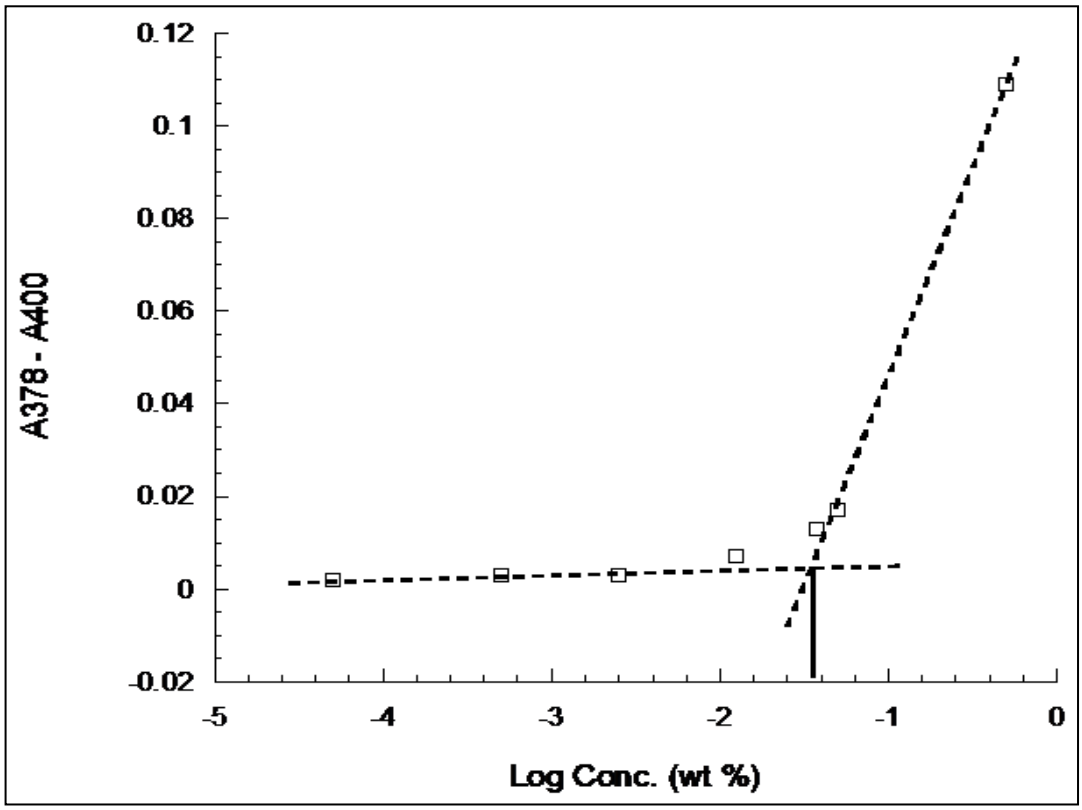

Figure 4.8 Plot of critical micelle concentration of PGPCPL-2

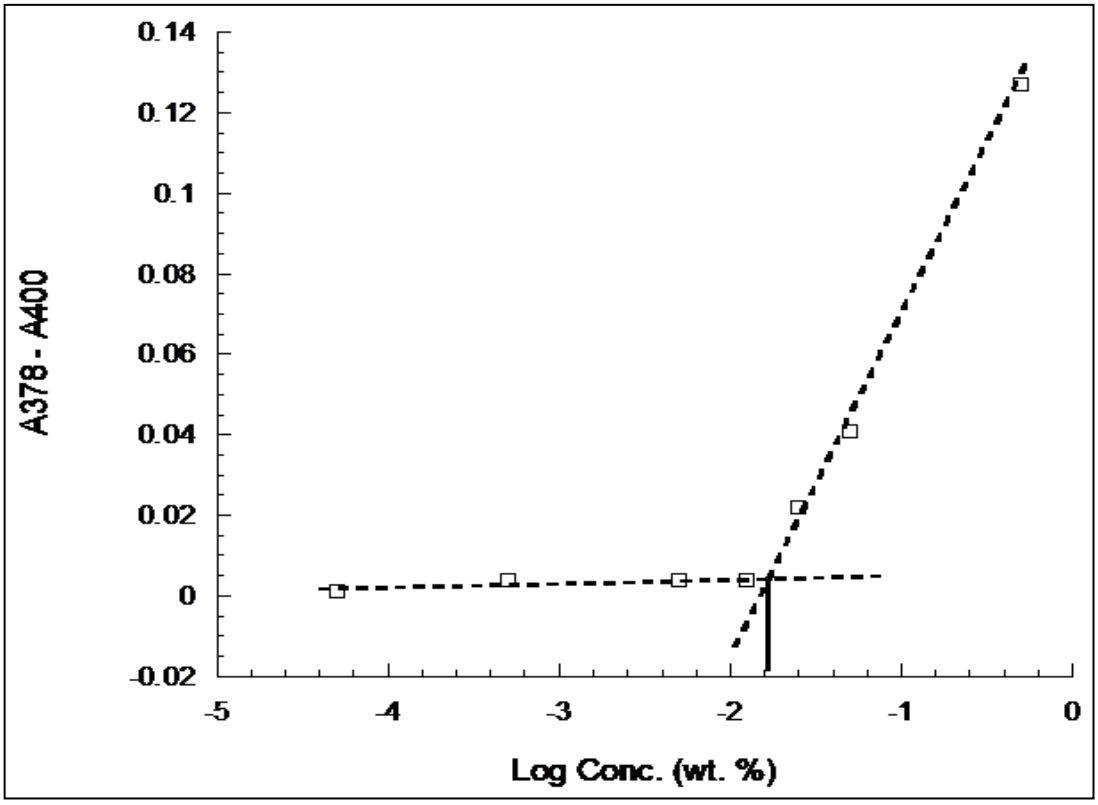

Figure 4.9 Plot of critical micelle concentration of PGPCPL-1

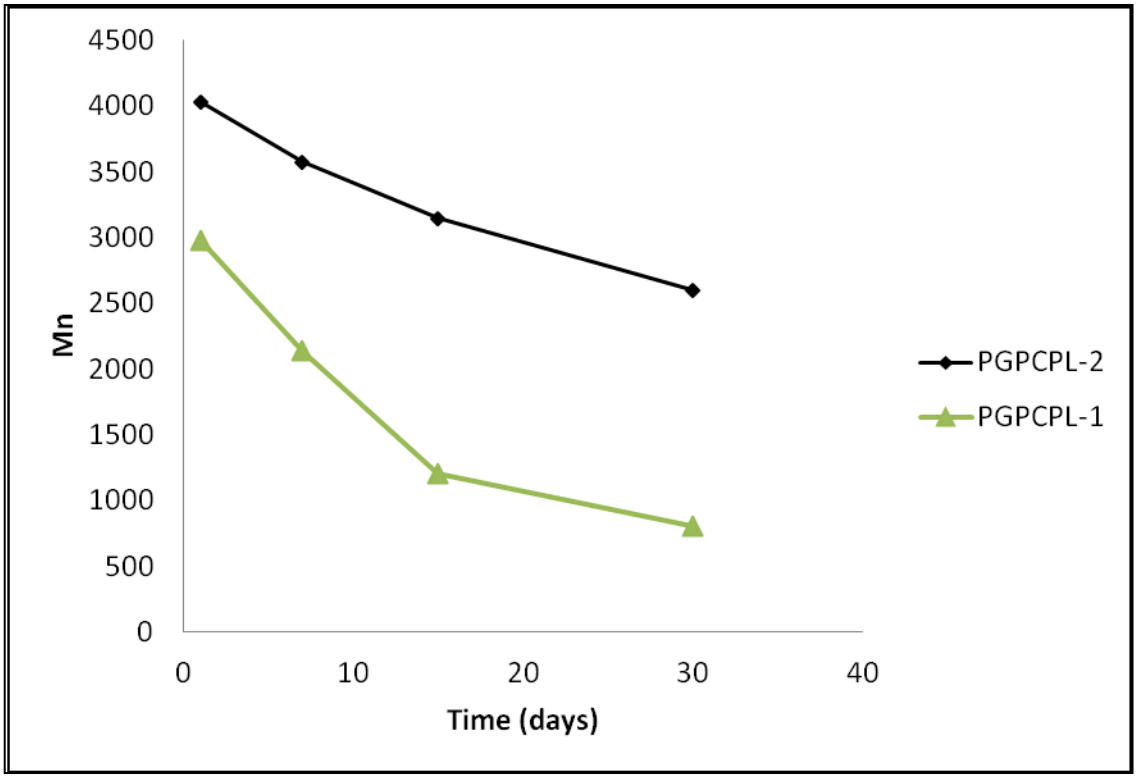

Figure 4.10 *In vitro* degradation study of PGPCPL-1 and 2 was performed in PBS pH 7.4 and analyzed by GPC

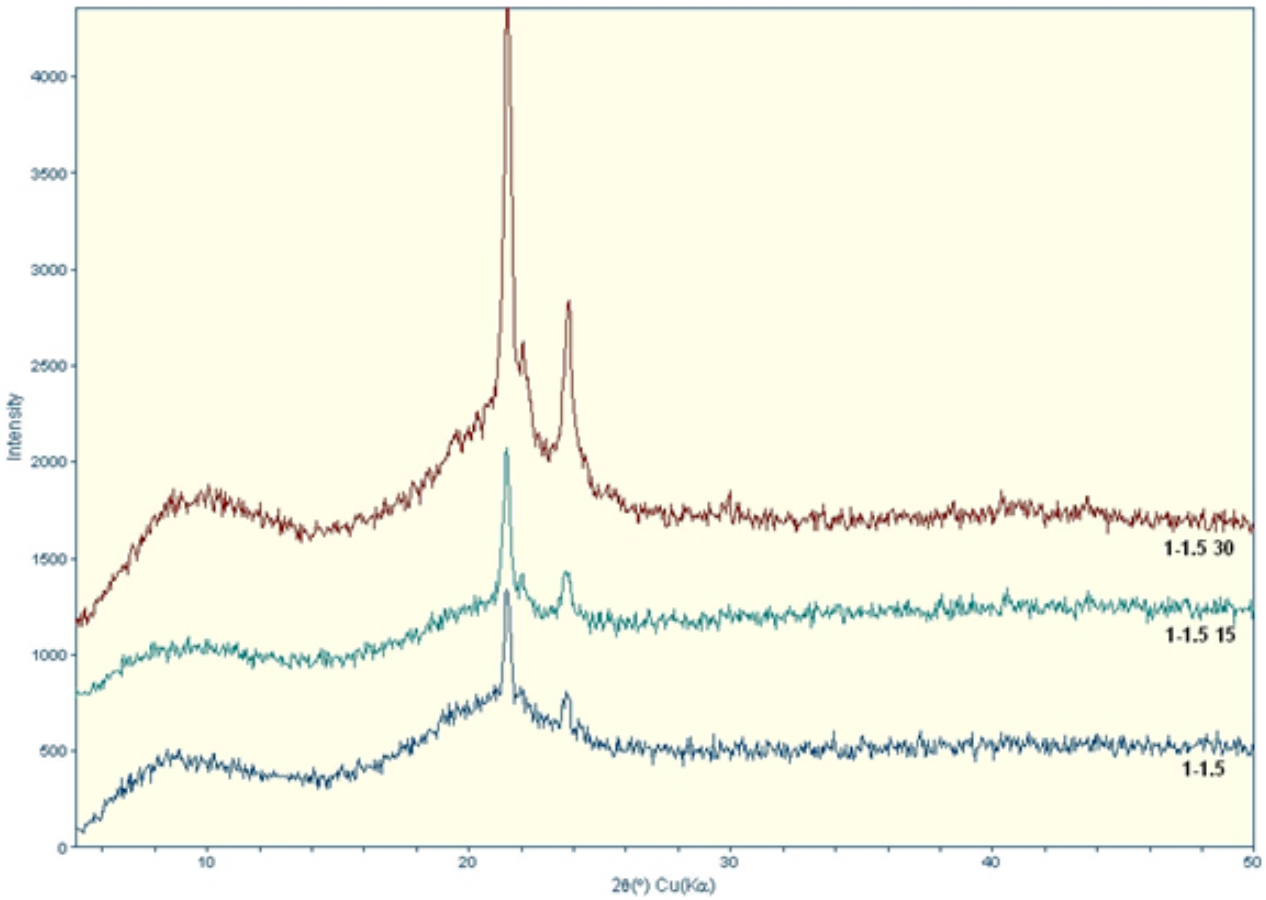

Figure 4.11 *In vitro* degradation study of PGPCPL-2 was performed in PBS pH 7.4 and analyzed by XRD

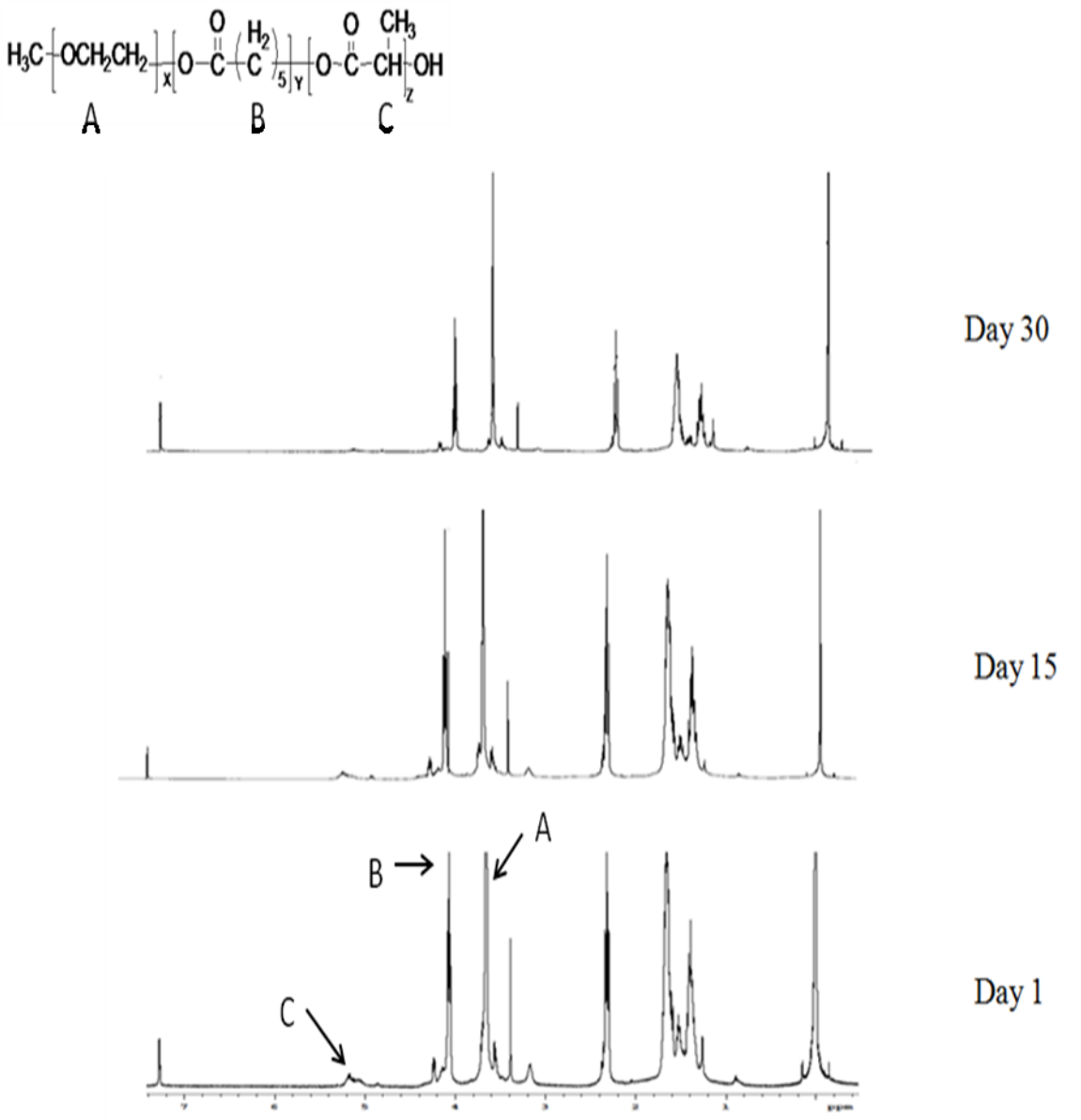

Figure 4.12 *In vitro* degradation analysis of PGPCPL-2 was performed in PBS pH 7.4 and analyzed by NMR

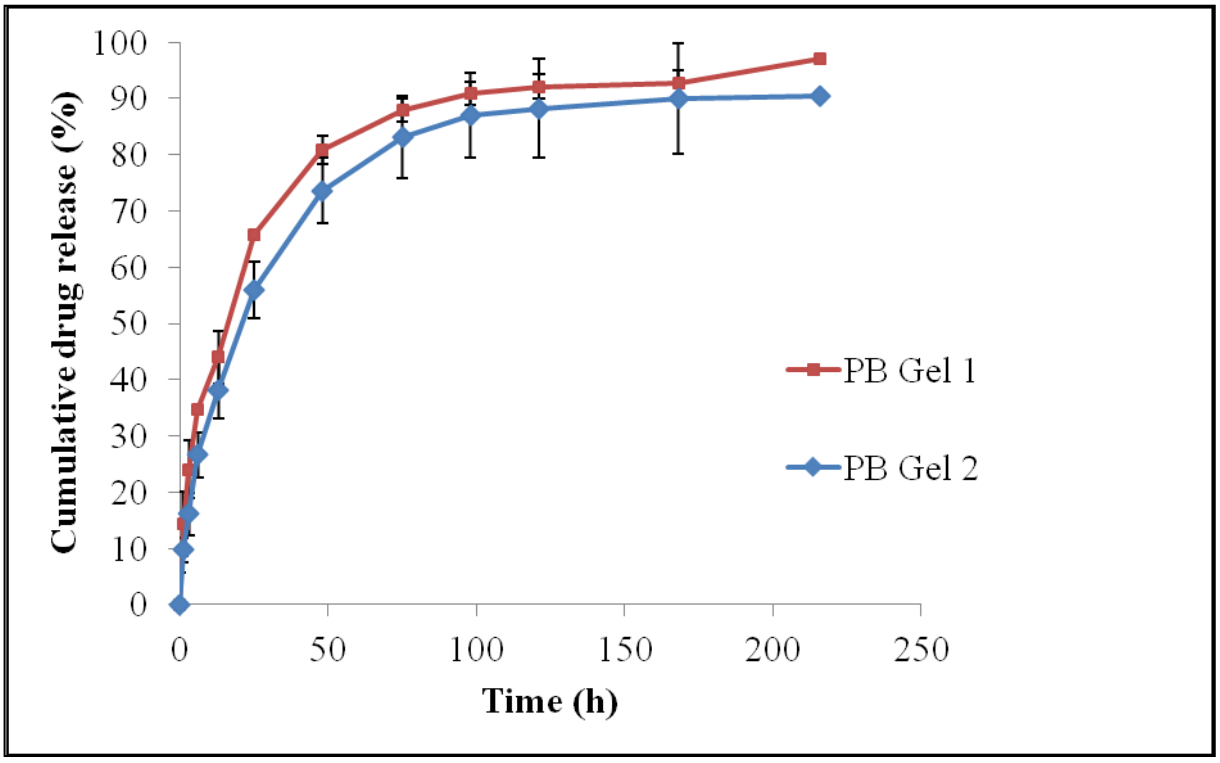

Figure 4.13 *In vitro* release of ofloxacin from thermosensitive hydrogel in PBS buffer (pH 7.4) at 37 °C. The values are represented as mean ± standard deviation of n = 3

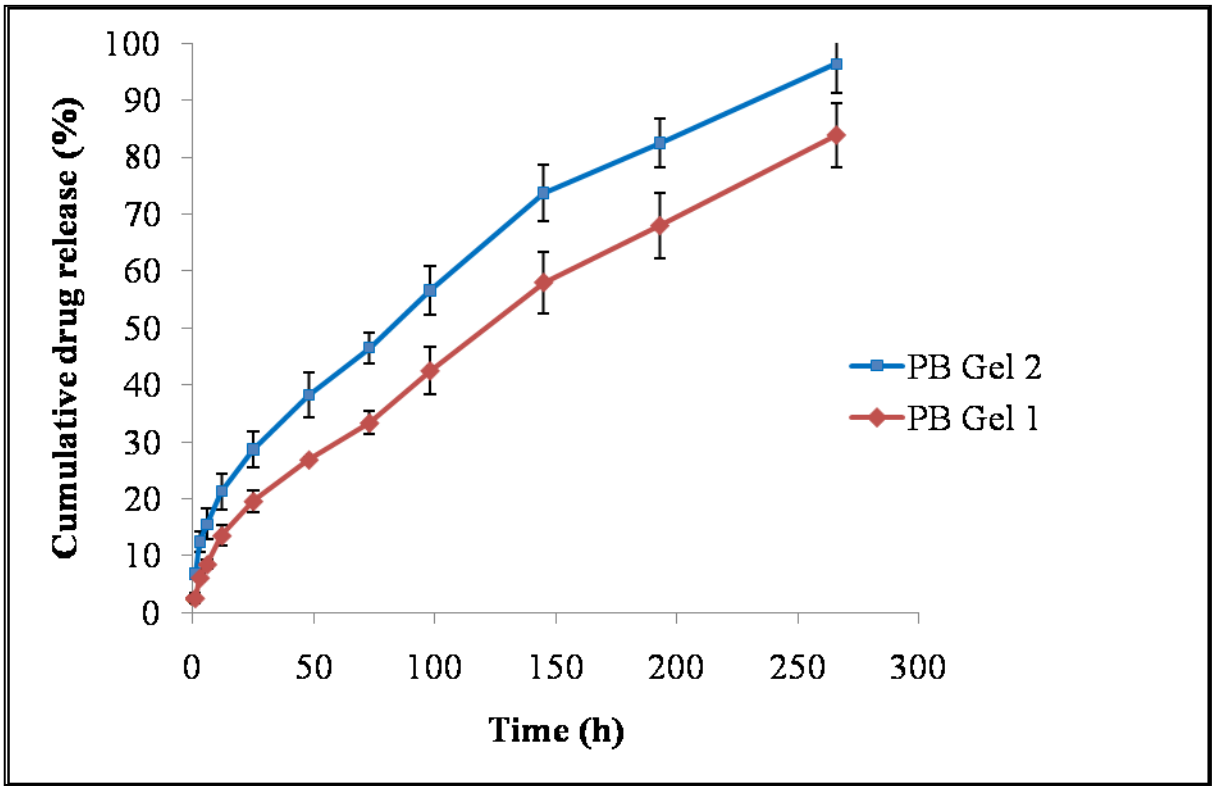

Figure 4.14 *In vitro* release of prednisolone acetate from thermosensitive hydrogel in PBS buffer (pH 7.4) at 37 °C. The values are represented as mean ± standard deviation of n = 3

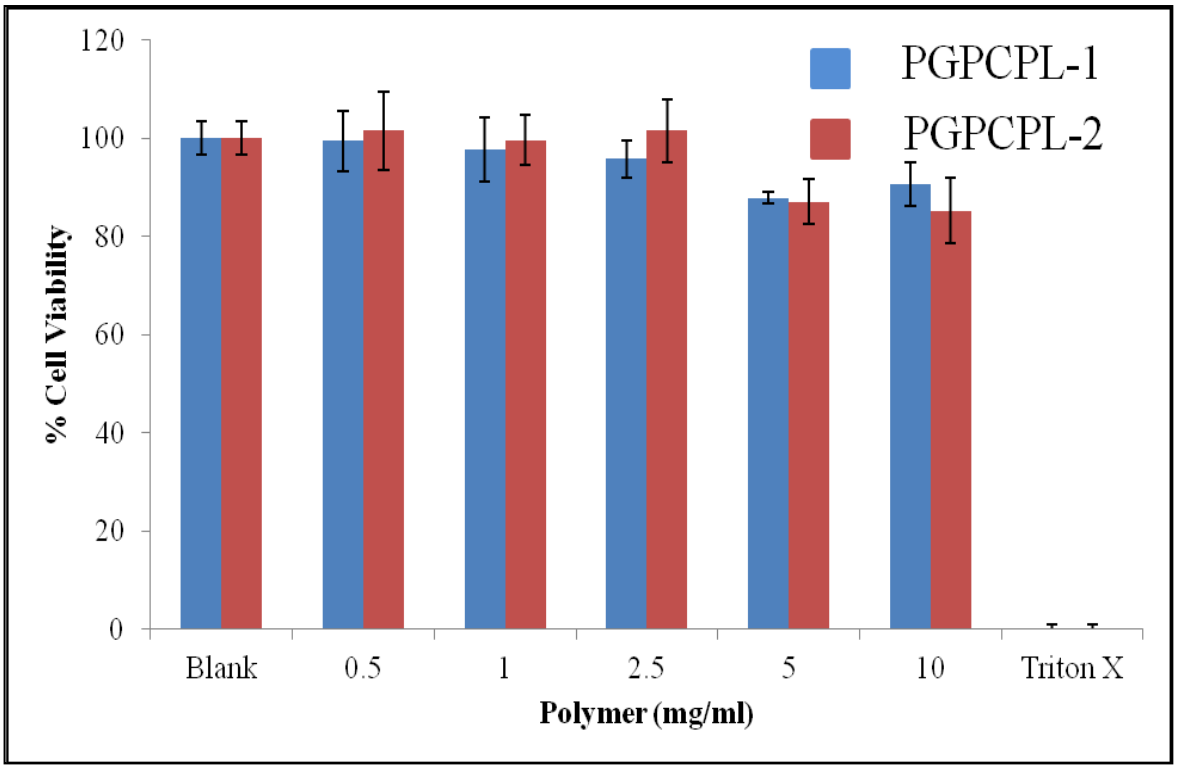

Figure 4.15 Rabbit primary corneal epithelial cell (rPCEC) viability study

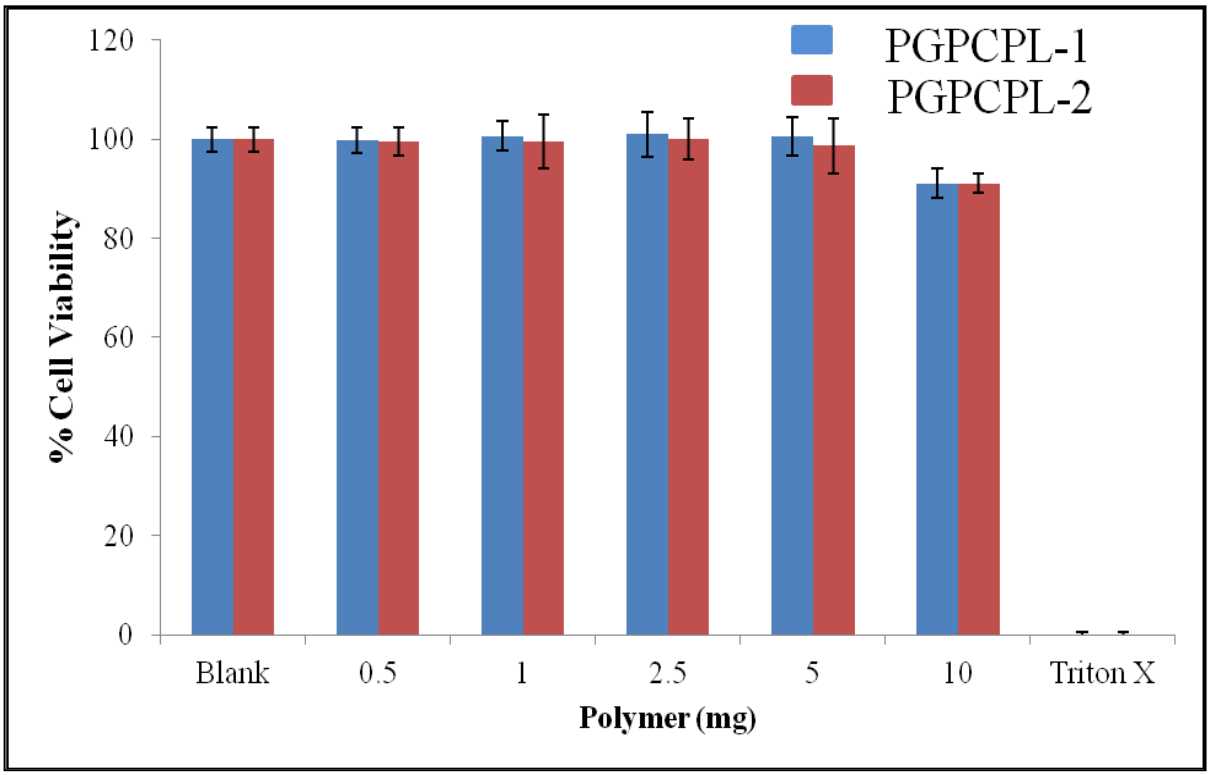

Figure 4.16 A Human retinal pigmented epithelial (ARPE-19) cell viability study

Cell Viability Studies

Cell viability response showed that PGPCPL-1 and 2 are not toxic to rPCEC and ARPE-19 cells. Fig. 4.15 and 4.16 suggested that cytotoxicity of hydrogel was concentration dependent. However, at low concentrations no statistically significant difference from control was observed. Cell viability studies suggest that pentablock hydrogel are biocompatible with the corneal epithelial and retinal cells.

Conclusions

We have successfully synthesized two different compositions of pentablock copolymers. We have shown the effect of block composition on the sol-gel transition, crystallinity, and drug release kinetics. We have observed that release kinetics of hydrophobic drug can be easily modulated by altering the hydrophobic block segment. Moreover, we have successfully delineated the effect of block composition on the sol-gel transition. Pentablock copolymers based hydrogel would be ideal for tailor-made drug delivery. Therefore, pentablock copolymers have potential for formulation of injectable drug delivery depots for the delivery of small molecules.

CHAPTER 5

SYNTHESIS AND CHARACTERIZATION OF DIFFERENT PENTABLOCK COPOLYMER COMPOSITIONS IN THE PREPARATION OF NANOPARTICLES

Rationale

Biodegradable nanoparticles prepared from block copolymers have received significant attention in the last decade. Polymeric nanoparticles are advantageous in enhancing the therapeutic outcome, minimizing the side-effects, protecting the drug molecules and regulating drug release kinetics (Hu et al., 2003; Soppimath et al., 2001; Wei et al., 2009). Amphiphilic block copolymers composed of PEG as hydrophilic segment and polyester such as PCL, PLA or PGA as hydrophobic block have tendency to form micelle like nanoparticles (Ge et al., 2002; Ryu et al., 2000; Yang et al., 2009). PCL as a hydrophobic segment has been extremely utilized due to its biodegradable and biocompatible nature. In addition, physical properties such as melting temperature and excellent permeability to various drug molecules further strengthen its growing application in the drug delivery field (Liggins and Burt, 2002) (Kwon, 1998; Lee et al., 2005). However, extremely slow degradation and higher crystallinity are the properties which limit the application of PCL to a wider extent. Therefore, polymerization of PCL with hydrophilic block such as PEG, and faster degrading blocks such as PGA or PLA can generate tailor made block copolymers. PEG will improve the hydrophilicity of block copolymers and form the hydrophilic corona of the nanoparticles which can avoid their recognition by reticuloendothelial system (RES) (Ge et al., 2002; Liu et al., 2010; Sheng et al., 2009). PLGA-PEG nanoparticles are well established for encapsulation of hydrophobic drugs (Gref

et al., 1994). In other investigations the effect of chemical composition of PLA-PEG on drug loading was elucidated. Investigators observed that PLA-PEG nanoparticle loading efficiency was independent of chemical composition (Govender et al., 2000; Xiao et al., 2010). In similar attempts, PEG-PLGA-PEG nanoparticles were also prepared for delivery of various therapeutic molecules. However, in past years researchers are trying to elucidate the role of hydrophilic/hydrophobic ratio by vary the molecular weight and block length of individual blocks. But limited investigations were performed in modification of hydrophobic block copolymers (Feng et al., 2008; Gou et al., 2009; Sheikh et al., 2009). So we have developed novel polymers with optimum degradation rate to achieve zero order drug release via both diffusion and degradation mediated pathway. These polymers will be utilized for the development of nanoparticles. In this work we have synthesized different compositions of pentablock copolymers and evaluated their effect on nanoparticles encapsulation and drug release profile.

Material and Methods

PEG, ε-caprolactone and stannous octoate were obtained from Sigma chemical company (St. Louis, MO). All chemicals were used without any further purification.

Synthesis of Pentablock Copolymers

Different compositions were prepared in two steps by sequential ring opening polymerization. In the first step, PEG of molecular weight 1,000 Da was allowed for polymerization with ε-caprolactone in presence of stannous octoate as a catalyst to form the triblock copolymer PCL-PEG-PCL (Step 1). In the second step, the triblock polymer was reacted with glycolide to form the pentablock copolymer (Step 2).

More specifically, in the first step, PEG was dissolved in anhydrous toluene followed by distillation to remove residual moisture. Polyethylene glycol (0.001 mol) and ε-caprolactone (0.13 mol) were taken and stannous octoate (0.5 w/w% of monomer concentration) was used as catalyst. The reaction was kept at 130 ºC for 24 hours and then the reaction mixture (RM) was degassed for 30 minutes. After degassing, RM was dissolved in methylene chloride followed by precipitation with petroleum ether. The precipitated polymer was filtered and dried for 24 hours in vacuum at room temperature.

As shown in step 2, for the synthesis of the pentablock polymer, the triblock copolymer was taken in a round bottom flask and glycolide (0.005 mol) or lactide was added to it and continued stirring for 24 hours at 130 ºC under inert atmosphere. For sequential polymerization stannous octoate (0.5 w/w% of monomer concentration) was added as a catalyst. The final PGA_{300}-PCL_{7500}-PEG_{1000}-PCL_{7500}-PGA_{300} (PB-A) compound was purified by similar precipitation method followed in the first step. Due to limited solubility of high molecular weight PGA in the common organic solvent we performed the synthesis of PB-A with smaller PGA block length. Similar procedure (Fig. 5.1) was followed for the synthesis of PLA_{1875}-PCL_{7500}-PEG_{1000}-PCL_{7500}-PLA_{1875} and PLA_{3750}-PCL_{7500}-PEG_{1000}-PCL_{7500}-PLA_{3750} (PB-B and C).

Step 1:

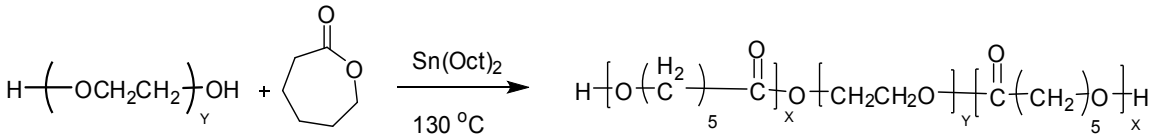

Step 2:

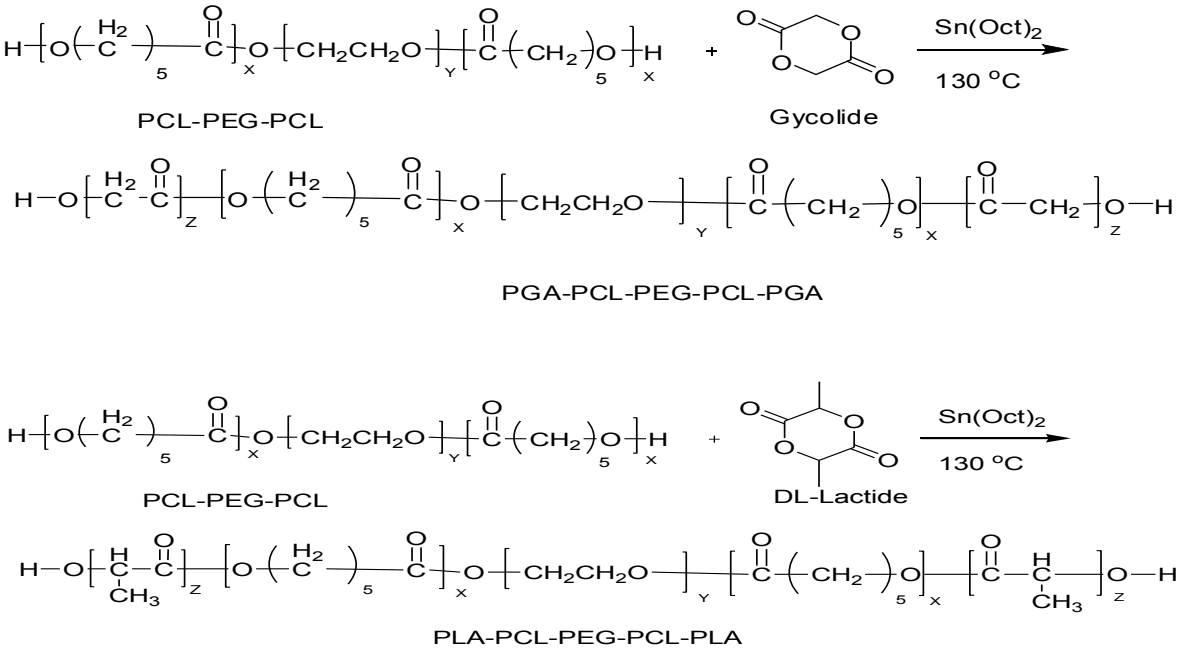

Figure 5.1 Synthetic schemes of PGA-PCL-PEG-PCL-PGA and PLA-PCL-PEG-PCL-PLA

Characterization of Polymeric Material

(i) NMR

^{1}H NMR spectroscopy was performed to characterize the composition of polymer. Spectra were recorded by dissolving polymeric material in $CDCl_3$ and then analyzing the proton NMR spectra recorded using Varian-400 NMR instrument.

(ii) FT-IR

The FT-IR spectra were recorded with a Nicolet-100 infrared spectrophotometer at a resolution of 4 sec^{-1}. Polymer was dissolved in methylene chloride and casted on KBr plates.

Preparation of Prednisolone Nanoparticles of Pentablock Copolymer

Nanoparticles were prepared by single emulsification method (Fig. 5.2) using the Pentablock Polymer A. Briefly, 100 mg of polymer and the 10 mg prednisolone were dissolved in methylene chloride. The resulting oil phase was emulsified in 2.0 w/v % aqueous solution of polyvinyl alcohol with the help of a tip sonicator at 60 W for 5 minutes to form oil in water (o/w) emulsion. The resulting organic solvent was evaporated under vacuum to form nanoparticles. The unreacted drug and PVA residue were washed three times with deionized water and the nanoparticles were collected by ultracentrifugation at 21,000 RPM for one hour. The drug entrapment efficiency was determined using high performance liquid chromatography (HPLC) using C-18 reverse-phase column at 254 nm.

Characterization of Nanoparticles

(i) Size and Zeta Potential Determination of Nanoparticles

Nanoparticles (1mg/ml) were dispersed in deionized water and analyses were performed with laser beam at 90° scattering angle at 25 °C. Dynamic light scattering was utilized to measure nanoparticles size and size distribution by 90 plus particle size analyzer (Brookhaven Instruments Corporation). Analysis was performed in triplicate and results were reported as the average of mean particle diameter.

(ii) *Drug Loading Content and Entrapment Efficiency*

Entrapment efficiency and drug loading of prepared nanoparticles were determined by dissolving freeze dried nanoparticles (5 mg) in dichloromethane (0.5 ml) and further diluted with deionized water. The entrapment efficiency of prednisolone was determined by the HPLC method reported in chapter 4.

$$\text{Entrapment Efficiency} = \frac{\text{Amount of drug in nanoparticles}}{\text{Amount of feeding drug}} \times 100$$

(iii) Surface morphology study

The surface morphology of lyophilized nanoparticles was observed by scanning electron microscopy (SEM). The lyophilized power of nanoparticles was coated with gold/palladium at 0.6 kV. The samples were examined by FEG ESEM XL 30 electron microscope.

(iv) X-ray Diffraction Analysis

X-ray diffraction analysis was utilized to determine the crystallinity of drug alone, blank nanoparticles and drug loaded nanoparticles prepared from pentablock copolymer-A by MiniFlex automated X-ray diffractometer (Rigaku, The Woodlands, Texas) using Ni-filtered Cu-kα radiation (30 kV and 15 mA) at 25 ° C.

In Vitro Release Studies

20 mg of prednisolone nanoparticles prepared from the pentablock polymer were dispersed in 500 µl of 0.1 M phosphate buffer saline (pH 7.4). The prepared solution was then added into the dialysis bag (MW cutoff 12,500) which was kept in a 15 ml tube containing 10 ml of release medium at 37 ºC. The entire release medium was replaced with fresh buffer at designated intervals to mimic the sink condition. The samples were stored at -20 ºC before further analysis. The release samples were analyzed by HPLC.

Statistical Analysis

All release experiments were conducted in triplicates and the results were reported as mean ± standard deviation. Statistical analyses were performed by one-way ANOVA. Statistical package for social science (SPSS) version 11 was used to compare mean of each group. A level of $p < 0.05$ was considered statistically significant in all cases.

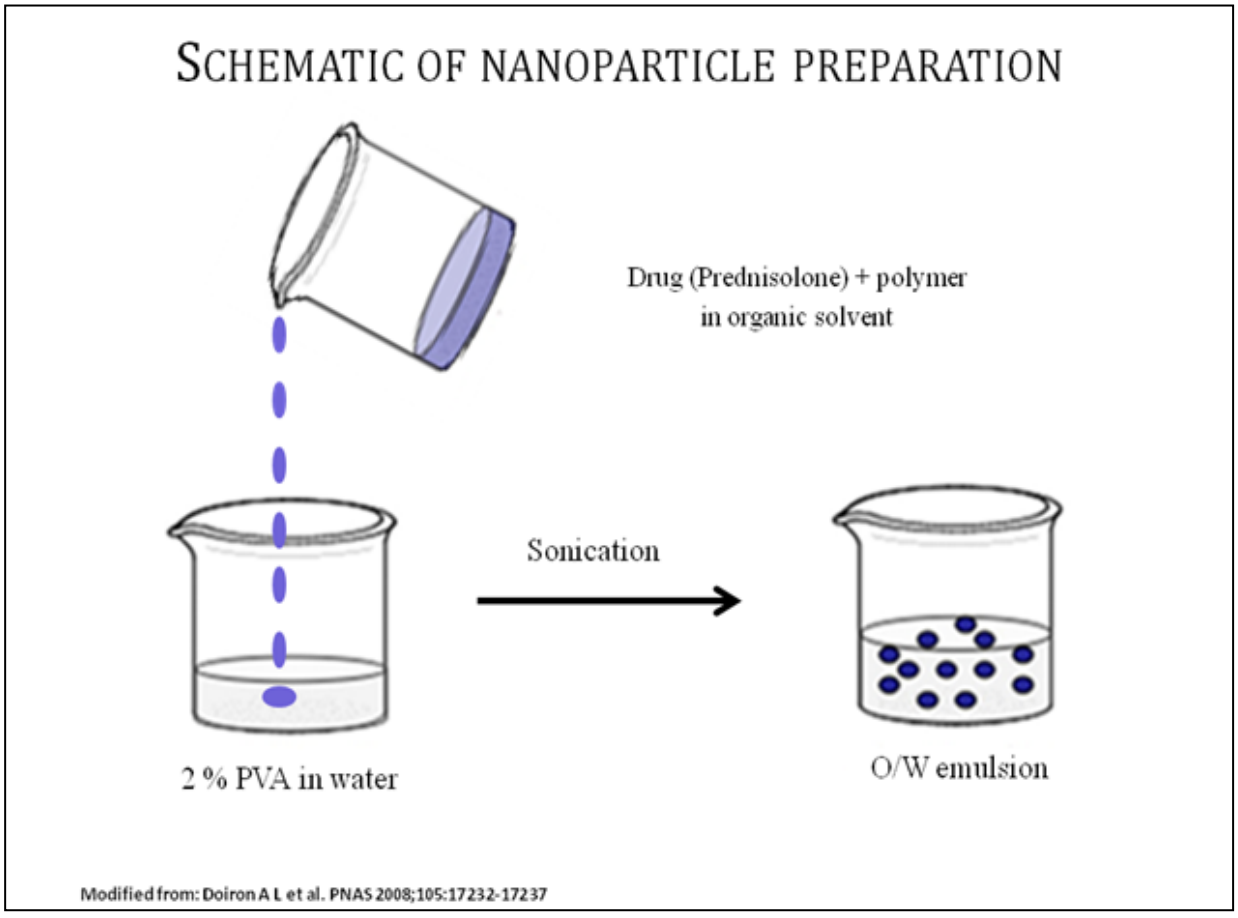

Figure 5.2 Nanoparticles preparation method

Result and Discussion

Synthesis and Characterization of Pentablock Copolymers

The pentablock copolymer was synthesized by ring opening polymerization method. ^{1}H NMR was utilized to confirm the composition and molecular weight. Fig. 5.3 shows main peaks of PCL at 1.4 and 1.65 ppm for protons of $–(CH_2)_3-$ and $–OCCH_2-$ respectively. Peaks at 2.32 and 4.06 ppm correspond to $–OCCH_2-$ and $–CH_2OOC-$ protons of PCL chain respectively. PEG major peak was evident at 3.6 ppm which confirmed the formation of polymer. For PB-A peaks at 4.5-4.8 confirms the conjugation of glycolide to form PGA-PCL-PEG-PCL-PGA. Pentablock copolymer-B and C has similar composition but different molecular weight. Therefore, peaks at 5.1 ppm in Fig. 5.4 and 5.5 confirmed the formation of PLA-PCL-PEG-PCL-PLA. The molecular weight was determined by integration ratio of peaks at 3.6 ppm for PEG block, 4.0 ppm for PCL block, and 5.1 ppm for PLA block. In the case copolymer-A instead of PLA, peak for PGA at 4.5 ppm was considered for the determination of molecular weight.

FT IR spectra (Fig. 5.6) of pentablock copolymers indicated the band for C=O stretching appeared at 1732 cm^{-1} and bands for C-H stretching appeared at 2941 cm^{-1} and 2860 cm^{-1} for PCL block. Absorption band at 1140 cm^{-1} was appeared because of C-O-C stretching vibrations of the repeated OCH_2CH_2 units of PEG and band at 1279 cm^{-1} was attributed to the -COO- stretching vibrations

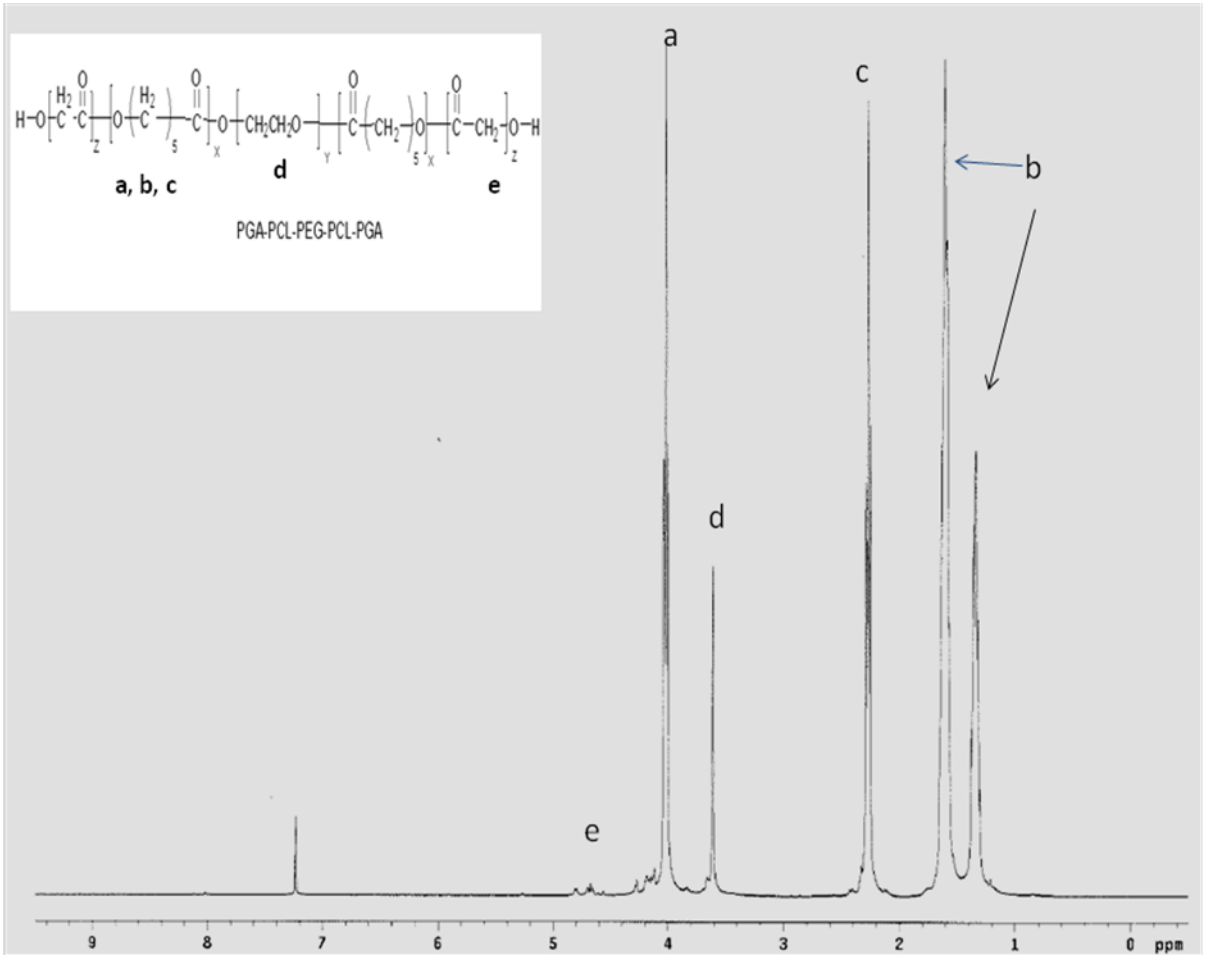

Figure 5.3 ^{1}H-NMR spectra of PGA-PCL-PLA-PCL-PGA pentablock copolymer in $CDCl_3$

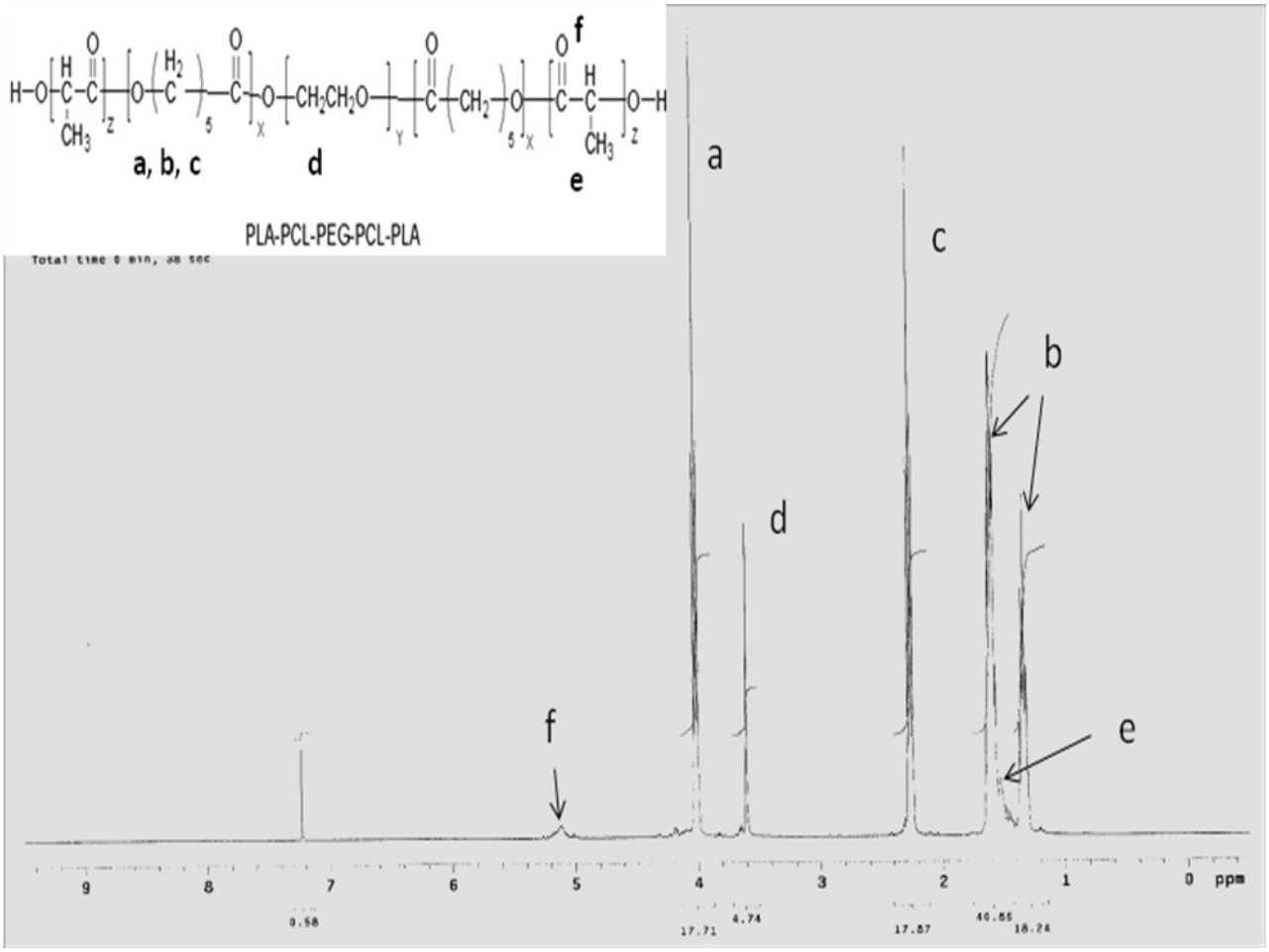

Figure 5.4 ^{1}H-NMR spectra of pentablock copolymer-B in $CDCl_3$

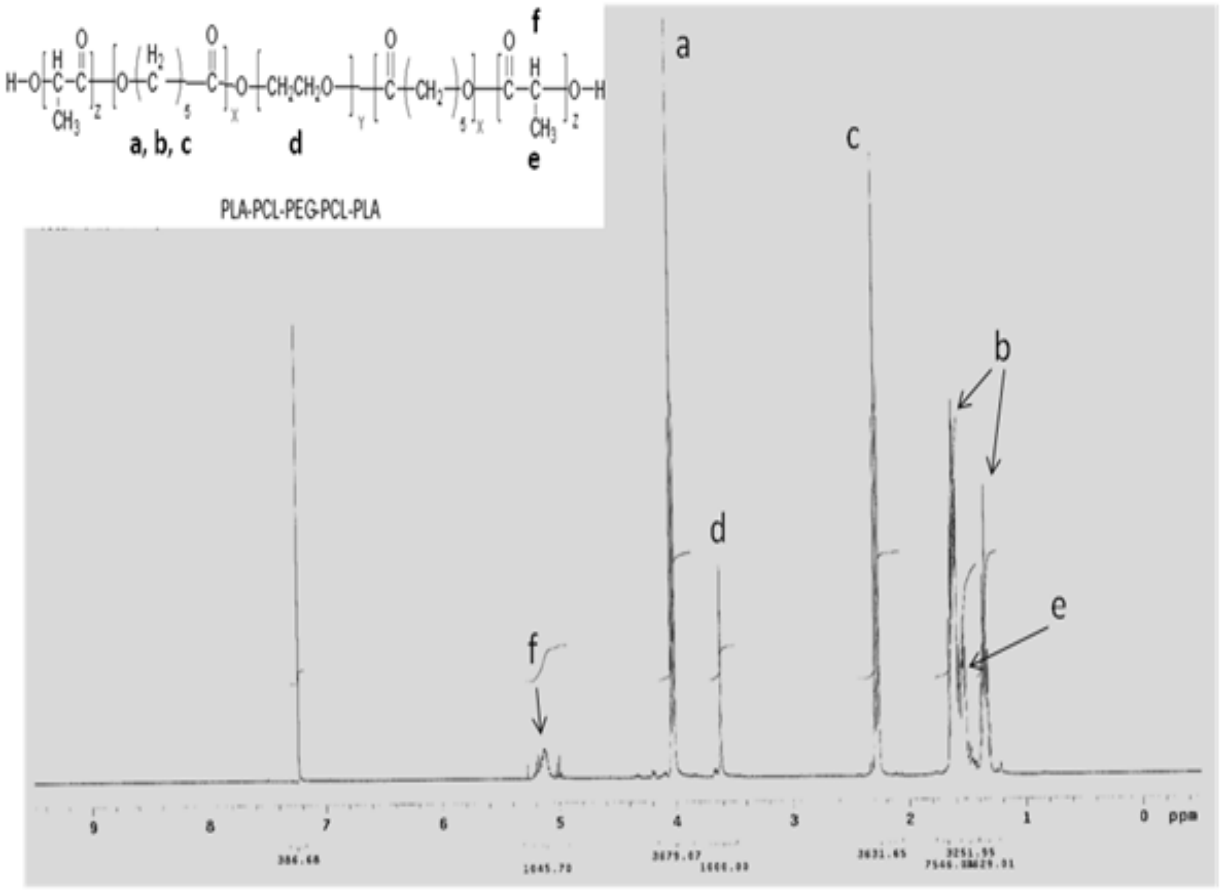

Figure 5.5 ^{1}H-NMR spectra of pentablock copolymer-C in $CDCl_3$

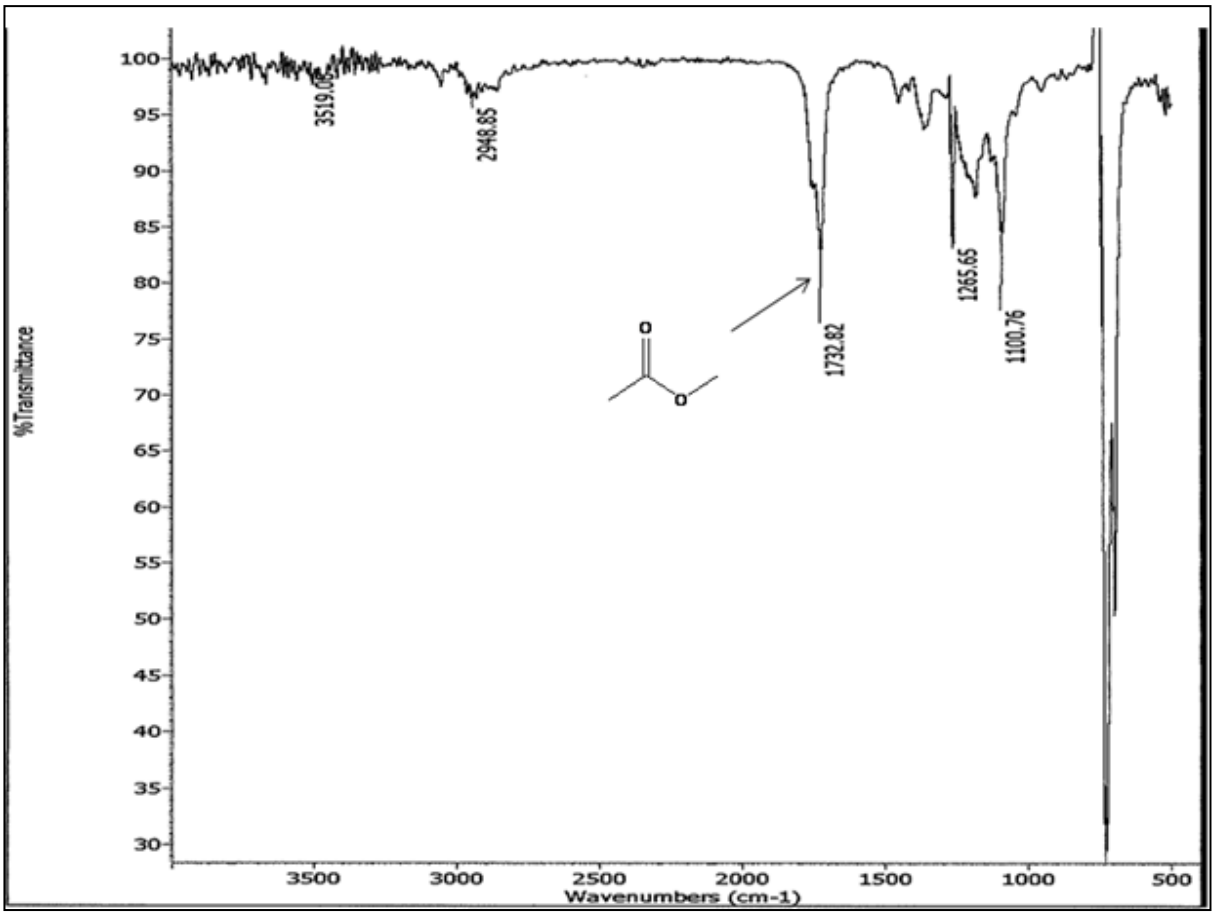

Figure 5.6 FTIR spectrum of pentablock copolymer

Preparation and Characterization of Nanoparticles

(i) Particle size

Prednisolone loaded nanoparticles were prepared by a single oil-in-water emulsification method utilizing PB-A, B and C. Particle size and drug encapsulation efficiency of nanoparticles were summarized in Table 5.1 Our study suggest that nanoparticles prepared from PB-A (Fig. 5.7) have larger particle size in comparison to PB-B and C (Fig. 5.9 and 5.12). Therefore, polymer composition has definite effect on the particle size but polymer molecular weight and hydrophobicity index did not exhibit any significant difference in particle size as evident in the case of PB-B and C.

(ii) Drug loading content and entrapment efficiency

Entrapment efficiency of prednisolone loaded nanoparticles mainly depended on the pentablock copolymer composition (Table 5.1). In the case of PB-A entrapment efficiency was around 65.4 ± 3.0%. On the other hand we found higher entrapment efficiency of prednisolone for PB-B and C which was 70.4 ± 2.7% and 71.2 ± 2.3% respectively. This difference in entrapment efficiency can be attributed to the difference in hydrophobicity of the copolymer. Polymer B and C are relatively more hydrophobic than polymer A. Prednisolone being a hydrophobic molecule tend to posses higher binding with the polymeric material having higher hydrophobicity. In addition, molecular weight of PB-B and C is higher than PB-A. Therefore, copolymer composition and molecular weight were the two dominant factors regulating the encapsulation efficiency.

(iii) Surface morphology and XRD analysis

Nanoparticles morphology was observed by SEM. Fig. 5.8, 5.10 and5.12 showed that all nanoparticles are spherical and possessed smooth surface morphology. Nanoparticles surface plays an important role in regulating translocation and interaction with biological membranes. These nanoparticles are spherical in shape and can be applicable for sustained and targeted delivery. The state of incorporated drug is an important factor that determines the release profile of drug delivery system. Fig. 5.13 examines XRD spectrum of polymer, drug and nanoparticles. We did not observed any diffraction peaks in the drug loaded nanoparticles matrix which suggested that drug existed in the amorphous state inside the nanoparticles. Therefore, nanoparticles processing parameter has a definite effect on the drug crystallinity.

Table 5.1 Nanoparticles characterization

Nanoparticles	Particle size (nm)	Polydispersity	Encapsulation efficiency
Polymer A	199.4 nm	0.231	65.4 ± 3.0 %
Polymer B	163.7 nm	0.182	70.4 ± 2.7%
Polymer C	157.1 nm	0.269	71.2 ± 2.3 %

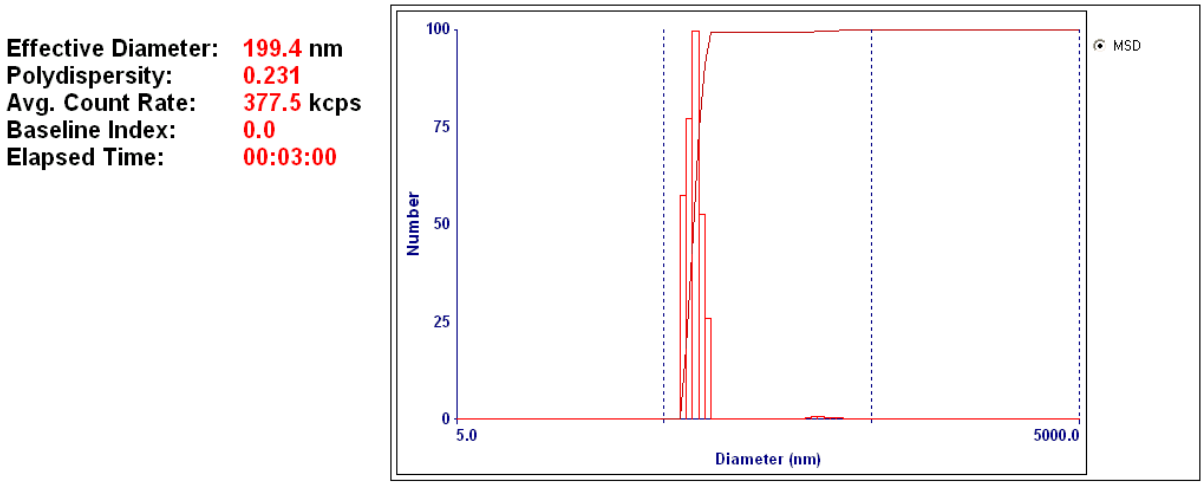

Run	Eff. Diam. (nm)	Half Width (nm)	Polydispersity	Baseline Index
1	198.7	91.3	0.211	0.0
2	201.0	99.8	0.246	0.0
3	198.8	96.0	0.233	5.6
Mean	199.5	95.7	0.230	1.9
Std. Error	0.8	2.4	0.010	1.9
Combined	199.4	95.9	0.231	0.0

Figure 5.7 DLS spectrum of nanoparticles prepared from pentablock copolymer-A

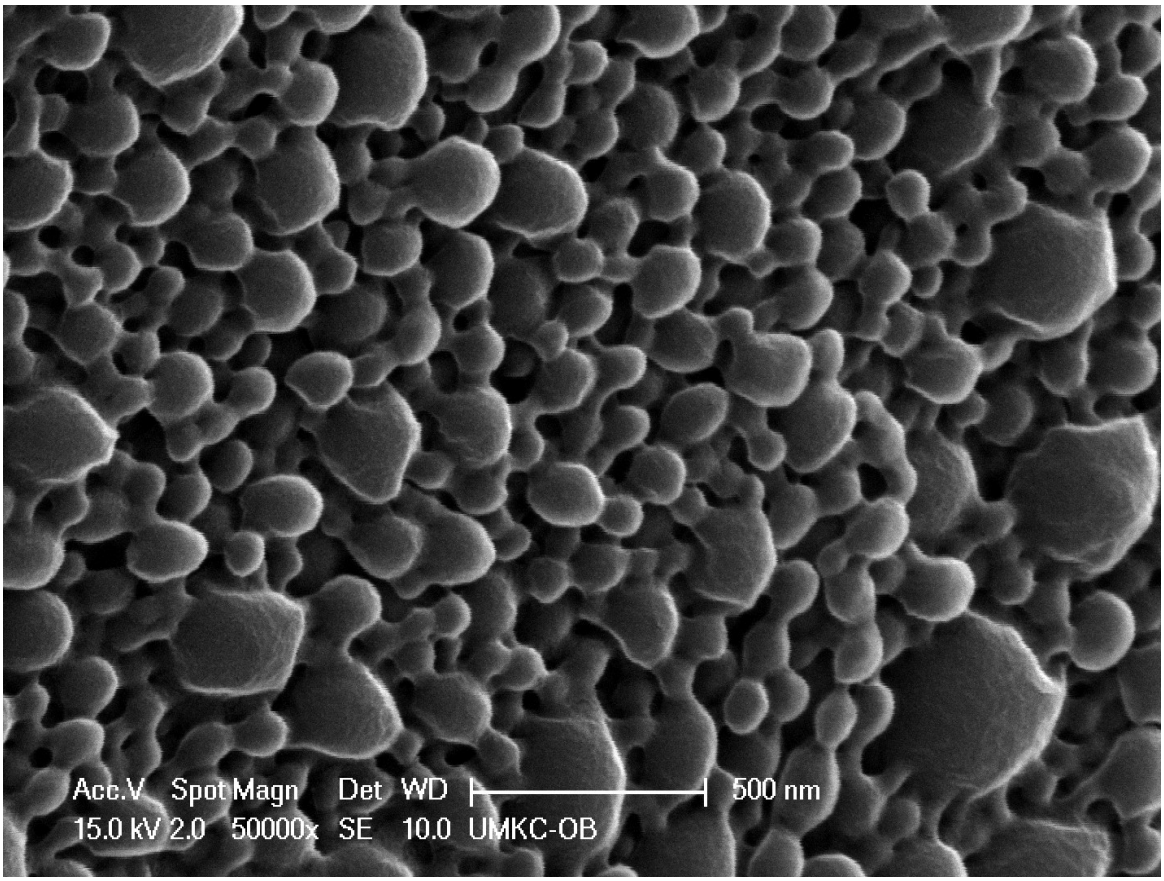

Figure 5.8 SEM image of nanoparticles prepared from pentablock copolymer-A

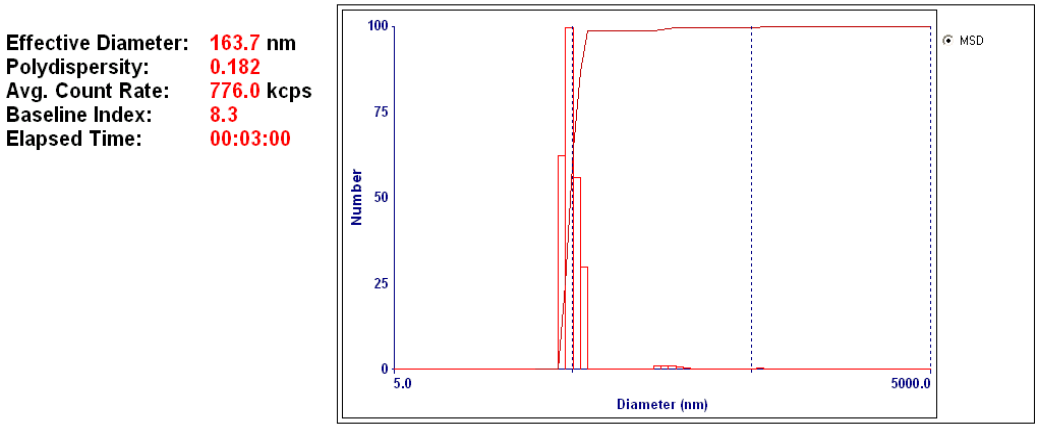

Run	Eff. Diam. (nm)	Half Width (nm)	Polydispersity	Baseline Index
1	162.1	68.2	0.177	8.2
2	164.0	69.0	0.177	7.5
3	162.9	69.8	0.183	9.5
Mean	163.0	69.0	0.179	8.4
Std. Error	0.5	0.5	0.002	0.6
Combined	163.7	69.8	0.182	8.3

Figure 5.9 DLS spectrum of nanoparticles prepared from pentablock copolymer-B

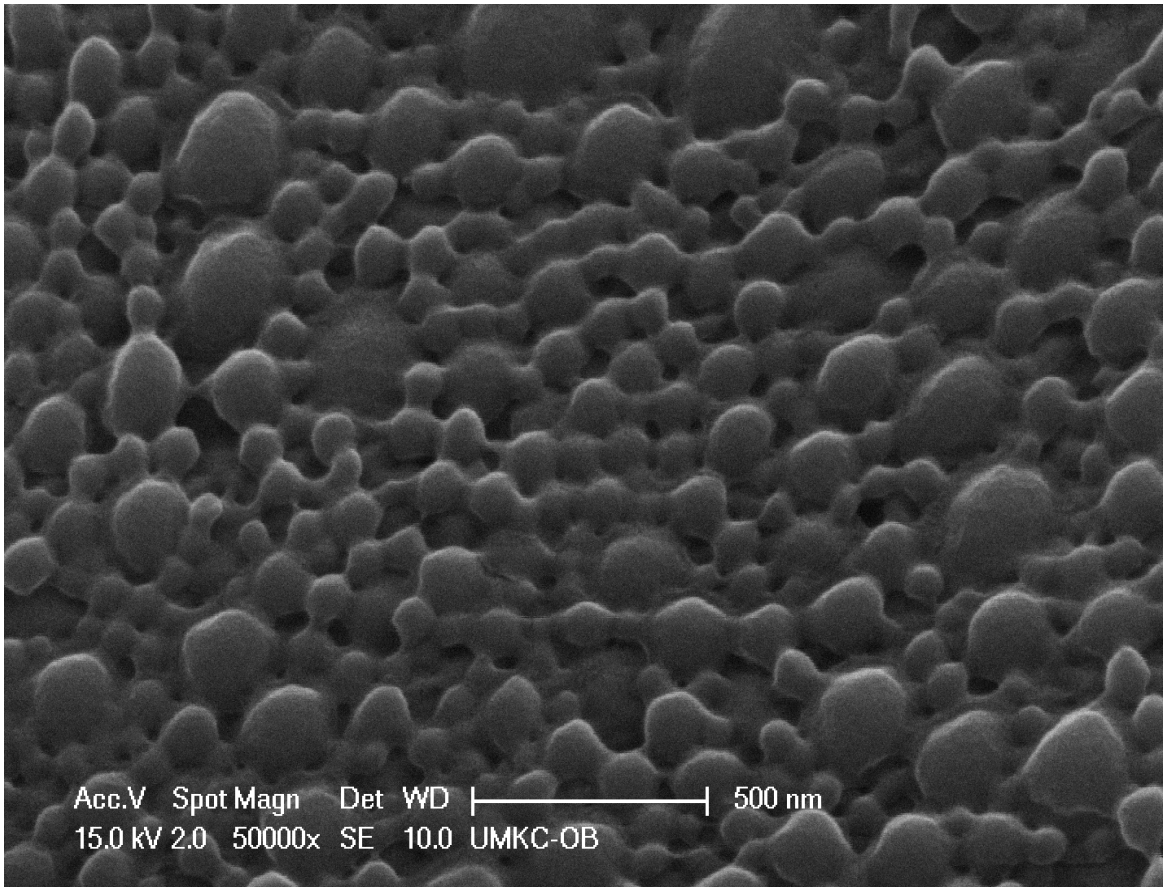

Figure 5.10 SEM image of nanoparticles prepared from pentablock copolymer-B

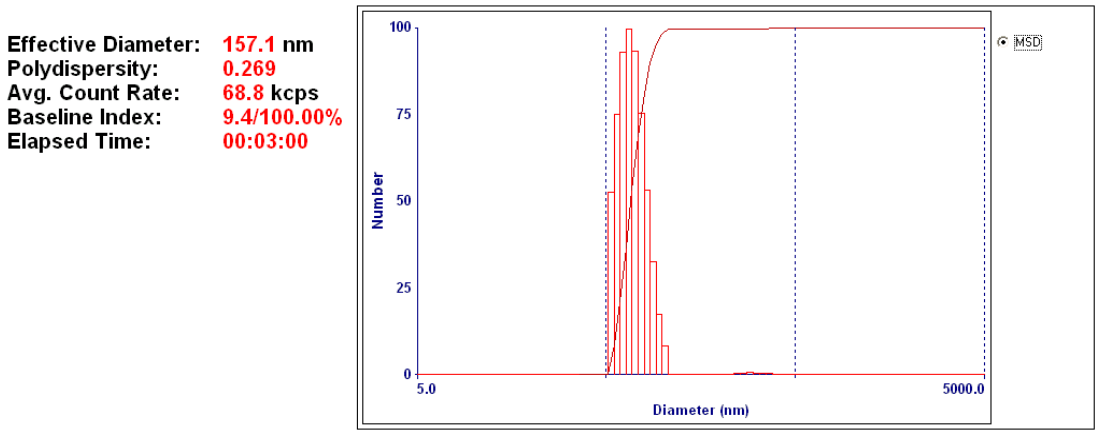

Run	Eff. Diam. (nm)	Half Width (nm)	Polydispersity	Baseline Index
1	154.7	81.2	0.275	9.7/100.00%
2	161.2	83.4	0.268	7.9/100.00%
3	155.6	80.1	0.265	9.2/100.00%
Mean	157.2	81.6	0.269	8.9/100.00%
Std. Error	2.0	1.0	0.003	0.5/ 0.00
Combined	157.1	81.5	0.269	9.4/100.00%

Figure 5.11 DLS spectrum of nanoparticles prepared from pentablock copolymer-C

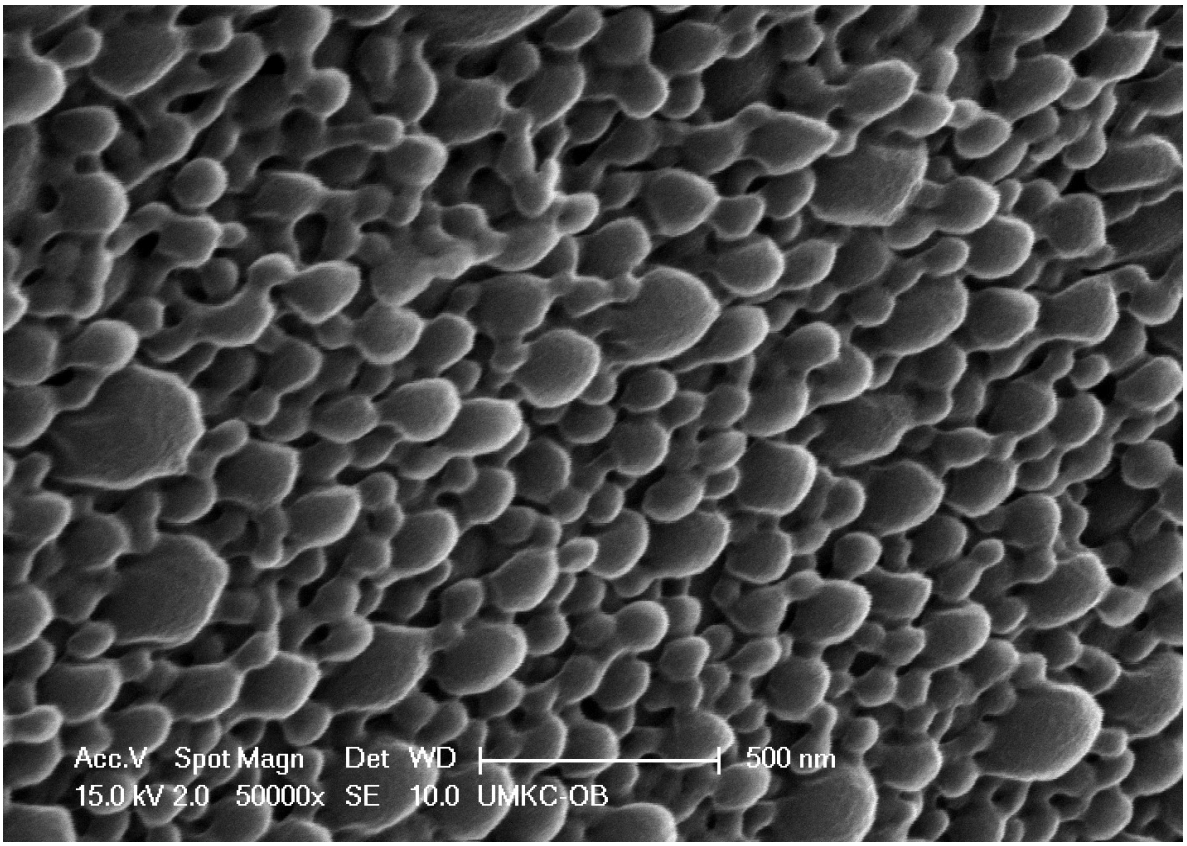

Figure 5.12 SEM image of nanoparticles prepared from pentablock copolymer-C

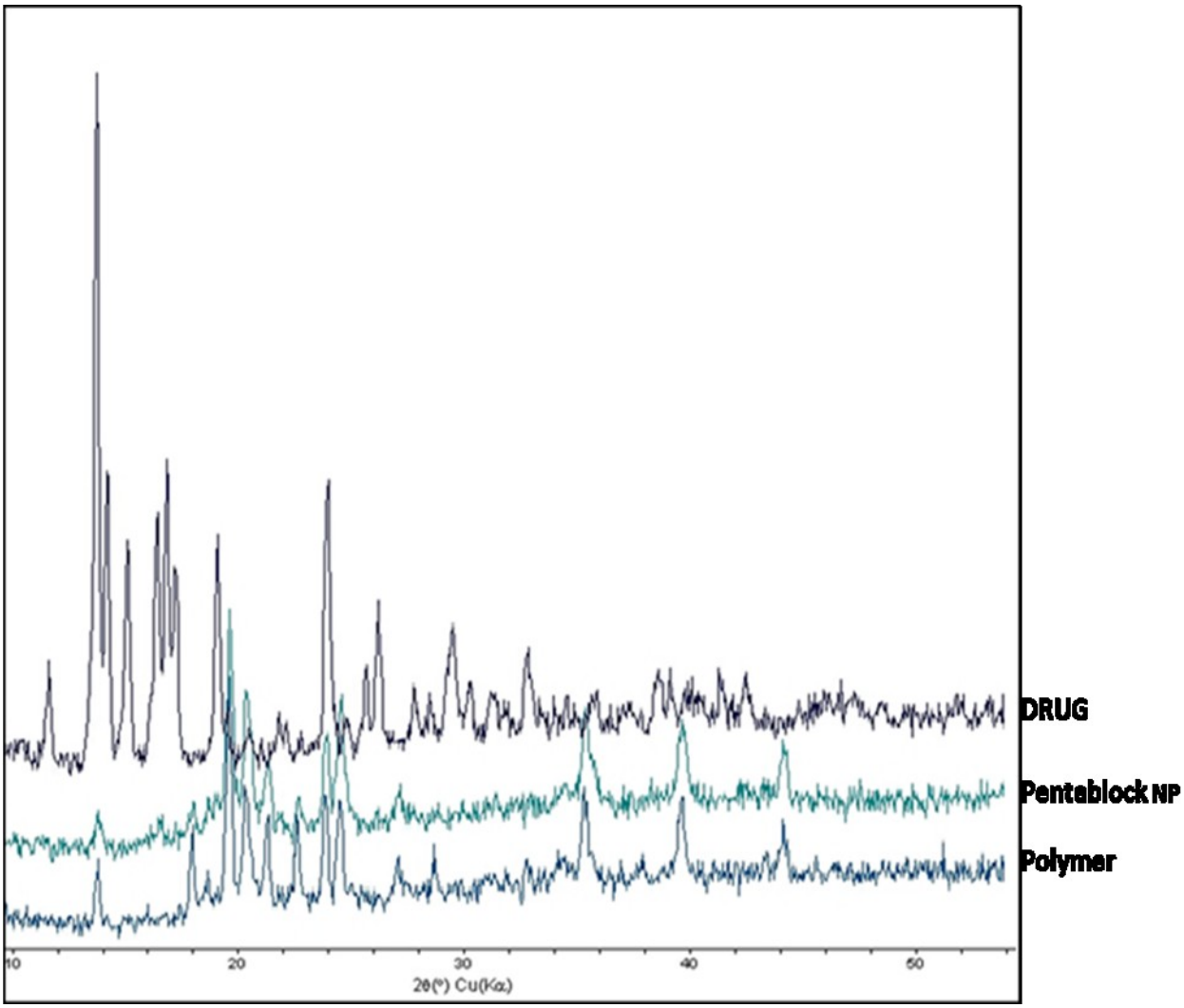

Figure 5.13 X-ray diffractogram of drug loaded nanoparticles, drug and polymer

In Vitro Drug Release Study

Fig. 5.14 and 5.15 demonstrated the release profile of prednisolone from pentablock copolymers nanoparticles. Our results indicate that 40.9 ± 2.9 % of drug release takes place within 23 h. These nanoparticles demonstrated high initial burst release phase due to surface adsorbed drug molecules. After high initial burst release phase, we observed that drug release rate was considerably reduced and continued upto 260 h. These results suggest that majority of the surface adsorbed drug molecules were responsible for high initial burst release phase. We speculate that PB-A is relatively hydrophilic and tends to have poor drug-polymer binding capacity. Therefore, majority of drug was not localized in the core of nanoparticles matrix. Moreover, PGA due to its faster degrading nature tends to contribute in the degradation mediated release profile. Nanoparticles composed of PB-C are relatively more hydrophobic and demonstrated slower release kinetics than PB-A. We observed that burst release phase was reduced in PB-C nanoparticles followed by continuous release kinetics. Polymer hydrophobicity and molecular weight are the two major factors responsible for slower drug release profile. PLA is relatively more hydrophobic and degrades slower than PGA. Therefore, contribution of degradation mediated drug release phase will not be significant in regulating the release kinetics. In addition, we presume that binding affinity of prednisolone acetate with PB-C was much higher than PB-A. Our results suggest that polymeric compositions can regulate the drug release kinetics. Future investigations in delineating the role of hydrophilic block molecular weight and crystallinity of PLA block can improve the understanding of drug release process.

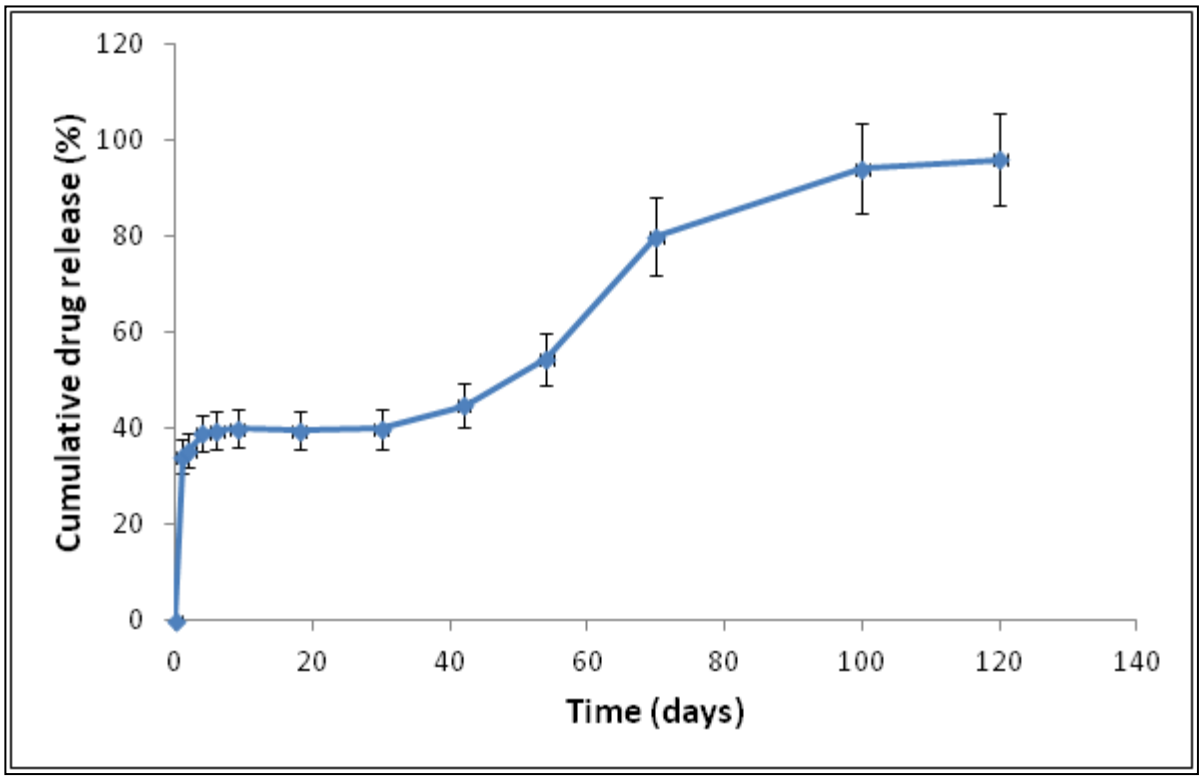

Figure 5.14 *In vitro* release of PB-A nanoparticles in PBS buffer (pH 7.4) at 37 °C. The values are represented as mean ± standard deviation of n = 3

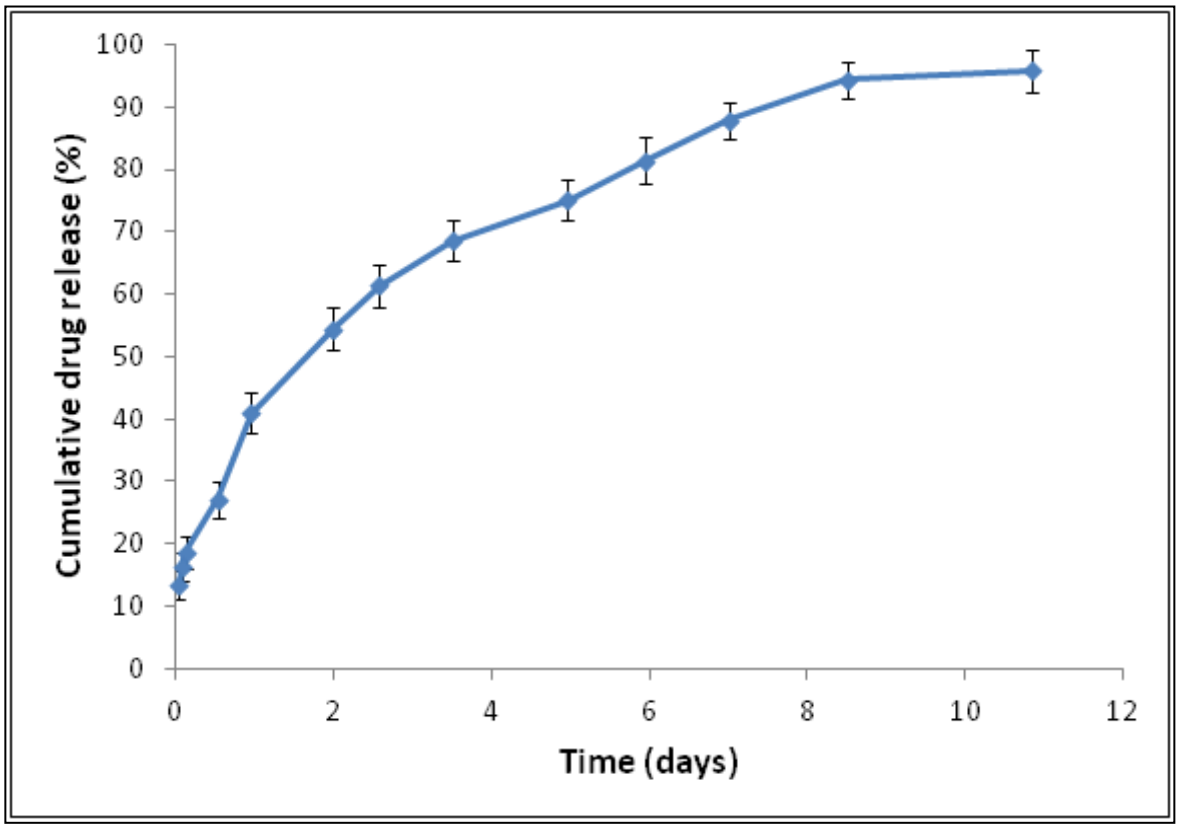

Figure 5.15 *In vitro* release of PB-C nanoparticles in PBS buffer (pH 7.4) at 37 °C. The values are represented as mean ± standard deviation of n = 3

Drug Release Kinetics

In vitro drug release from nanoparticles generally demonstrated burst release phase followed by continuous release phase. Evaluations of drug release profile through three different models (Higuchi, First order, and Korsmeyer model) provide more insight into the drug release mechanisms. We have observed that release rate constant was significantly decreased (Table 5.2) in the case of nanoparticles prepared from PB-C. Analysis of release data through Korsmeyer model suggested that nanoparticles of PB-A displayed K_{KP} value of 33.4 whereas in the case of nanoparticles from PB-C it was 12.6. Therefore, these results suggest that polymeric compositions significantly decrease the drug release rate. In addition, diffusion exponent value is less than 0.5 which suggested diffusion controlled drug release from both the compositions.

Table 5.2 Kinetic parameters of *in vitro* release profile of nanoparticles

Nanoparticles	First order		Higuchi		Korsmeyer-Peppas		
	r^2	k_o (h^{-1})	r^2	k_H ($h^{-1/2}$)	r^2	K_{KP} (h^{-n})	n
Pentablock copolymer-A	0.934	0.009	0.823	6.155	0.704	33.517	0.083
Pentablock copolymer-C	0.712	0.007	0.983	5.859	0.981	12.604	0.369

Conclusions

We have successfully synthesized and characterized different compositions of pentablock copolymers. In this work we have successfully delineated the role of polymeric compositions on nanoparticles size, encapsulation efficiency and drug release profile. We have observed that nanoparticles are spherical in shape with a mean diameter in the range of 150-250 nm. We observed that polymer compositions can modulate the drug release profile. Therefore, these polymeric compositions can be further optimized to achieve controlled release of therapeutic molecules of different size and polarity.

CHAPTER 6

EVALUATION OF DIFFERENT PENTABLOCK COPOLYMER COMPOSITIONS BIOCOMPATIBILITY UTLIZING VARIOUS CELL LINES

Rationale

Biodegradable polyesters such as PLA, PCL, and PLGA possess excellent biocompatible nature. Polymeric component utilized for the synthesis of pentablock copolymers are FDA approved. However, earlier investigations suggest that biocompatibility depends on processing method and properties of final polymeric material.

TNF-α is major inflammatory cytokine synthesized by macrophages. It has key role in apoptosis and also responsible for inducing tissue injury. IL-6 is a cytokine which perform functions such as acute phase reactions and nerve cell response. Production of IL-6 by macrophage is elevated after exposure to lipopolysaccharide (LPS) (main constituent of gram-negative bacteria cell membrane). It plays a key role in signal transition to immune cells such as neutrophils and macrophages resulting in the release of inflammatory mediators (Mishra et al., 2011). Biomaterial utilized for drug delivery should be non-toxic and non-immunogenic. Considering this we have evaluated the cytotoxicity of novel pentablock copolymers by direct exposure to various cell lines. However, cytotoxicity studies may not reveal the inflammatory response of the polymeric material. It is possible that non-cytotoxic material can trigger inflammatory response. Therefore, we evaluated the inflammatory response through macrophage activation by exposing the RAW 264.7 cell line to different polymeric concentrations. Considering this our investigation involves evaluating cell

viability and characterizing the inflammatory response on mouse macrophage cell line i.e. RAW 264.7. We have monitored the released of cytokines such as TNF-α, IL-6 and IL-1β after exposure to two different concentration of pentablock copolymers.

Material and Methods

The cytotoxicity and biocompatibility of the PB-A, B, C and PLGA were investigated in several cell lines. ARPE-19, SIRC and RAW 264.7 were procured from American Type Culture Collection (ATCC).

Cell Culture

ARPE-19 cells were grown in Dubelcco's modified Eagle's medium (DMEM/F12) supplemented with 10% fetal bovine serum (FBS), 100 U/mL penicillin and 100 μg/mL of streptomycin. SIRC cells were grown in minimum essential medium (MEM) and supplemented with 10% FBS, 100 U/mL of penicillin and 100 μg/mL of streptomycin. RAW 264.7 (Mouse macrophage cells) cells were cultured in DMEM/F12supplemented with 10% FBS, 10% of nonessential amino acids, 100 U/mL penicillin and 100 μg/mL of streptomycin. The pH of the medium was adjusted to 7.4 and cells were incubated in humidified atmosphere at 37 ºC temperature with 5% CO_2 environment. The cell were exposed directly to different concentrations of Pentablock Polymer A, B, C and PLGA.

Cell Viability Assay

Cell viability studies were performed utilizing MTS assays in which novel tetrazolium compound, 3-(4, 5-dimethylthiazole-2-yl)-5- (3-carboxymethoxyphenyl)-2-(4-sulfophenyl)-2H-tetrazolium (MTS) was reduced into a colored formazan product by live

cells. Rabbit primary corneal epithelial culture cells (rPCEC) were grown in the culture media comprising MEM, 10% FBS, HEPES, sodium bicarbonate, penicillin, and streptomycin sulfate. Cells were maintained under a humidified atmosphere of 5% CO_2 at 37°C and then sub cultured and seeded in 96-well culture plates at a density of 10,000 cells/well. After 24 h incubation, fresh media containing hydrogels of different concentrations ranging from 0.5 mg/ml to 20 mg/ml were added alone and with 5 wt% (PVA or PCL) polymeric additives. Triton X-100 (0.1%) was used as positive control while the blank (without treatment) was considered as negative control. Following 24 h incubation, 100 µL serum free medium containing 20 µL of MTS solution was added to the 96 well plates and were incubated at 37 °C and 5% CO_2 for 4 h. After incubation, the absorbance of each well was measured at 450 nm by an ELISA plate reader. Absorbance was directly proportional to viability of cells which was calculated by following equation.

$$\text{Cell Viability} = \frac{\text{(Abs. of sample) - (Abs. of negative control) * 100}}{\text{(Abs. of positive control) - (Abs. of negative control)}}$$

Cytotoxicity Assay/Lactate Dehydrogenase (LDH) Assay

To estimate the cytotoxicity of polymeric nanoparticles to the exposed cells lactate Dehydrogenase (LDH) assay was performed. Cell growth conditions were kept same as the MTS assay. Cells were seeded in 96-well culture plates at a density of 10,000 cells per well. At 70 % confluency, 200 µl fresh medium containing blank nanoparticles at different concentrations were added. Cells were incubated for 48 h at the humidified atmosphere at

37° C and 5% CO_2. Damage of the cell membrane or cell death releases the lactate dehydrogenase (LDH) in the supernatant. Concentration of LDH released in the supernatant of the rPCEC and ARPE-19 cells was measured by Cytotoxicity Detection Kit (Takara Bio Inc., Japan). Amount of the LDH release is directly proportional to the number of damaged cells. Less than 10% LDH release was considered as non toxic in our experiment and spectrophotometric determination was carried out at 450 nm.

Inflammatory Mediators Release Study

RAW 264.7 cells were cultured and incubated as described above in cytotoxicity studies. 1mg/50µL and 0.1mg/50µL of the polymer solutions (Pentablock polymer A, B, C and PLGA 50:50) were prepared in acetonitrile. These polymer solutions (300µL) were aliquot in 24 well plates, followed by overnight UV exposure. After getting 80% confluence, cells were trypsinised and 50000 cells were seeded per well. One set of wells were kept without polymers and considered as blank. Cells were incubated for 24 hours at 37° C and 5% CO_2 in humidified atmosphere. Sample volume of 120µL was collected at 6 and 24 hour from each well and stored at -80° C for ELISA assay.

Determination of TNFα, IL-6 and IL-1 β Levels in Cell Supernatant of RAW 264.7

The levels of TNFα, IL-6 and IL-1 β were measured by enzyme-linked immunosorbent assay (eBIOSCIENCE, USA). ELISA assay (Fig. 6.1) was performed as standard manufacturer protocol. Calibration curve of TNFα, IL-6 and IL-1β were prepared in the range of 10 pg/mL to 750 pg/mL, 5 pg/mL to 500 pg/mL and 10 pg/mL to 500 pg/mL respectively. Absorbance was measured at 450 nm by ELISA plate reader. Capture

antibodies for TNF α, IL 6 and IL 1β were diluted in coating buffer and 100 μL of resulting solutions were aliquoted in each well of 96 well plate. Assay plate was incubated overnight at 4°C. After aspiration of solutions, plate was washed three times with wash buffer followed by addition of 200 μL of blocking solution in each well and incubated for 2 hours at room temperature. A 100 μL of samples and standard solutions (ranging from 10 – 1000 pg/mL for TNF α, 5 – 500 pg/mL for IL 6 and 10 – 1000 pg/mL for IL 1β) were aliquoted in each well and kept overnight at 4 °C. Plates were washed and aliquoted with 100 μL/well of detection antibodies, and incubated at room temperature for 1 hour. After washing, Avadin-HRP conjugate (100 μL/well) was added in the plates and incubated for 30 mins. After final washing, 100 μL of substrate solution was added and incubated for 10 – 15 mins followed by addition of 50 μL of stop solution. Samples were analyzed at 450 nm and 570 nm wavelengths. Absorption values of 570 nm were subtracted from 450 nm for final calculation.

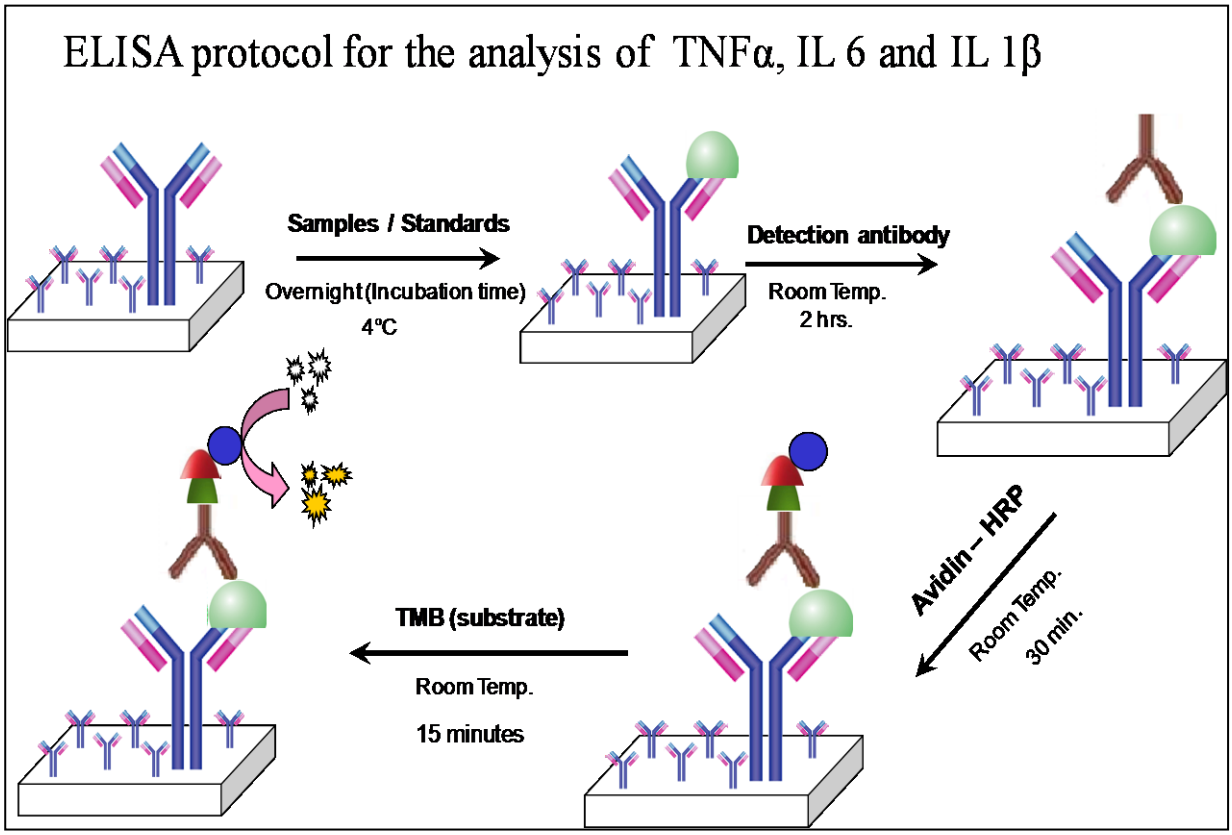

Figure 6.1 Schematic of ELISA assay

Result and Discussion

Cytotoxicity Studies on ARPE 19 Cells

Cytotoxicity studies suggested that pentablock copolymers were not cytotoxic (Fig. 6.2 and 6.3) to ARPE-19 cells. At the concentration of 20 mg/ml pentablock copolymers showed 10.24 ± 1.73 % of cytotoxicity in comparison to control whereas polymers PB-B and PB-C demonstrated 7.54 ± 0.79 and 4.2 ±1.5 % of cytotoxicity respectively. These results are comparable to PLGA which showed 8.1 ± 5.0 % of cytotoxicity. Our results suggest that PB-B and PB-C were more biocompatible to ARPE-19 cells in comparison to PB-A and PLGA. At lower concentration (2 mg/ml) we did not observed any significant cytotoxicity. This difference in cytotoxicity may be attributed to low molecular weight of PGA block in PB-A which has higher tendency to degrade faster. PB-A possesses PGA of molecular weight 300 on either side of the polymeric chain. Earlier reports suggest that degradation of polyester depends on the molecular weight. Therefore, in the case of PB-A faster degradation of PGA may lead to higher cytotoxicity.

In addition, it is well known that PGA degrades at faster rate in comparison to PLA. PB-A, PB-B and PB-C differs primarily in the molecular weight of end block. In the case of PB-A, PGA is of low molecular weight whereas PB-B and PB-C possess PLA of high molecular weight. Therefore, molecular weight and composition of block copolymers are the key factors responsible for the difference in cell cytotoxicity.

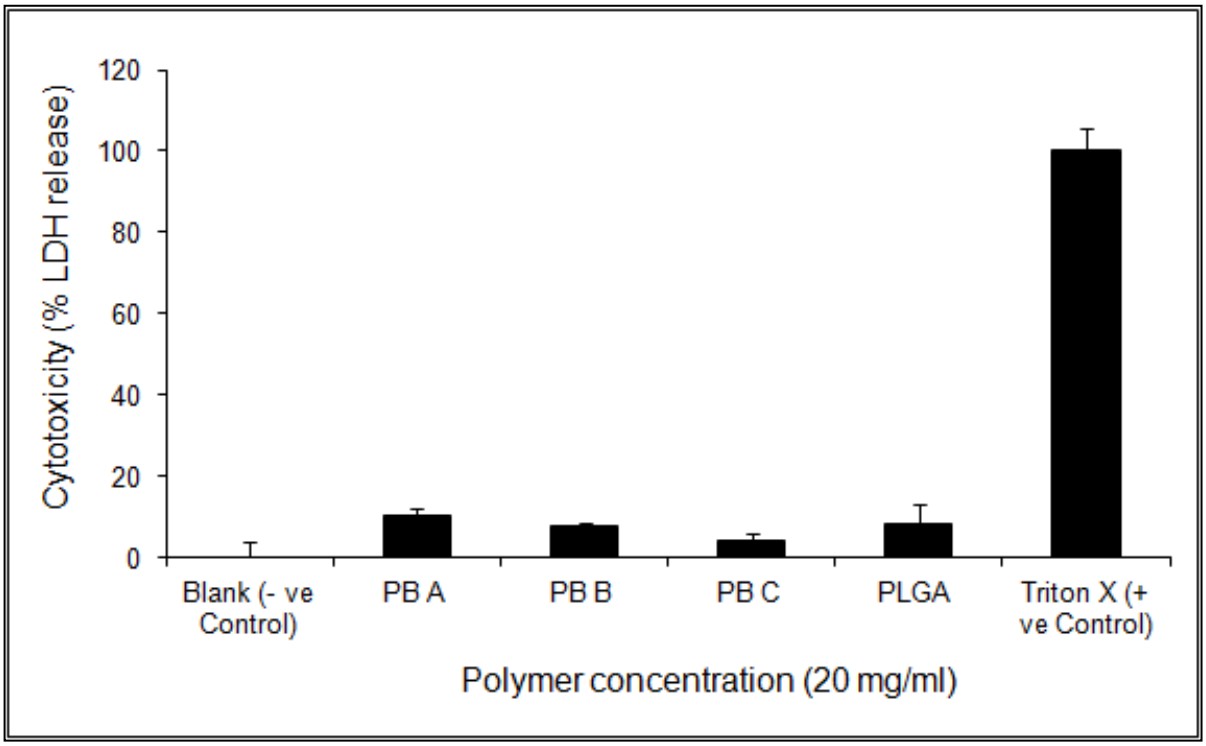

Figure 6.2 LDH (%) release from the ARPE 19 cells when exposed to the 20 mg/ml of PB-A, PB-B, PB-C and PLGA (50:50)

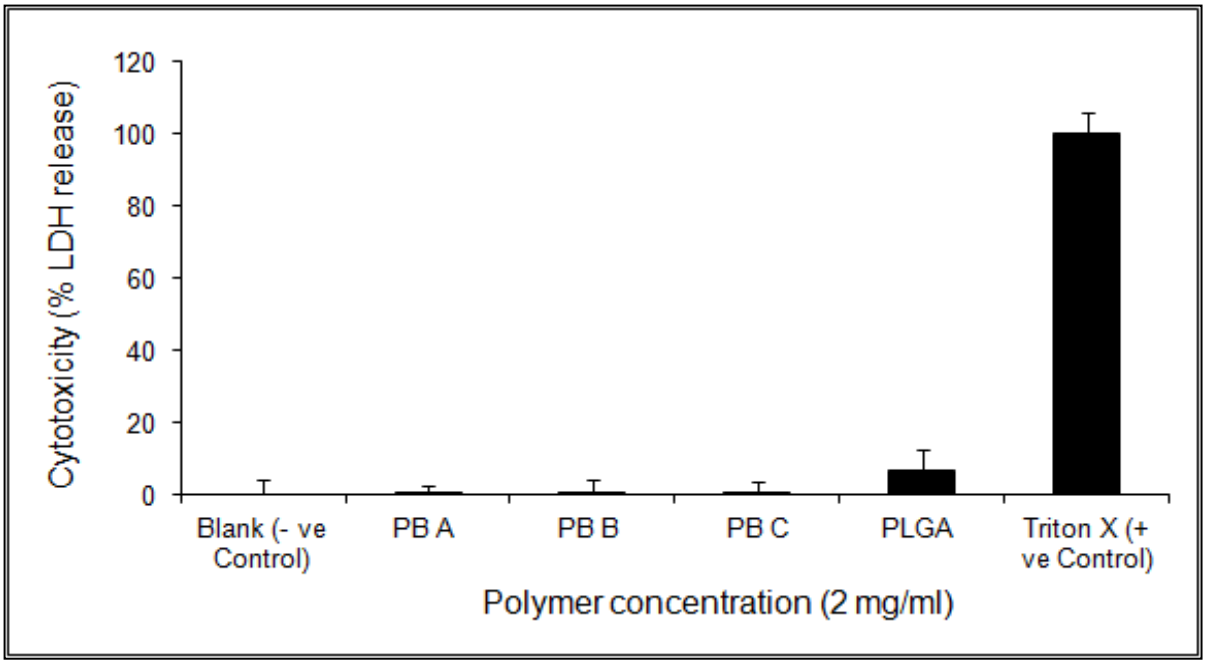

Figure 6.3 LDH (%) release from the ARPE 19 cells when exposed to the 2 mg/ml of PB-A, PB-B, PB-C and PLGA (50:50)

Cell Viability Studies on RAW 264.7 Cell Line

Cell viability studies demonstrate that in the presence of PB-A, B and C at the concentration of 20 mg/ml viability of RAW 264.7 cells were 83.7 ± 4.2%, 86.5 ± 4.2% and 94.0 ± 1.3% respectively. In all the cases cell viability was higher in comparison to PLGA. Assessment of cell viability in RAW 264.7 provided a clear evidence that pentablock copolymers were biocompatible and can be applicable for ocular drug delivery. Our results indicated a difference in cell viability between PB-A, B and C. This difference can be attributed to the polymer compositions (Fig. 6.4 and 6.5). In PB-A faster degradation of PGA block might have resulted in less viability in comparison to pentablock copolymers B and C. However, at low concentration of 2 mg/ml cell viability was not significantly different in the case of polymer PB-A, B and C. We presume that no significant difference in cell viability was not evident because the concentration of glycolic acid released after degradation was very low to induce any cytotoxicity. Furthermore, we observed similar trend in cytotoxicity studies performed on ARPE-19 cell-line. In this study, we have prepared polymeric film and then seeded the cells. Therefore, our result also indicated cell attachment tendency on the polymeric surface. Other reports also suggest that attachment of macrophages to hydrophilic surface is less in comparison to hydrophobic surface. PB-A is relatively less hydrophobic in comparison to PB-B and C. Therefore, PB-B and C may not favor cell attachment. Difference in the polymer hydrophobicity index may be another potential reason for the difference in cell viability. Our study indicate that PB-C is more cytocompatible in comparison to PB-A. Further studies with PEG of high molecular weight may elucidate the role of hydrophilic block in cell attachment and proliferation.

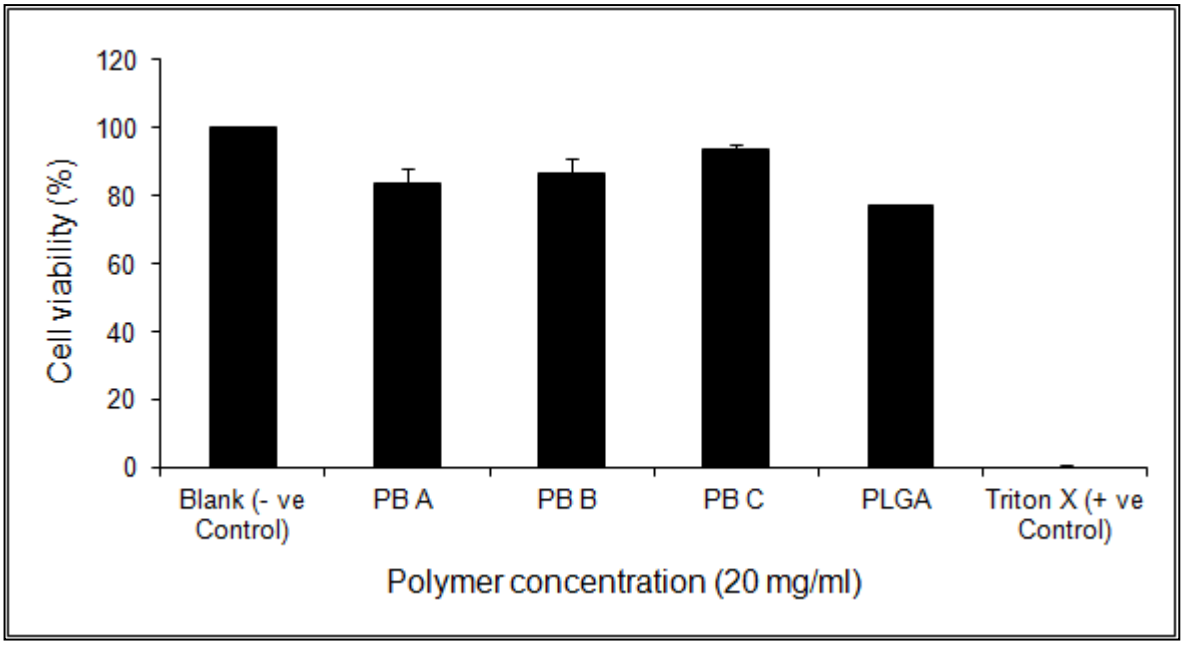

Figure 6.4 Cell viability (%) of the RAW 264.7 cells when exposed to the 20 mg/ml of PB-A, PB-B, PB-C and PLGA (50:50)

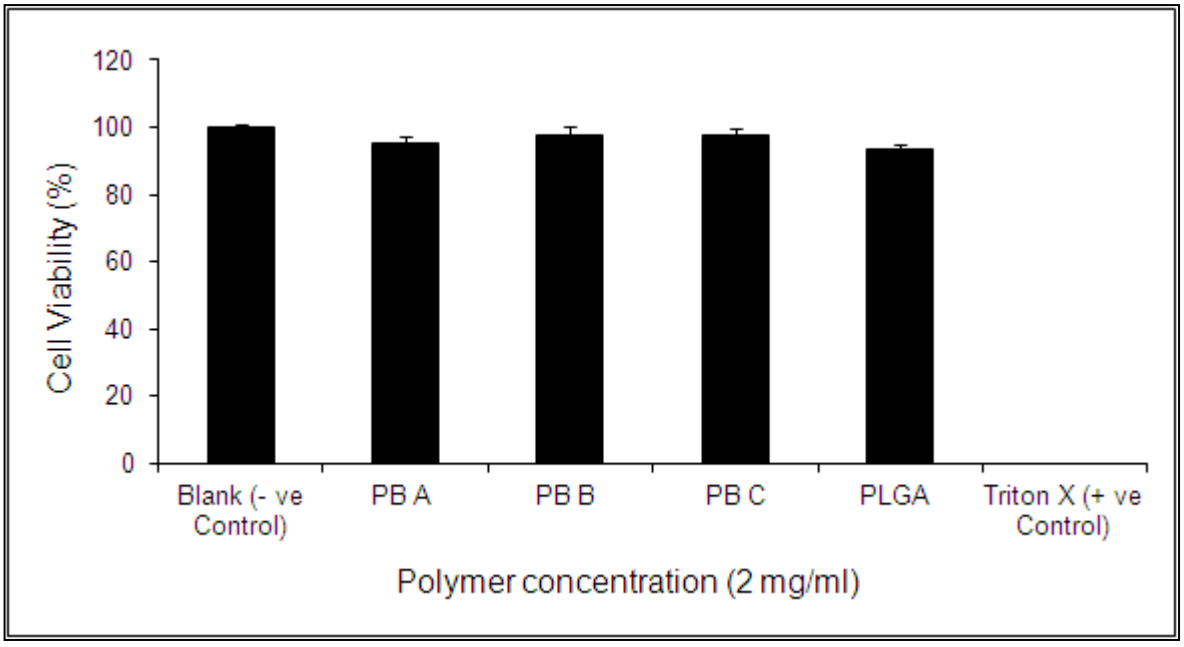

Figure 6.5 Cell viability (%) of the RAW 264.7 cells when exposed to the 2 mg/ml of PB-A, PB-B, PB-C and PLGA (50:50)

Inflammatory Response after Exposure to Pentablock Copolymers

Release of inflammatory mediators TNF-α, IL-6 AND IL-1β were measured after exposure to PB-A,B and C for 24 h. Cells without treatment were considered as negative control and LPS was considered as positive control. LPS is recognized through toll like receptor which subsequently phosphorylates and send signal for the activation of mitogen activated kinase. This process followed by translocation of genes which is mainly responsible for cytokine generation. Our result indicates negligible release (Fig. 6.6 and 6.7) of inflammatory mediator TNF-α after exposure to PB-A, B and C in comparison to control. We observed similar release of TNF-α at two different concentrations. These results suggested that even higher cytotoxicity was observed in the case of PB-A but in terms of immunogenic response different composition demonstrated comparable release of TNF-α. In addition, we did not observed concentration dependent repose which further confirms that pentablock copolymers were non-immunogenic in nature. We have selected RAW 264.7 cell line because it is recommended by American Society of Testing and Materials for the evaluation of biocompatibility of novel biomaterials. We also monitored the release of IL-6 (Fig. 6.8 and 6.9) which is responsible for late phase of innate response and IL-1β (Fig. 6.10 and 6.11) which is involved in the acute phase response. We did not observe any significant release of IL-6 and IL-1β in comparison to control at two different concentrations (0.6 and 6 mg/ml) after exposure for 24 h. Therefore, our results provided strong evidence for the future application of pentablock copolymers for drug delivery. Studies performed by other investigators with biomaterials such as PEG/Polyacrylic acid and crosslinked PEG demonstrated release of TNF-α in a time and dose dependent manner (Sethi et al., 2003; Yim et al., 2009).

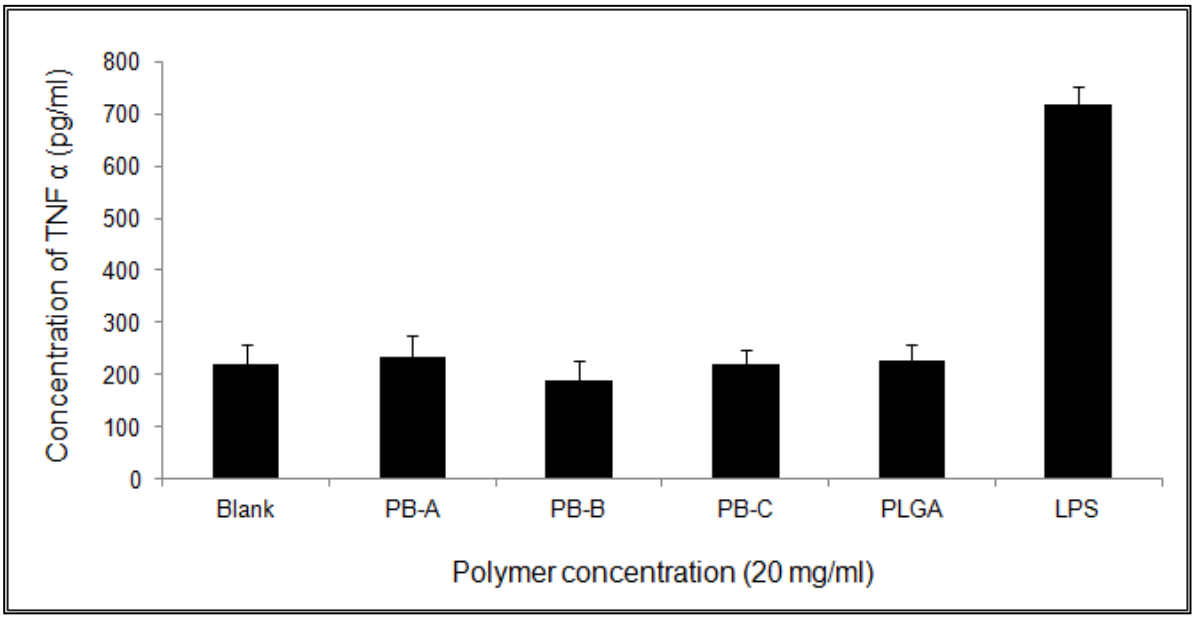

Figure 6.6 TNF-α release from RAW 264.7 cell after exposure to 20 mg/ml of different polymers

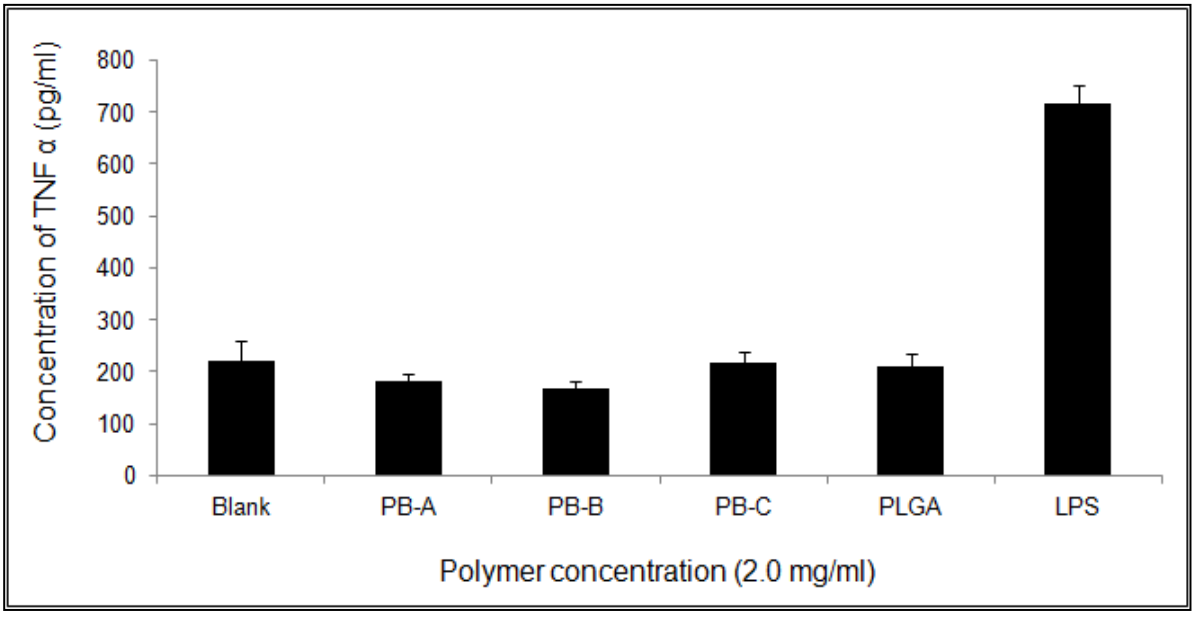

Figure 6.7 TNF-α release from RAW 264.7 cell after exposure to 2 mg/ml of different polymers

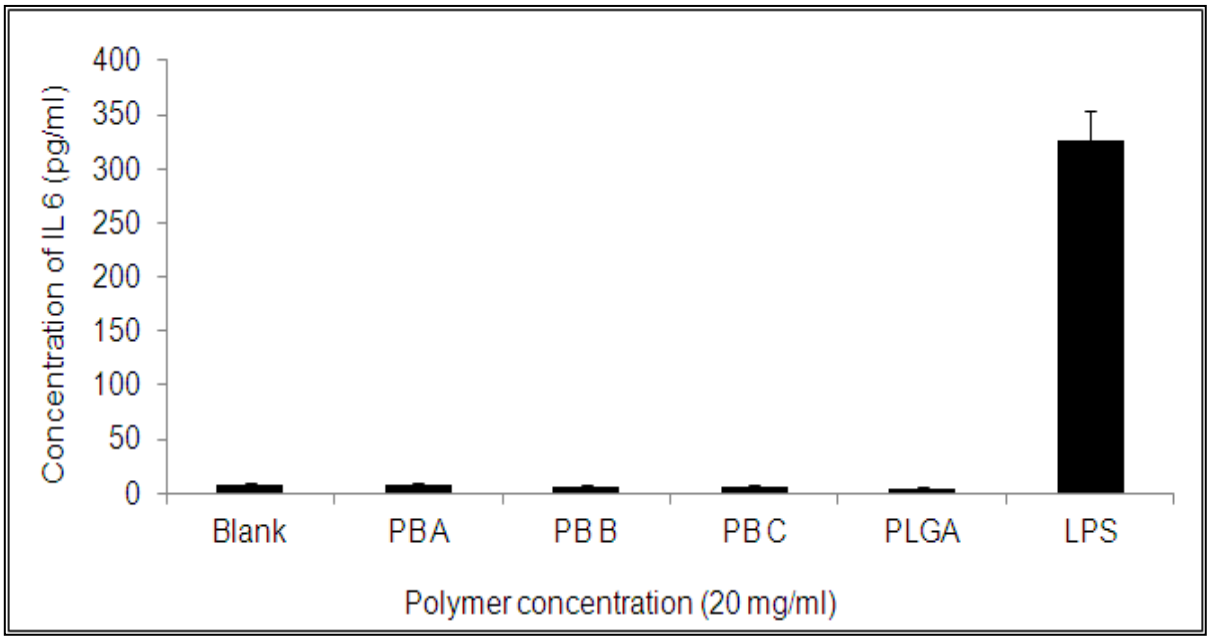

Figure 6.8 IL-6 release from RAW 264.7 cell after exposure to 20 mg/ml of different polymers

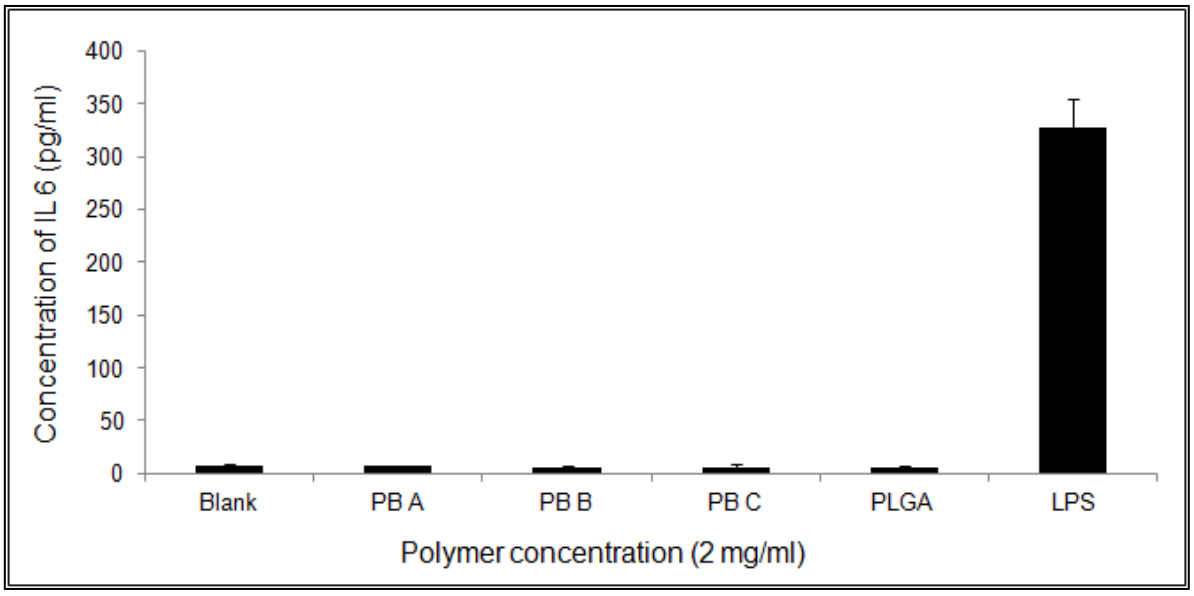

Figure 6.9 IL-6 release from RAW 264.7 cell after exposure to 2 mg/ml of different polymers

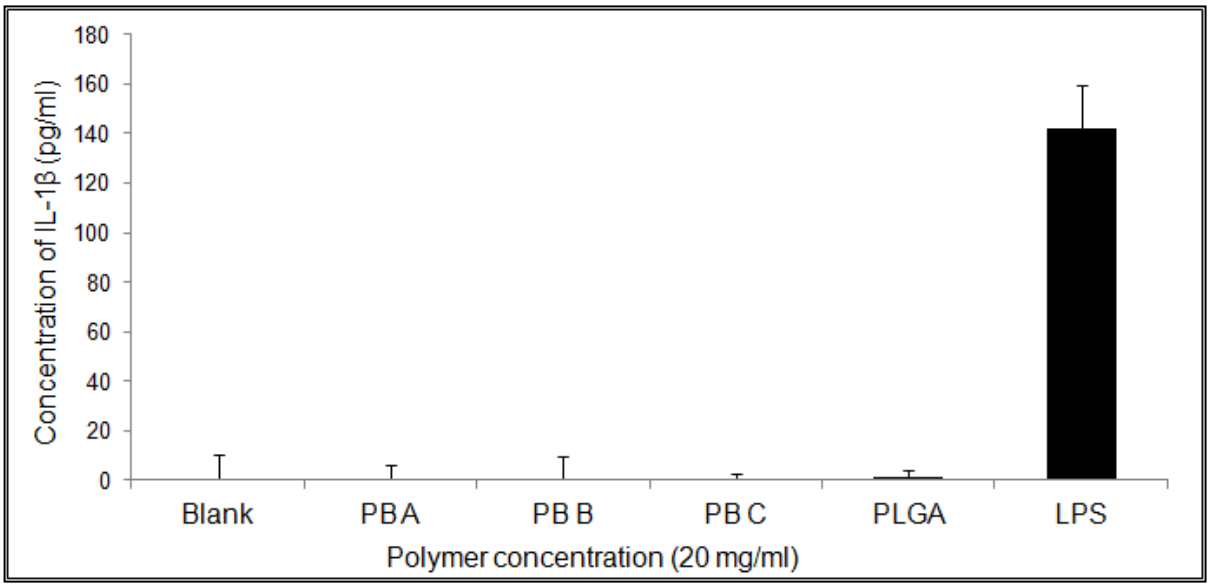

Figure 6.10 IL-1β release from RAW 264.7 cell after exposure to 20 mg/ml of different polymers

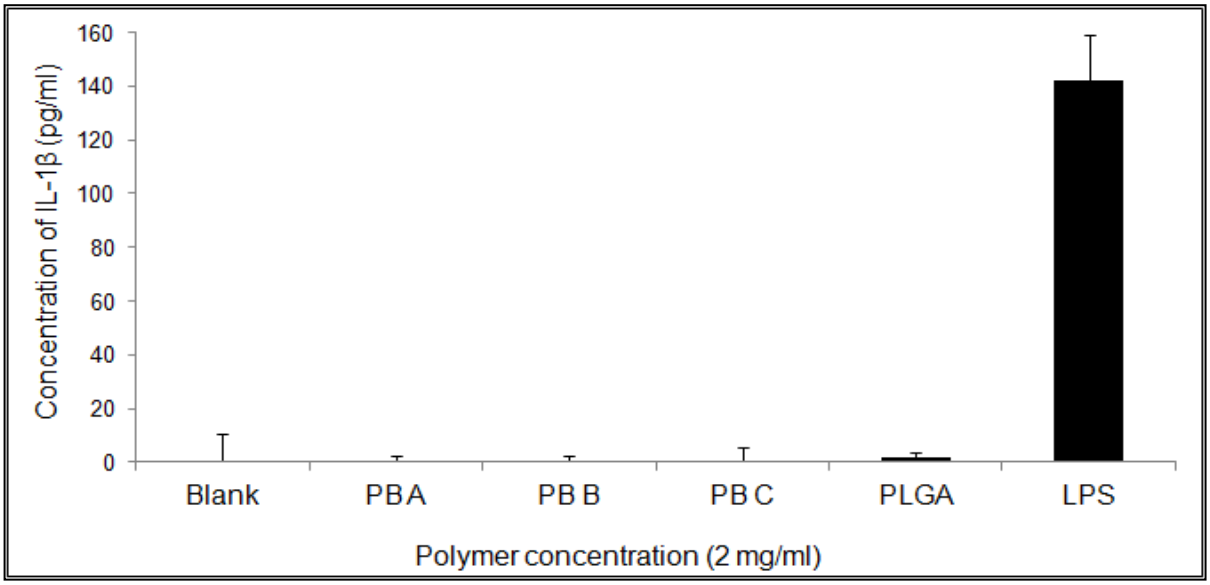

Figure 6.11 IL-1β release from RAW 264.7 cell after exposure to 2 mg/ml of different polymers

Thus, our polymeric material has superior biocompatibility profile in comparison to other materials which are commonly utilized for biomedical applications.

Conclusions

Our results suggest that pentablock copolymer is biocompatible to ocular cell line i.e. ARPE-19. We observed that pentablock copolymer block composition and molecular weight has definite effect on the cell viability. Pentablock copolymer-B and C are lees cytotoxic in comparison to copolymer-A. However, all the compositions displayed negligible release of major inflammatory mediators i.e. TNF-α, IL-6 and IL-1β from macrophage cell line. Therefore our novel pentablock copolymers could be applicable for ophthalmic drug delivery.

CHAPTER 7

DEVELOPMENT AND EVALAUTION OF COMPOSITE FORMULATIONS OF NANOPARTICLES SUSPENDED IN THERMOSENSITIVE HYDROGEL

Rationale

In this work composite formulations of nanoparticles suspended in thermosensitive hydrogel were evaluated. By varying the block ratio, copolymer molecular weight and block rearrangement pentablock could be utilized for the preparation of nanoparticles and thermosensitive hydrogel (Gong et al., 2009a). Earlier we have dispersed the hydrophobic drug (prednisolone acetate) into the aqueous polymeric solution at room temperature. The drug loaded solution eventually transform into hydrogel matrix as the temperature changes to 37 °C. Thermosensitive hydrogel demonstrate solution to gel state transition in response to temperature stimuli. The temperature at which sol-gel transition takes place is known as critical solution temperature. At critical solution temperature conformational changes occurs due to physical crosslinking of polymeric chain matrix which are reversible in nature and returns to its original state after removal of thermal stimulus (Jeong et al., 2000). Physical cross linking results in the formation of three dimensional matrices, which act as a reservoir for controlled drug delivery. Thermosensitive block copolymers have gained significant attention due to their potential application in the development of *in situ* depot forming injectable controlled release formulations (Packhaeuser and Kissel, 2007; Ryu et al.). Block copolymers such as poly (N-isopropylacrylamide), poly vinyl ether, pluronic and PEG conjugated polyesters are commonly explored over the past decade (Chung et al., 2002; Derakhshandeh et al. 2010; Lee et al., 2006; Sun et al., 2006; Zhang et al., 2009).

Release of drug from the polymeric matrix takes place through diffusion and degradation mechanism (Lao et al., 2011; Siepmann and Gopferich, 2001). However, uniform dispersion of hydrophobic molecule inside the polymeric matrix is difficult to achieve. In this regard, nano encapsulation of hydrophobic drug in the polymeric matrix may provide enhanced stability and solubility (Shuai et al., 2004; Zhang et al., 2011). It is interesting to note that both the pentablock copolymers have PEG and PCL but the block arrangement and molecular weight was different. We have used PEG-PCL-PLA-PCL-PEG for the preparation of thermosensitive hydrogel whereas PGA-PCL-PEG-PCL-PGA for the fabrication of nanoparticles. We expect that composite delivery system of nanoparticles suspended in thermosensitive hydrogel will remain in solution state at room temperature and eventually transform in to hydrogel (Duvvuri et al., 2005; Gong et al., 2009a; Gou et al.). In addition, it will reduce the chances of precipitation of hydrophobic drug and also prolonged the drug release. We have monitored the in vitro drug release profile and also performed biocompatibility studies on human conjunctival cell line.

Material and Methods

PEG (Mn=1000) was purchased from Sigma (USA). PEG was dried under vacuum at 60 °C. ε-caprolactone, glycolide, stannous octoate, mPEG (Mn=550) were obtained from Sigma chemical company (St. Louis, MO). Hexamethylene diisocyanate (HMDI) (Aldrich) was procured from Acros organics (Morris Plains, NJ). Methylene chloride and petroleum ether was obtained from Fischer Scientific (USA). All other reagents utilized for this study are of analytical grade and used without further processing. Human conjunctival epithelial cells (HCEC) cells were procured from ATCC (USA).

Synthesis of PGA-PCL-PEG-PCL-PGA/PLA-PCL-PEG-PCL-PLA for Nanoparticles

Pentablock copolymers were synthesized in two steps by sequential ring opening polymerization method. Detailed synthetic scheme was mentioned in chapter 5.

Synthesis of PEG-PCL-PLA-PCL-PEG for the Preparation of Thermosensitive Hydrogel

Synthetic method discussed in chapter 4 was utilized for the preparation of thermosensitive hydrogel.

In Vitro Release Study

20 wt. % of PGPCPL-2 was solubilized in 10 mM PBS by keeping overnight at 4 ºC. Then prednisolone acetate nanoparticles (140 mg) drug equivalent to 250 µg, prepared from Pentablock Polymer A were dispersed in 20% w/w thermosensitive polymer solution. Then polymeric aqueous solution (0.4 ml) was injected into 10 ml vial with 12 mm internal diameter. Vials were kept in shaker bath at 37 $^{\circ}$C with a stroke rate of 30 rpm. The polymeric solution was allowed to gel for 2 min. Then 5 ml of the release medium containing phosphate buffer (pH 7.4) and sodium azide (0.02 wt%) were added in order to prevent microbial contamination during a release study. The entire release medium was replaced with fresh buffer at predetermined intervals to mimic the sink condition. Samples were stored at -20^{0} C until further analysis. The release samples were analyzed by high performance liquid chromatography (HPLC).

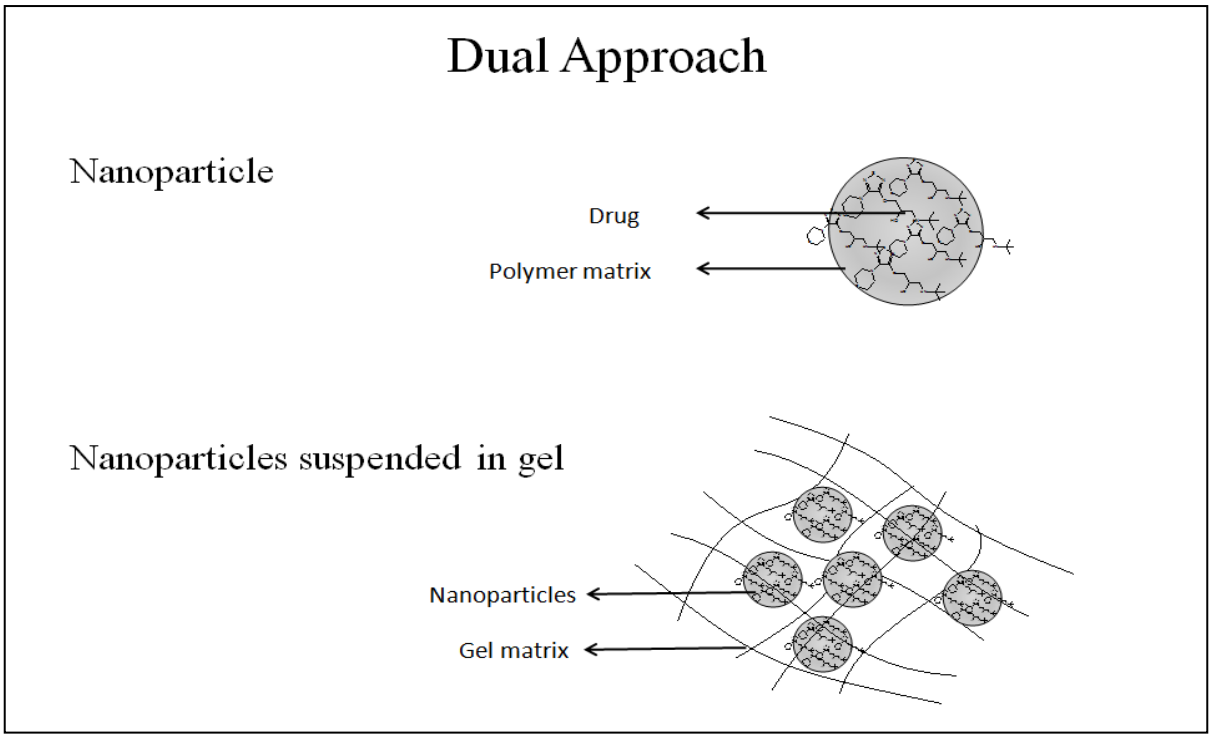

Figure 7.1 Schematic representation of composite approach

Release of Inflammatory Mediators

Lipoteichoic acid (LTA) is a component of Gram-positive bacterial cell wall. LTA can interact with Toll-like receptor 2 (TLR2) of HCEC cells and stimulates release of cytokines such as TNFα, IL 6 and IL 1β. Hence, in this study LTA (50 μg/mL) was used as positive control and blank was considered as negative control. The levels of TNFα, IL-6 and IL-1 β were measured by enzyme-linked immunosorbent assay (eBIOSCIENCE, USA). ELISA assay was performed as standard manufacturer protocol. Calibration curve of TNFα,

IL-6 and IL-1β were prepared in the range of 10 pg/mL to 750 pg/mL, 5 pg/mL to 500 pg/mL and 10 pg/mL to 500 pg/mL respectively. Absorbance was measured at 450 nm by ELISA plate reader.

Result and Discussion

Application of pentablock copolymers for ophthalmic delivery depends on the absence of release of inflammatory mediators from HCEC upon exposure for different time duration. Release of TNF-α, IL-6 and IL-β were monitored at 24, 48, and 72 h after exposure to two different compositions of pentablock copolymers based hydrogel. Our results indicated that release of inflammatory mediators was comparable to negative control (Cells without treatment). Lipoteichoic acid was taken as the positive control and release of inflammatory mediators from HCEC was increased with time duration. For instance, at 24 h, 48 and 72 h increase in TNF-α concentration (Fig. 7.2 and 7.3) in the cell supernatant was observed.

These findings suggested that release of inflammatory mediators was negligible even up to concentration of 20 mg/ml. Furthermore, concentration we have utilized for the studies are very high for *in vitro* experiments. Therefore, our results validate our hypothesis that these materials could be applicable for subconjunctival delivery. In comparison to the studies performed with other biomaterial, we did not observed any significant dose and time dependent release of TNF-α, IL-6 and Il-1β (Fig. 7.4, 7.5, 7.6 and 7.7) after exposure to two different compositions of pentablock hydrogel. Since our target site for application of these polymeric material is conjunctival space. Therefore, monitoring the release of inflammatory indicators such as TNF-α, IL-6 and IL-1β was a definite indication of their non-inflammatory nature.

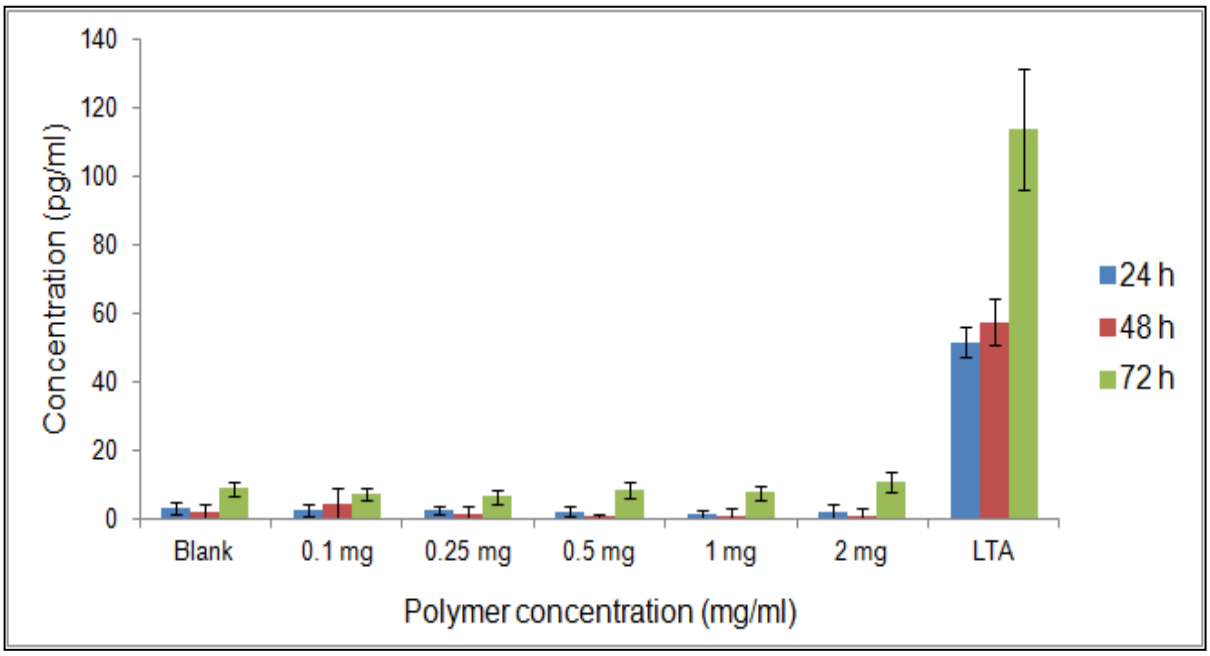

Figure 7.2 TNF-α release from HCEC cell line after exposure to PGPCPL-1

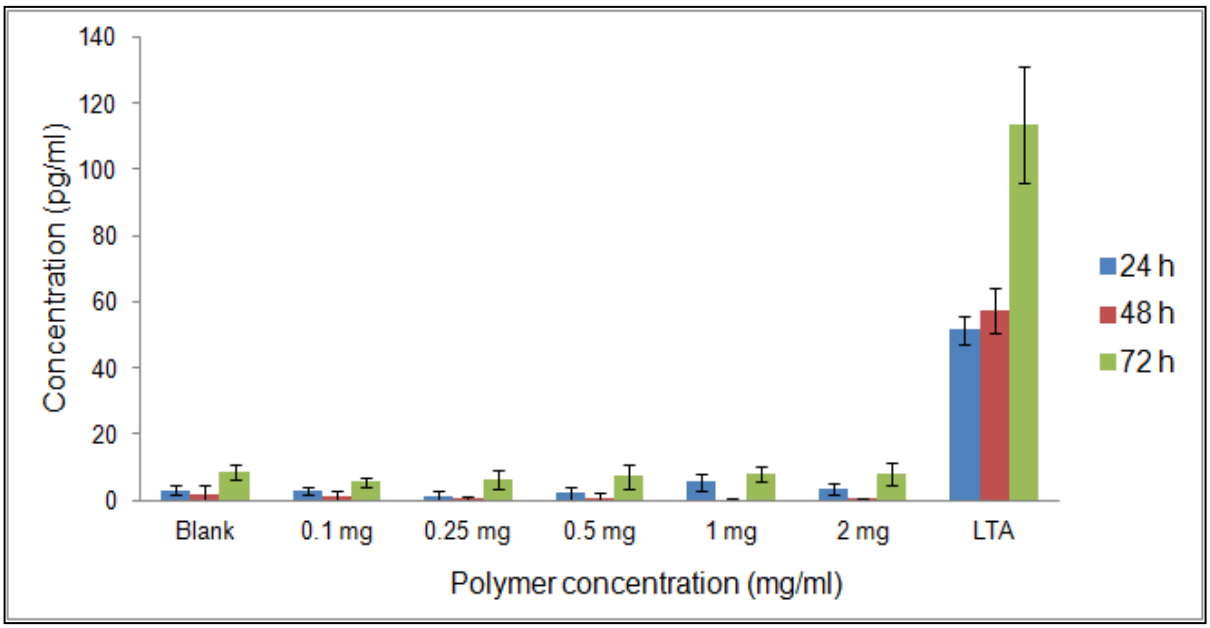

Figure 7.3 TNF-α release from HCEC cell line after exposure to PGPCPL-2

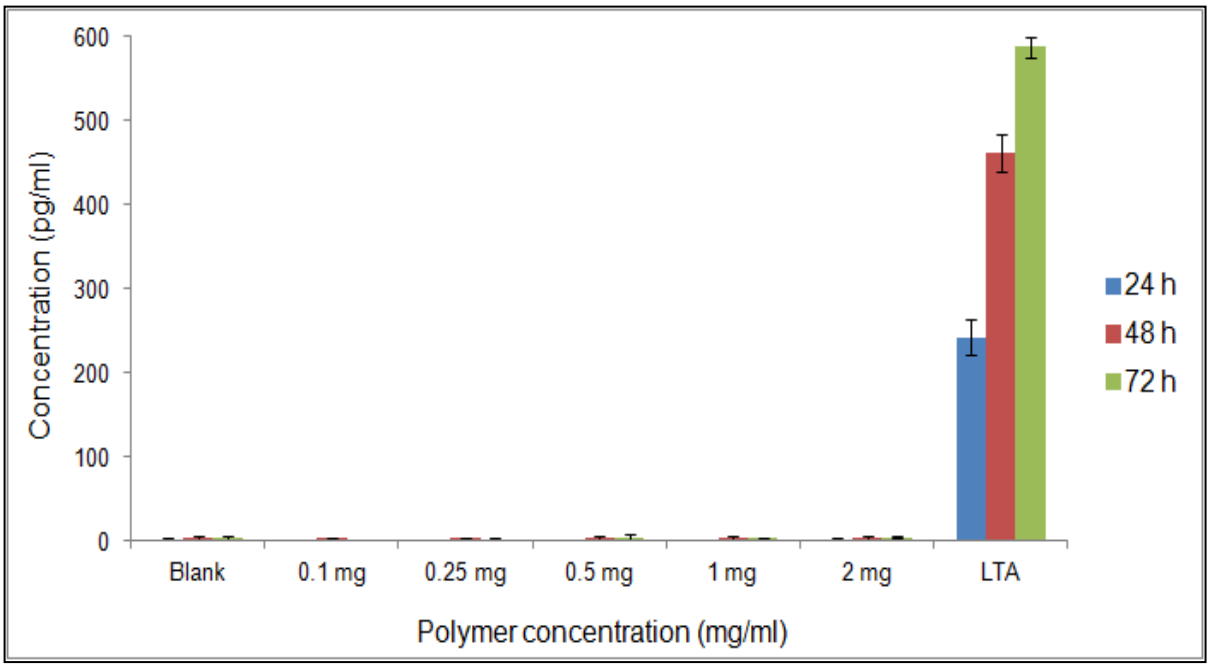

Figure 7.4 IL-6 release from HCEC cell line after exposure to PGPCPL-1

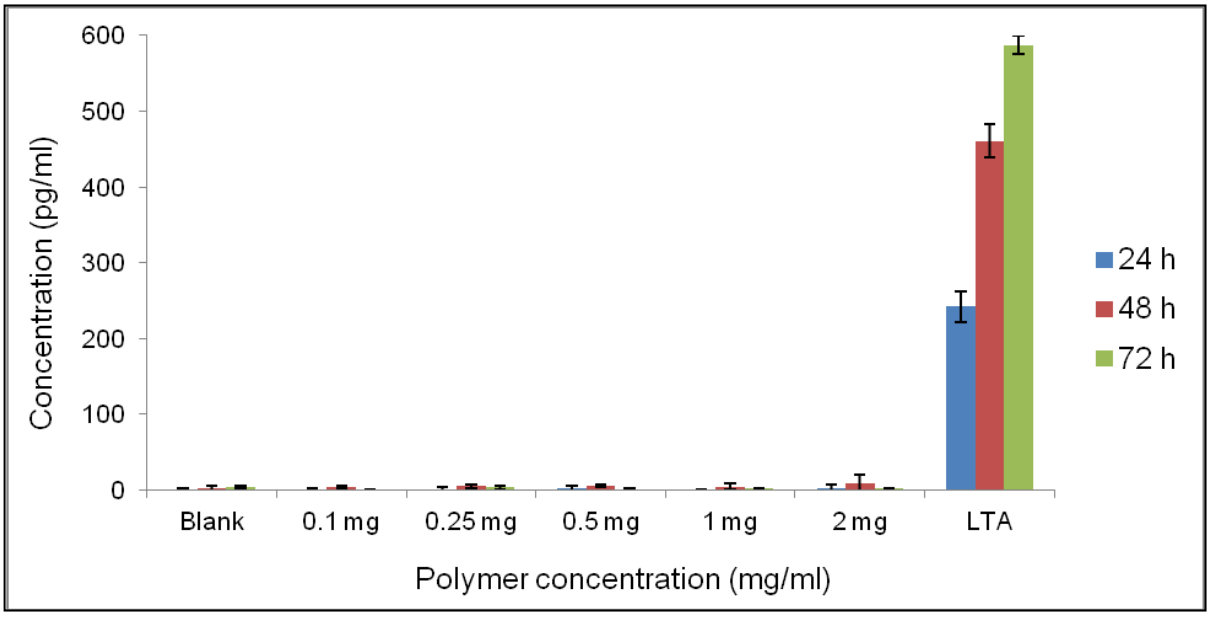

Figure 7.5 IL-6 release from HCEC cell line after exposure to PGPCPL-2

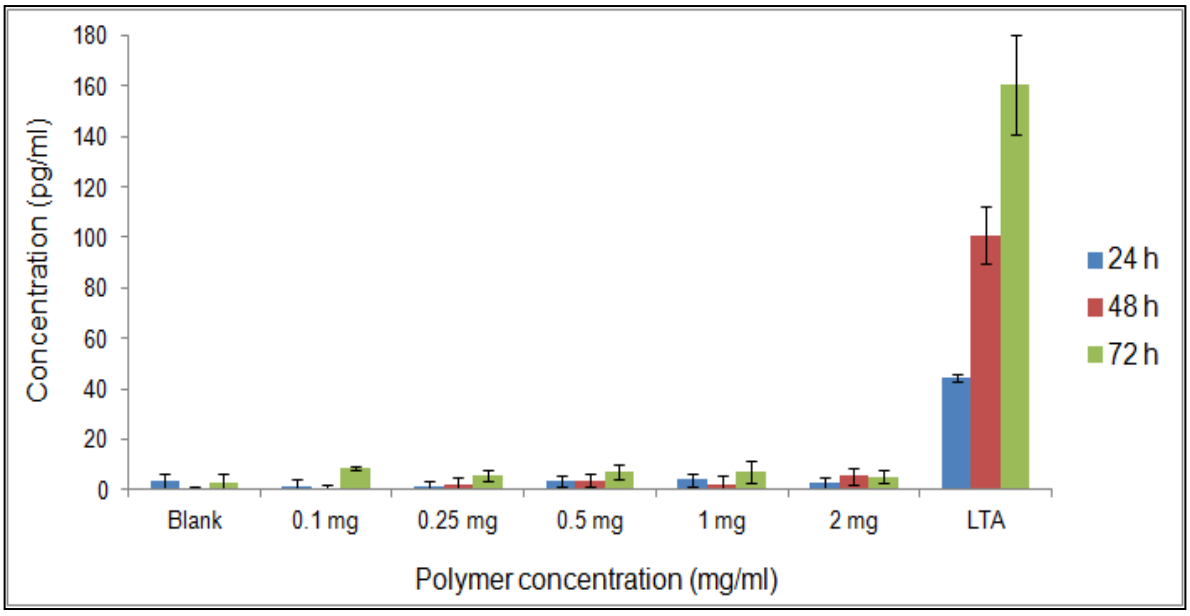

Figure 7.6 IL-1β release from HCEC cell line after exposure to PGPCPL-1

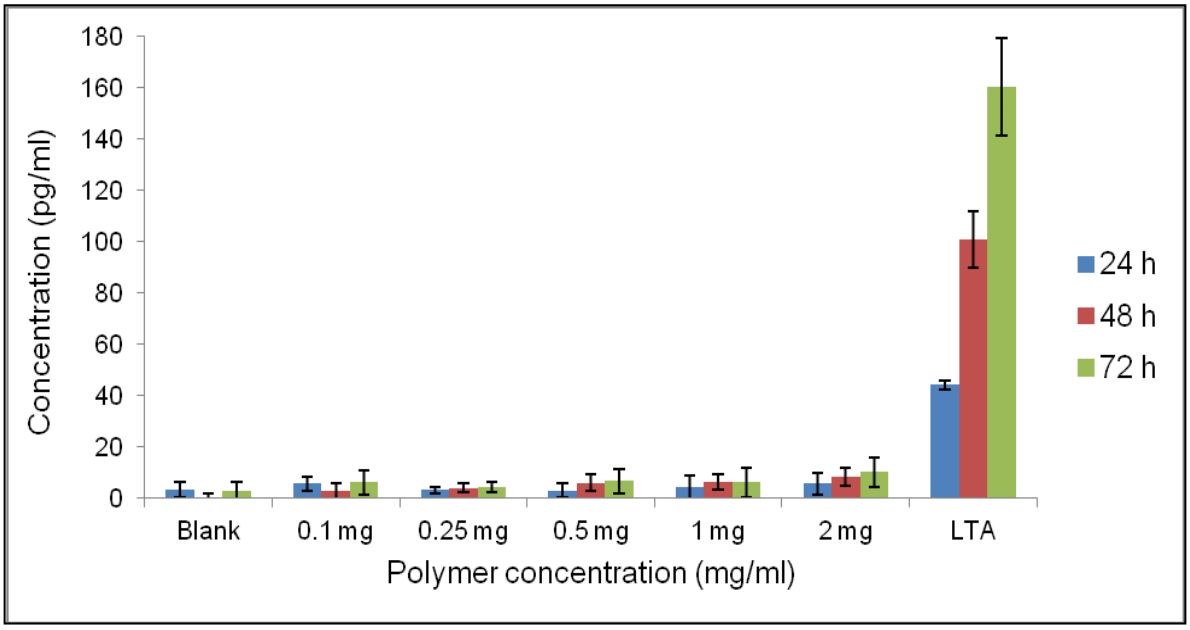

Figure 7.7 IL-1β release from HCEC cell line after exposure to PGPCPL-2

Moreover, suspension of nanoparticles in to the thermosensitive hydrogel also significantly restricts the diffusion of water molecules in to polymeric matrix. In the case of PB-A nanoparticles alone, 94.0 ± 9.4% drug release takes place in 129 h whereas in composite formulation 90.9 ± 1.9 % of release was observed in 19 days. These results suggest that our strategy has minimized the burst release phase and significantly prolonged the drug release duration. We have selected two different nanoparticulate formulation composed of pentablock copolymers A and C. Our results suggest that PB-A nanoparticles suspended in hydrogel displayed faster drug release in comparison to PB-C nanoparticles dispersed hydrogel in similar time duration. We observed that 90.9 ± 1.9 % release take place in 19 days from PB-A nanoparticles suspended in thermosensitive gel whereas in similar time duration only 65.0 ± 3.2% drug release was observed in the case of PB-C dispersed hydrogel. This difference can be explained by the fact that PB-C being more hydrophobic than PB-A tends to have better drug polymer compatibility. Prednisolone is a hydrophobic drug molecule and tends to partition into hydrophobic polymeric matrix. Therefore, difference in the hydrophobicity of polymeric materials is mainly responsible for the difference in drug release.

Drug Release Kinetics

We have evaluated the drug release profile of composite formulations through Higuchi, First order and Korsmeyer model. In the case of nanoparticles alone release was primarily depended (Table 7.1) on diffusion mechanisms whereas in the case of composite formulations diffusion exponent value is greater than 0.5 which suggest that release process was mediated by diffusion and degradation mechanisms. We also observed that release rate constant was significantly decreased in the case of composite formulations in comparison to

nanoparticles alone. We observed that higher diffusion exponent in the case of PB-A nanoparticles suspended in hydrogel in comparison to PB-C nanoparticles in hydrogel was mainly due to faster degradation of PB-A. Pentablock copolymer PB-C was composed of higher molecular weight PLA, therefore release process is primarily regulated through diffusion and less prominent effect of degradation mediated release was observed.

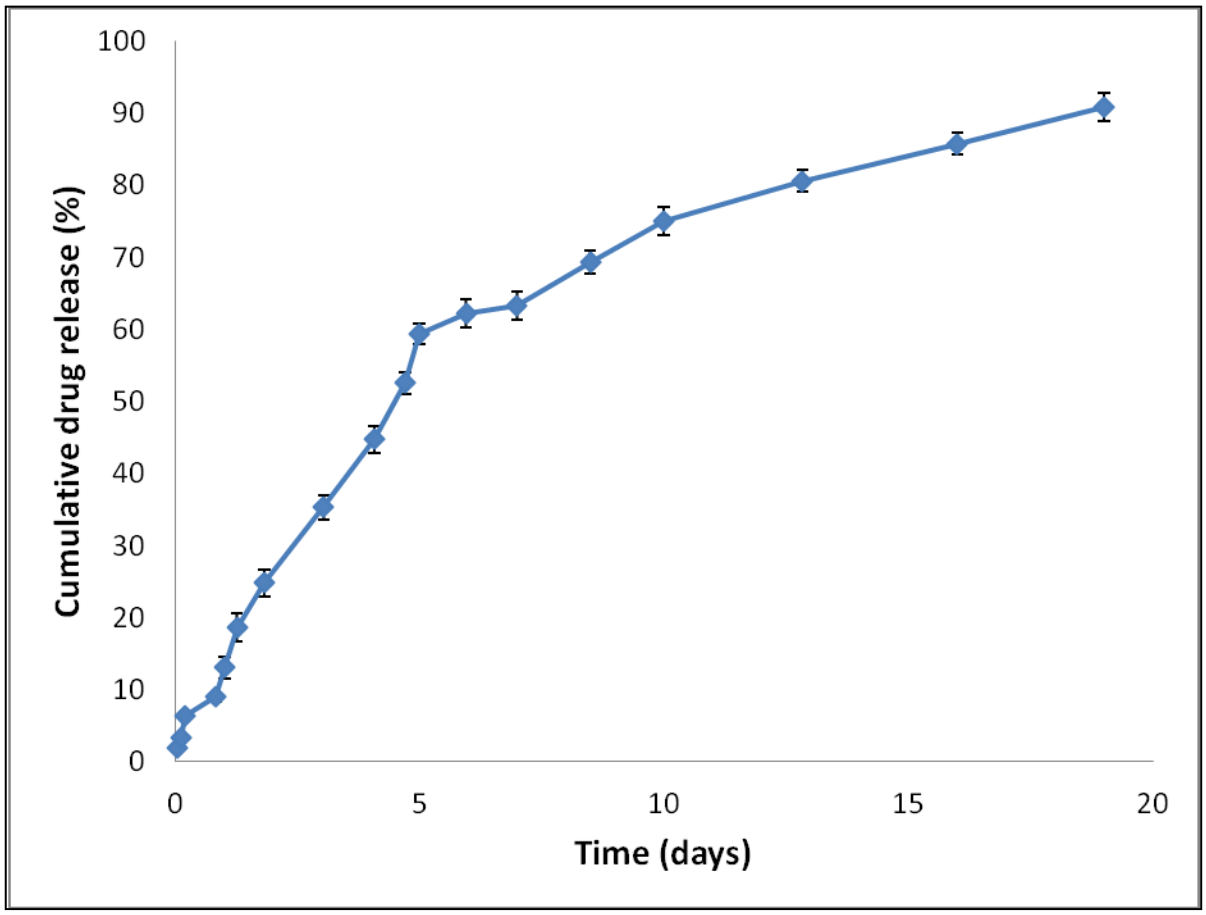

Figure 7.8 *In vitro* release of pentablock copolymer- A nanoparticles suspended in thermosensitive hydrogel in PBS buffer (pH 7.4) at 37 °C. The values are represented as mean ± standard deviation of n=3

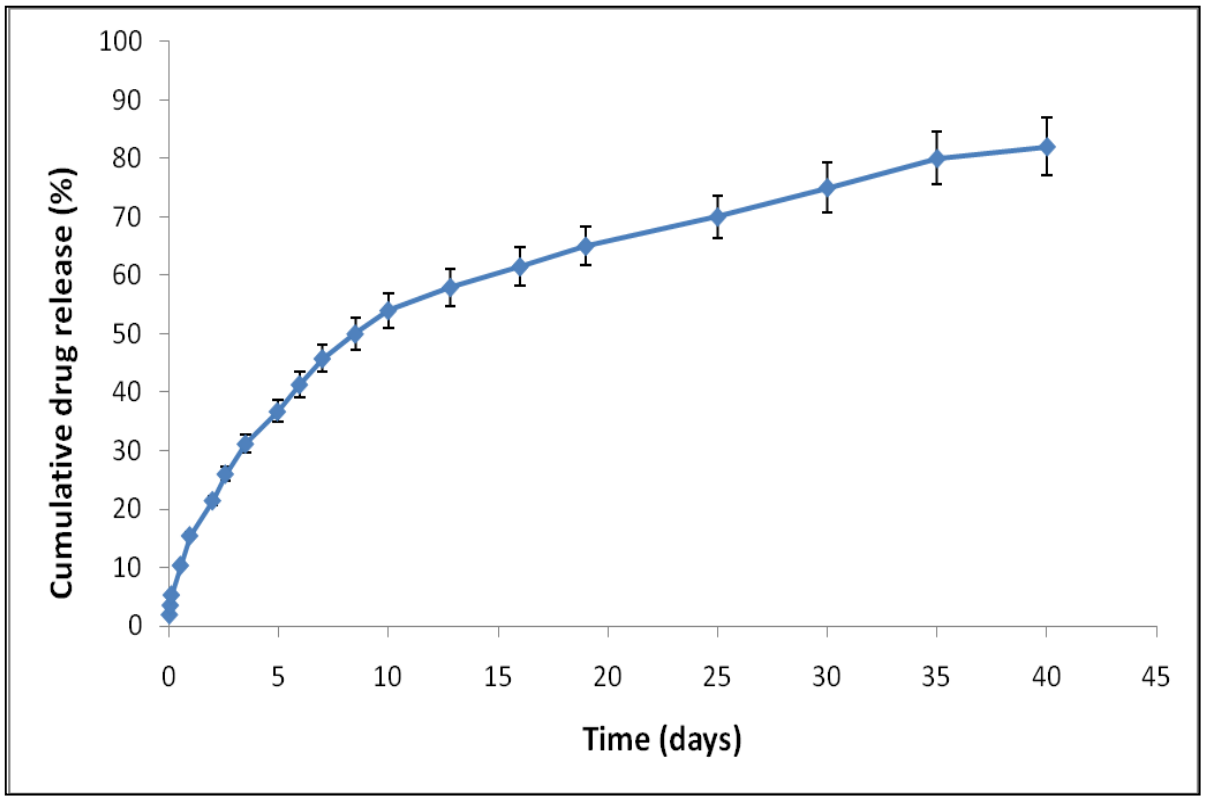

Figure 7.9 *In vitro* release of pentablock copolymer- C nanoparticles suspended in thermosensitive hydrogel in PBS buffer (pH 7.4) at 37 °C. The values are represented as mean ± standard deviation of n=3

Table 7.1 Kinetic parameters of *in vitro* release profile of nanoparticles suspended in thermosensitive hydrogel

Nanoparticles	First order		Higuchi		Korsmeyer-Peppas		
	r^2	k_o (h^{-1})	r^2	k_H ($h^{-1/2}$)	r^2	K_{KP} (h^{-n})	n
Pentablock copolymer-A suspended in gel	0.576	0.007	0.968	4.923	0.975	1.677	0.79
Pentablock copolymer-C suspended in gel	0.493	0.003	0.973	2.767	0.994	2.459	0.563

Conclusions

We have successfully prepared composite formulations of nanoparticles suspended in the hydrogel matrix. Composite formulations provided extended release profile in comparison to hydrogel or nanoparticles alone. These formulations successfully minimized the burst release phase and provided extended release profile in comparison to hydrogel or nanoparticles alone. These formulations have potential for clinical application based on their excellent biocompatible nature. Future investigations with different percentage of nanoparticles in the hydrogel matrix will further improve the understanding of composite systems.

CHAPTER 8

SUMMARY AND RECOMMENDATIONS

Summary

We have evaluated four different approaches to optimize drug release profile. In this regard, our first approach of incorporating polymeric additives was applicable to modulate the sol-gel transition and drug release kinetics from hydrogel. So in this study attempts has been made to study the effects of additives on sol-gel transition and drug release from hydrogel with the addition of hydrophilic and hydrophobic polymers. Hydrogel polymeric matrix is porous in nature and TM molecules can diffuse through the pores of polymeric chains. Polymeric additives can easily fit into the spaces of a hydrogel matrix and modify drug release rate.

PCL was selected as a hydrophobic and polyvinyl alcohol (PVA) as a hydrophilic additive. Addition of PVA and PCL increased the viscosity of hydrogel and improved the gelling efficiency possibly by providing better packing of the gel matrix. We observed more pronounced effect of PCL on sol-gel transition in comparison to PVA because PCL is a hydrophobic polymer and promotes better micellar aggregation for the formation of gel. Addition of PCL promoted the aggregation of polymeric chains at 37 °C but did not alter the porosity of the hydrogel matrix due to its low molecular weight whereas high molecular weight PVA uniformly cover the porous matrix of hydrogel and thereby reduced the diffusion of drug molecules from the hydrogel matrix. We found that PVA being a hydrophilic polymer tends to localize with hydrophilic block of the hydrogel where majority of TM molecules are dispersed. Higher percentage of PVA favors micellar aggregation due to presence of polar hydroxyl groups. Majority of TM dispersed in the hydrophilic block

therefore addition of PCL did not significantly modulate the release of TM. The effect of PVA on release kinetics was more pronounced than PCL. In hydrogel alone K_{KP} value was 3.03 whereas with PVA, K_{KP} was found to be 1.368 and for PCL it was 2.455. Cell viability studies suggest that polycaprolactone based hydrogels alone and with polymeric additives are biocompatible with the corneal epithelial cells (Mishra et al., 2011).

In our second approach we have incorporated PLA block in the center of PEG-PCL-PEG, in an attempt to accelerate degradation rate of highly crystalline and hydrophobic PCL block. PCL based block copolymers have primarily diffusion mediated drug release due to extremely slow degradation. So we have successfully developed novel pentablock copolymers by introducing faster degrading polymeric block with optimum degradation rate and achieved zero order drug release via both diffusion and degradation mediated pathway. Prednisolone and ofloxacin was utilized as model drugs of varying lipophilicity for *in vitro* release studies. Pentablock copolymers were successfully synthesized and characterized by ^{1}H NMR, GPC and FT IR. Sol-gel transition of two different copolymer of varying ε-caprolactone and L-lactide ratio suggested that upon increasing the block length of PCL, CGC decreased from 20 to 18 wt%. These results suggest that increasing the L-lactide to ε-caprolactone ratio with similar block length of mPEG resulted in lowering the CGC and increasing the stability of gel at higher temperature. The decrease in CGC was attributed to better micellar packing of copolymer with higher content of ε-caprolactone. Release of ofloxacin was not significantly different from both the polymeric compositions whereas release rate of PA was affected by hydrophilic/hydrophobic balance of the polymer. In addition, relatively longer PCL block length may have restricted the permeation of water

molecules across the polymeric matrix. Hence, slower hydration of gel resulted in decreased diffusion coefficient of the drug across the hydrogel matrix.

Release profile of OFX was not significantly different from both the compositions. OFX being a hydrophilic drug molecule tend to partition in the PEG domain of the hydrogel whereas hydrophobic drug molecule (PA) partition into PCL core. Therefore, OFX dispersed in PEG domain was easily diffused out in the release medium irrespective of polymer composition whereas change in hydrophobic component altered the release profile of PA by altering the micellar aggregation which influenced the porosity of hydrogel matrix.

A specific combination of different molecular weight and block ratio can generate copolymers, which can be used to prepare nanoparticles. Therefore, in our third approach we have successfully we have synthesized different compositions of pentablock copolymers and evaluated their effect on nanoparticles encapsulation and drug release profile. Our study suggest that nanoparticles prepared from pentablock copolymer-A have larger particle size in comparison to pentablock copolymer-B and C. Therefore, polymer composition has definite effect on the particle size but polymer molecular weight and hydrophobicity index did not exhibit any significant difference in particle size. We found higher entrapment efficiency of prednisolone for pentablock copolymer-B and C in comparison to pentablock copolymer-A. This difference in entrapment efficiency can be attributed to the difference in hydrophobicity of the copolymer. Polymer B and C are relatively more hydrophobic than polymer A. Prednisolone being a hydrophobic molecule tend to posses higher binding with the polymeric material having higher hydrophobicity. In addition, molecular weight of pentablock copolymer B and C is higher than polymer A. Therefore, copolymer composition and

molecular weight are the two dominant factors regulating the encapsulation efficiency and *in vitro* release profile.

Nanoparticles or thermosensitive hydrogel alone demonstrated initial burst release due to surface adsorbed drug molecule. Therefore, in our final approach we have utilized composite formulations of nanoparticles suspended in thermosensitive gel that successfully minimized the burst release of drugs due to longer diffusion pathway of drug molecules from the delivery system.

In addition, we have evaluated the cytotoxicity and inflammatory response of novel pentablock copolymers by direct exposure to various cell lines. Our results indicate a difference in cell viability between PB-A, B and C. This difference can be attributed to the polymer compositions. In PB-A faster degradation of PGA block might have resulted in less viability in comparison to pentablock copolymers B and C. However, all the compositions displayed negligible release of major inflammatory mediators i.e. TNF-α, IL-6 and IL-1β from macrophage cell line and Human conjunctival epithelial cells. Therefore our novel pentablock copolymers have potential for ophthalmic drug delivery.

Recommendations

Pentablock copolymers employed for nanoparticles preparation (PGA-PCL-PEG-PCL-PGA) have hydrophobic blocks at the terminal whereas copolymers utilized for thermosensitive gel (PEG-PCL-PLA-PCL-PEG) contains hydrophilic blocks at the terminal. Pentablock copolymers can be easily rearranged to accommodate both hydrophilic and hydrophobic drug molecules. Major challenge for controlled delivery of therapeutic macromolecules is to maintain structural integrity and biological activity of protein for

prolonged periods. These copolymers are amphiphilic in nature which can assist in optimizing the release profile of therapeutic macromolecules by varying the molecular weight of hydrophilic and hydrophobic blocks. Moreover, we can control the hydrolytic degradation of PB copolymers that will preserve structural integrity and immunogenicity of macromolecules. Our dual approach of nanoparticles suspended in a thermosensitive gel can eliminate the burst release of drugs due to longer diffusion pathway of drug molecules through both nanoparticles and gel layers. Such innovative system can be introduced in to episcleral space through subconjunctival administration. Such a delivery system may result in prolonged duration of action, thereby completely eliminates the need for repeated intravitreal injections. Moreover, uptake of nanoparticles could be enhanced by functionalizing the surface groups such that the surface modified nanoparticles might be recognized by peptide transporter present on the basolateral side of the RPE and Bruch's membrane. Subconjunctival administration of surface modified nanoparticles suspended in thermosensitive gel may provide prolonged delivery with improved conformational stability and targeted delivery of therapeutic macromolecules. Scientific and clinical impact of developing a controlled polymeric delivery of therapeutic macromolecules for age related macular degeneration treatment may cause a paradigm shift in the treatment of retinal diseases. Our composite formulations may serve as a platform for delivery of other therapeutic proteins, peptides, siRNA, antibody and fragments. Subconjunctival injection of optimized formulation will overcome common side effects associated with intravitreal injections. Investigation would also provide insight into transscleral pharmacokinetics of macromolecules following subconjunctival administration of controlled release formulation, which would provide new mechanistic approaches to biomaterial design.

REFERENCES

Ambati, J., Gragoudas, E.S., Miller, J.W., You, T.T., Miyamoto, K., Delori, F.C., Adamis, A.P., 2000. Transscleral delivery of bioactive protein to the choroid and retina. Invest Ophthalmol Vis Sci 41, 1186-1191.

Andersen, H.L., Sander, B., 2003. The vitreous, in: Kaufman, P.L., Alam, A., Adler, F.H. (Eds.), Adler's physiology of the eye: clinical application. Mosby, St. Louis, pp. 293-318.

Arias, J.L., Gallardo, V., Ruiz, M.A., Delgado, A.V., 2008a. Magnetite/poly(alkylcyanoacrylate) (core/shell) nanoparticles as 5-Fluorouracil delivery systems for active targeting. Eur J Pharm Biopharm 69, 54-63.

Arias, J.L., Ruiz, M.A., Lopez-Viota, M., Delgado, A.V., 2008b. Poly(alkylcyanoacrylate) colloidal particles as vehicles for antitumour drug delivery: a comparative study. Colloids Surf B Biointerfaces 62, 64-70.

Ban, Y., Rizzolo, L.J., 1997. A culture model of development reveals multiple properties of RPE tight junctions. Mol Vis 3, 18.

Baum, J., Peyman, G.A., Barza, M., 1982. Intravitreal administration of antibiotic in the treatment of bacterial endophthalmitis. III. Consensus. Surv Ophthalmol 26, 204-206.

Beeley, N.R., Rossi, J.V., Mello-Filho, P.A., Mahmoud, M.I., Fujii, G.Y., de Juan, E., Jr., Varner, S.E., 2005. Fabrication, implantation, elution, and retrieval of a steroid-loaded polycaprolactone subretinal implant. J Biomed Mater Res A 73, 437-444.

Brechue, W.F., Maren, T.H., 1993. pH and drug ionization affects ocular pressure lowering of topical carbonic anhydrase inhibitors. Invest Ophthalmol Vis Sci 34, 2581-2587.

Brem, H., 1990. Polymers to treat brain tumours. Biomaterials 11, 699-701.

Chen, S., Pieper, R., Webster, D.C., Singh, J., 2005. Triblock copolymers: synthesis, characterization, and delivery of a model protein. Int J Pharm 288, 207-218.

Cheng, L., Hostetler, K.Y., Lee, J., Koh, H.J., Beadle, J.R., Bessho, K., Toyoguchi, M., Aldern, K., Bovet, J.M., Freeman, W.R., 2004. Characterization of a novel intraocular drug-delivery system using crystalline lipid antiviral prodrugs of ganciclovir and cyclic cidofovir. Invest Ophthalmol Vis Sci 45, 4138-4144.

Cheong, H.I., Johnson, J., Cormier, M., Hosseini, K., 2008. In vitro cytotoxicity of eight beta-blockers in human corneal epithelial and retinal pigment epithelial cell lines: comparison with epidermal keratinocytes and dermal fibroblasts. Toxicol In Vitro 22, 1070-1076.

Chien, D.S., Sasaki, H., Bundgaard, H., Buur, A., Lee, V.H., 1991. Role of enzymatic lability in the corneal and conjunctival penetration of timolol ester prodrugs in the pigmented rabbit. Pharm Res 8, 728-733.

Chung, Y.M., Simmons, K.L., Gutowska, A., Jeong, B., 2002. Sol-gel transition temperature of PLGA-g-PEG aqueous solutions. Biomacromolecules 3, 511-516.

Ciolino, J.B., Hoare, T.R., Iwata, N.G., Behlau, I., Dohlman, C.H., Langer, R., Kohane, D.S., 2009. A drug-eluting contact lens. Invest Ophthalmol Vis Sci 50, 3346-3352.

Cour, M., 2003. The retinal pigmented epithelium, in: Kaufman, P.L., Alam, A., Adler, F.H. (Eds.), Adler's physiology of the eye: clinical application. Mosby, St. Louis, pp. 348-357.

Cunha-Vaz, J., Bernardes, R., Lobo, C., Blood-retinal barrier. Eur J Ophthalmol 21, 3-9.

Cunha-Vaz, J.G., 2004. The blood-retinal barriers system. Basic concepts and clinical evaluation. Exp Eye Res 78, 715-721.

Davson, H., Duke-Elder, W.S., et al., 1949. The penetration of some electrolytes and non-electrolytes into the aqueous humour and vitreous body of the cat. J Physiol 108, 203-217.

Derakhshandeh, K., Fashi, M., Seifoleslami, S., 2010. Thermosensitive Pluronic hydrogel: prolonged injectable formulation for drug abuse. Drug Des Devel Ther 4, 255-262.

Desai, S.D., Blanchard, J., 2000. Pluronic F127-based ocular delivery system containing biodegradable polyisobutylcyanoacrylate nanocapsules of pilocarpine. Drug Deliv 7, 201-207.

Duvvuri, S., Janoria, K.G., Mitra, A.K., 2005. Development of a novel formulation containing poly(d,l-lactide-co-glycolide) microspheres dispersed in PLGA-PEG-PLGA gel for sustained delivery of ganciclovir. J Control Release 108, 282-293.

Ebner, R., Devoto, M.H., Weil, D., Bordaberry, M., Mir, C., Martinez, H., Bonelli, L., Niepomniszcze, H., 2004. Treatment of thyroid associated ophthalmopathy with periocular injections of triamcinolone. Br J Ophthalmol 88, 1380-1386.

Edelhauser, H.F., Ubels, J.L., 2003. Cornea and sclera, in: Kaufman, P.L., Alam, A., Adler, F.H. (Eds.), Adler's physiology of the eye: clinical application. Mosby, St. Louis, pp. 47-116.

Einmahl, S., Behar-Cohen, F., D'Hermies, F., Rudaz, S., Tabatabay, C., Renard, G., Gurny, R., 2001a. A new poly(ortho ester)-based drug delivery system as an adjunct treatment in filtering surgery. Invest Ophthalmol Vis Sci 42, 695-700.

Einmahl, S., Capancioni, S., Schwach-Abdellaoui, K., Moeller, M., Behar-Cohen, F., Gurny, R., 2001b. Therapeutic applications of viscous and injectable poly(ortho esters). Adv Drug Deliv Rev 53, 45-73.

Einmahl, S., Ponsart, S., Bejjani, R.A., D'Hermies, F., Savoldelli, M., Heller, J., Tabatabay, C., Gurny, R., Behar-Cohen, F., 2003. Ocular biocompatibility of a poly(ortho ester) characterized by autocatalyzed degradation. J Biomed Mater Res A 67, 44-53.

Eperon, S., Bossy-Nobs, L., Petropoulos, I.K., Gurny, R., Guex-Crosier, Y., 2008. A biodegradable drug delivery system for the treatment of postoperative inflammation. Int J Pharm 352, 240-247.

Feng, N., Wu, P., Li, Q., Mei, Y., Shi, S., Yu, J., Xu, J., Liu, Y., Wang, Y., 2008. Oridonin-loaded poly(epsilon-caprolactone)-poly(ethylene oxide)-poly(epsilon-caprolactone) copolymer nanoparticles: preparation, characterization, and antitumor activity on mice with transplanted hepatoma. J Drug Target 16, 479-485.

Fresta, M., Fontana, G., Bucolo, C., Cavallaro, G., Giammona, G., Puglisi, G., 2001. Ocular tolerability and in vivo bioavailability of poly(ethylene glycol) (PEG)-coated polyethyl-2-cyanoacrylate nanosphere-encapsulated acyclovir. J Pharm Sci 90, 288-297.

Garripelli, V.K., Kim, J.K., Namgung, R., Kim, W.J., Repka, M.A., Jo, S., 2010. A novel thermosensitive polymer with pH-dependent degradation for drug delivery. Acta Biomater 6, 477-485.

Ge, H., Hu, Y., Jiang, X., Cheng, D., Yuan, Y., Bi, H., Yang, C., 2002. Preparation, characterization, and drug release behaviors of drug nimodipine-loaded poly(epsilon-caprolactone)-poly(ethylene oxide)-poly(epsilon-caprolactone) amphiphilic triblock copolymer micelles. J Pharm Sci 91, 1463-1473.

Geroski, D.H., Edelhauser, H.F., 2000. Drug delivery for posterior segment eye disease. Invest Ophthalmol Vis Sci 41, 961-964.

Gong, C., Shi, S., Wang, X., Wang, Y., Fu, S., Dong, P., Chen, L., Zhao, X., Wei, Y., Qian, Z., 2009a. Novel composite drug delivery system for honokiol delivery: self-assembled poly(ethylene glycol)-poly(epsilon-caprolactone)-poly(ethylene glycol) micelles in thermosensitive poly(ethylene glycol)-poly(epsilon-caprolactone)-poly(ethylene glycol) hydrogel. J Phys Chem B 113, 10183-10188.

Gong, C.Y., Dong, P.W., Shi, S., Fu, S.Z., Yang, J.L., Guo, G., Zhao, X., Wei, Y.Q., Qian, Z.Y., 2009b. Thermosensitive PEG-PCL-PEG hydrogel controlled drug delivery system: sol-gel-sol transition and in vitro drug release study. J Pharm Sci 98, 3707-3717.

Gong, C.Y., Shi, S., Dong, P.W., Yang, B., Qi, X.R., Guo, G., Gu, Y.C., Zhao, X., Wei, Y.Q., Qian, Z.Y., 2009c. Biodegradable in situ gel-forming controlled drug delivery system

based on thermosensitive PCL-PEG-PCL hydrogel: part 1--Synthesis, characterization, and acute toxicity evaluation. J Pharm Sci 98, 4684-4694.

Gou, M., Gong, C., Zhang, J., Wang, X., Gu, Y., Guo, G., Chen, L., Luo, F., Zhao, X., Wei, Y., Qian, Z., Polymeric matrix for drug delivery: honokiol-loaded PCL-PEG-PCL nanoparticles in PEG-PCL-PEG thermosensitive hydrogel. J Biomed Mater Res A 93, 219-226.

Gou, M., Zheng, X., Men, K., Zhang, J., Zheng, L., Wang, X., Luo, F., Zhao, Y., Zhao, X., Wei, Y., Qian, Z., 2009. Poly(epsilon-caprolactone)/poly(ethylene glycol)/poly(epsilon-caprolactone) nanoparticles: preparation, characterization, and application in doxorubicin delivery. J Phys Chem B 113, 12928-12933.

Govender, T., Riley, T., Ehtezazi, T., Garnett, M.C., Stolnik, S., Illum, L., Davis, S.S., 2000. Defining the drug incorporation properties of PLA-PEG nanoparticles. Int J Pharm 199, 95-110.

Gref, R., Minamitake, Y., Peracchia, M.T., Trubetskoy, V., Torchilin, V., Langer, R., 1994. Biodegradable long-circulating polymeric nanospheres. Science 263, 1600-1603.

Gupta, H., Aqil, M., Khar, R.K., Ali, A., Bhatnagar, A., Mittal, G., 2010. Sparfloxacin-loaded PLGA nanoparticles for sustained ocular drug delivery. Nanomedicine 6, 324-333.

Hamalainen, K.M., Kananen, K., Auriola, S., Kontturi, K., Urtti, A., 1997. Characterization of paracellular and aqueous penetration routes in cornea, conjunctiva, and sclera. Invest Ophthalmol Vis Sci 38, 627-634.

Hazin, R., Hendrick, A.M., Kahook, M.Y., 2009. Primary open-angle glaucoma: diagnostic approaches and management. J Natl Med Assoc 101, 46-50.

He, C., Kim, S.W., Lee, D.S., 2008. In situ gelling stimuli-sensitive block copolymer hydrogels for drug delivery. J Control Release 127, 189-207.

Heller, J., 2005. Ocular delivery using poly(ortho esters). Adv Drug Deliv Rev 57, 2053-2062.

Heller, J., Barr, J., Ng, S.Y., Abdellauoi, K.S., Gurny, R., 2002. Poly(ortho esters): synthesis, characterization, properties and uses. Adv Drug Deliv Rev 54, 1015-1039.

Heller, J., Barr, J., Ng, S.Y., Shen, H.R., Schwach-Abdellaoui, K., Einmahl, S., Rothen-Weinhold, A., Gurny, R., 2000. Poly(ortho esters) - their development and some recent applications. Eur J Pharm Biopharm 50, 121-128.

Henke, M., Brandl, F., Goepferich, A.M., Tessmar, J.K., 2010. Size-dependent release of fluorescent macromolecules and nanoparticles from radically cross-linked hydrogels. Eur J Pharm Biopharm 74, 184-192.

Hu, Y., Jiang, X., Ding, Y., Zhang, L., Yang, C., Zhang, J., Chen, J., Yang, Y., 2003. Preparation and drug release behaviors of nimodipine-loaded poly(caprolactone)-poly(ethylene oxide)-polylactide amphiphilic copolymer nanoparticles. Biomaterials 24, 2395-2404.

Hughes, P.M., Olejnik, O., Chang-Lin, J.E., Wilson, C.G., 2005. Topical and systemic drug delivery to the posterior segments. Adv Drug Deliv Rev 57, 2010-2032.

Huynh, D.P., Im, G.J., Chae, S.Y., Lee, K.C., Lee, D.S., 2009. Controlled release of insulin from pH/temperature-sensitive injectable pentablock copolymer hydrogel. J Control Release 137, 20-24.

Huynh, D.P., Nguyen, M.K., Pi, B.S., Kim, M.S., Chae, S.Y., Lee, K.C., Kim, B.S., Kim, S.W., Lee, D.S., 2008. Functionalized injectable hydrogels for controlled insulin delivery. Biomaterials 29, 2527-2534.

Hwang, M.J., Joo, M.K., Choi, B.G., Park, M.H., Hamley, I.W., Jeong, B., 2010. Multiple Sol-Gel Transitions of PEG-PCL-PEG Triblock Copolymer Aqueous Solution. Macromol Rapid Commun 31, 2064-2069.

Hwang, M.J., Suh, J.M., Bae, Y.H., Kim, S.W., Jeong, B., 2005. Caprolactonic poloxamer analog: PEG-PCL-PEG. Biomacromolecules 6, 885-890.

Hyndiuk, R.A., Reagan, M.G., 1968. Radioactive depot-corticosteroid penetration into monkey ocular tissue. I. Retrobulbar and systemic administration. Arch Ophthalmol 80, 499-503.

Hyon, S.H., Jamshidi, K., Ikada, Y., 1997. Synthesis of polylactides with different molecular weights. Biomaterials 18, 1503-1508.

Jain, J.P., Chitkara, D., Kumar, N., 2008. Polyanhydrides as localized drug delivery carrier: an update. Expert Opin Drug Deliv 5, 889-907.

Jain, R., Shah, N.H., Malick, A.W., Rhodes, C.T., 1998. Controlled drug delivery by biodegradable poly(ester) devices: different preparative approaches. Drug Dev Ind Pharm 24, 703-727.

Jeong, B., Bae, Y.H., Kim, S.W., 2000. Drug release from biodegradable injectable thermosensitive hydrogel of PEG-PLGA-PEG triblock copolymers. J Control Release 63, 155-163.

Jiang, Z., Hao, J., You, Y., Gu, Q., Cao, W., Deng, X., 2009. Biodegradable thermogelling hydrogel of P(CL-GL)-PEG-P(CL-GL) triblock copolymer: degradation and drug release behavior. J Pharm Sci 98, 2603-2610.

Jiang, Z., Hao, J., You, Y., Liu, Y., Wang, Z., Deng, X., 2008. Biodegradable and thermoreversible hydrogels of poly(ethylene glycol)-poly(epsilon-caprolactone-co-glycolide)-poly(ethylene glycol) aqueous solutions. J Biomed Mater Res A 87, 45-51.

Jones, D.S., McLaughlin, D.W., McCoy, C.P., Gorman, S.P., 2005. Physicochemical characterisation and biological evaluation of hydrogel-poly(epsilon-caprolactone) interpenetrating polymer networks as novel urinary biomaterials. Biomaterials 26, 1761-1770.

Kan, P., Lin, X.Z., Hsieh, M.F., Chang, K.Y., 2005. Thermogelling emulsions for vascular embolization and sustained release of drugs. J Biomed Mater Res B Appl Biomater 75, 185-192.

Kang, Y.M., Lee, S.H., Lee, J.Y., Son, J.S., Kim, B.S., Lee, B., Chun, H.J., Min, B.H., Kim, J.H., Kim, M.S., A biodegradable, injectable, gel system based on MPEG-b-(PCL-ran-PLLA) diblock copolymers with an adjustable therapeutic window. Biomaterials 31, 2453-2460.

Kaur, I.P., Kanwar, M., 2002. Ocular preparations: the formulation approach. Drug Dev Ind Pharm 28, 473-493.

Kent, A.R., King, L., Bartholomew, L.R., 2006. Vitreous concentration of topically applied brimonidine-purite 0.15%. J Ocul Pharmacol Ther 22, 242-246.

Kim, H., Robinson, M.R., Lizak, M.J., Tansey, G., Lutz, R.J., Yuan, P., Wang, N.S., Csaky, K.G., 2004a. Controlled drug release from an ocular implant: an evaluation using dynamic three-dimensional magnetic resonance imaging. Invest Ophthalmol Vis Sci 45, 2722-2731.

Kim, M.S., Seo, K.S., Khang, G., Cho, S.H., Lee, H.B., 2004b. Preparation of poly(ethylene glycol)-block-poly(caprolactone) copolymers and their applications as thermo-sensitive materials. J Biomed Mater Res A 70, 154-158.

Kim, S.W., Bae, Y.H., Okano, T., 1992. Hydrogels: swelling, drug loading, and release. Pharm Res 9, 283-290.

Kim, T.W., Lindsey, J.D., Aihara, M., Anthony, T.L., Weinreb, R.N., 2002. Intraocular distribution of 70-kDa dextran after subconjunctival injection in mice. Invest Ophthalmol Vis Sci 43, 1809-1816.

Klouda, L., Mikos, A.G., 2008. Thermoresponsive hydrogels in biomedical applications. Eur J Pharm Biopharm 68, 34-45.

Klyce, S.D., Beuerman, R.W., 1988. Structure and function of the cornea, in: Kaufman, H.E. (Ed.), The Cornea. Churchill Livingstone, New York, p. 3.

Koevary, S.B., 2003. Pharmacokinetics of topical ocular drug delivery: potential uses for the treatment of diseases of the posterior segment and beyond. Curr Drug Metab 4, 213-222.

Kumar, N., Langer, R.S., Domb, A.J., 2002. Polyanhydrides: an overview. Adv Drug Deliv Rev 54, 889-910.

Kundu P, K.M., Sinha M, Choe S, Chattopadhayay D, 2003. Effect of alcoholic, glycolic, and polyester resin additives on the gelation of dilute solution (1%) of methylcellulose. . Carbohydrate Polymers 51, 57-61.

Kwon, G.S., 1998. Diblock copolymer nanoparticles for drug delivery. Crit Rev Ther Drug Carrier Syst 15, 481-512.

Lao, L.L., Peppas, N.A., Boey, F.Y., Venkatraman, S.S., 2011. Modeling of drug release from bulk-degrading polymers. Int J Pharm.

Lee, H., Zeng, F., Dunne, M., Allen, C., 2005. Methoxy poly(ethylene glycol)-block-poly(delta-valerolactone) copolymer micelles for formulation of hydrophobic drugs. Biomacromolecules 6, 3119-3128.

Lee, J., Bae, Y.H., Sohn, Y.S., Jeong, B., 2006. Thermogelling aqueous solutions of alternating multiblock copolymers of poly(L-lactic acid) and poly(ethylene glycol). Biomacromolecules 7, 1729-1734.

Lee, J.W., Hua, F., Lee, D.S., 2001. Thermoreversible gelation of biodegradable poly(epsilon-caprolactone) and poly(ethylene glycol) multiblock copolymers in aqueous solutions. J Control Release 73, 315-327.

Lee, K.B., Yoon, K.R., Woo, S.I., Choi, I.S., 2003. Surface modification of poly(glycolic acid) (PGA) for biomedical applications. J Pharm Sci 92, 933-937.

Li, F., Li, S., Ghzaoui, A.E., Nouailhas, H., Zhuo, R., 2007. Synthesis and gelation properties of PEG-PLA-PEG triblock copolymers obtained by coupling monohydroxylated PEG-PLA with adipoyl chloride. Langmuir 23, 2778-2783.

Liggins, R.T., Burt, H.M., 2002. Polyether-polyester diblock copolymers for the preparation of paclitaxel loaded polymeric micelle formulations. Adv Drug Deliv Rev 54, 191-202.

Lindstrom, R., Kim, T., 2006. Ocular permeation and inhibition of retinal inflammation: an examination of data and expert opinion on the clinical utility of nepafenac. Curr Med Res Opin 22, 397-404.

Liu, D., Wang, L., Liu, Z., Zhang, C., Zhang, N., 2010. Preparation, characterization, and in vitro evaluation of docetaxel-loaded poly(lactic acid)-poly(ethylene glycol) nanoparticles for parenteral drug delivery. J Biomed Nanotechnol 6, 675-682.

Lopez-Cortes, L.F., Pastor-Ramos, M.T., Ruiz-Valderas, R., Cordero, E., Uceda-Montanes, A., Claro-Cala, C.M., Lucero-Munoz, M.J., 2001. Intravitreal pharmacokinetics and retinal concentrations of ganciclovir and foscarnet after intravitreal administration in rabbits. Invest Ophthalmol Vis Sci 42, 1024-1028.

Lu, J.M., Wang, X., Marin-Muller, C., Wang, H., Lin, P.H., Yao, Q., Chen, C., 2009. Current advances in research and clinical applications of PLGA-based nanotechnology. Expert Rev Mol Diagn 9, 325-341.

Lu, L., Peter, S.J., Lyman, M.D., Lai, H.L., Leite, S.M., Tamada, J.A., Uyama, S., Vacanti, J.P., Langer, R., Mikos, A.G., 2000. In vitro and in vivo degradation of porous poly(DL-lactic-co-glycolic acid) foams. Biomaterials 21, 1837-1845.

Macha, S., Mitra, A.K., 2001. Ocular pharmacokinetics in rabbits using a novel dual probe microdialysis technique. Exp Eye Res 72, 289-299.

Macha, S., Mitra, A.K., 2002. Ocular disposition of ganciclovir and its monoester prodrugs following intravitreal administration using microdialysis. Drug Metab Dispos 30, 670-675.

Makino, K., Hiyoshi, J., Ohshima, H., 2001. Effects of thermosensitivity of poly (N-isopropylacrylamide) hydrogel upon the duration of a lag phase at the beginning of drug release from the hydrogel. Colloids Surf B Biointerfaces 20, 341-346.

Mather, C.M., Kirkpatrick, J.N., 2003. Sub-Tenon's administration of local anaesthetic: a review of the technique. Br J Anaesth 91, 922;author reply 922-923.

Middleton, J.C., Tipton, A.J., 2000. Synthetic biodegradable polymers as orthopedic devices. Biomaterials 21, 2335-2346.

Mishra, G.P., Bagui, M., Tamboli, V., Mitra, A.K., 2011. Recent applications of liposomes in ophthalmic drug delivery. J Drug Deliv 2011, 863734.

Mishra, G.P., Gaudana, R., Tamboli, V.M., Mitra, A.K., 2010. Recent advances in ocular drug delivery: role of transporters, receptors and nanocarriers, in: Narang, A.S., Mahato, R.I. (Eds.), Targeted Delivery of Small and Macromolecular Drugs. CRC press, Taylor & francis group.

Mishra, G.P., Tamboli, V., Jwala, J., Mitra, A.K., 2011. Recent patents and emerging therapeutics in the treatment of allergic conjunctivitis. Recent Pat Inflamm Allergy Drug Discov 5, 26-36.

Mishra, G.P., Tamboli, V., Mitra, A.K., 2011. Effect of hydrophobic and hydrophilic additives on sol-gel transition and release behavior of timolol maleate from polycaprolactone-based hydrogel. Colloid Polym Sci 289, 1553-1562.

Mitra, A.K., 2009. Role of transporters in ocular drug delivery system. Pharm Res 26, 1192-1196.

Mohan, N., Nair, P.D., 2008. Polyvinyl alcohol-poly(caprolactone) semi IPN scaffold with implication for cartilage tissue engineering. J Biomed Mater Res B Appl Biomater 84, 584-594.

Munroe, W.P., Rindone, J.P., Kershner, R.M., 1985. Systemic side effects associated with the ophthalmic administration of timolol. Drug Intell Clin Pharm 19, 85-89.

Nemoto, E., Takahashi, H., Kobayashi, D., Ueda, H., Morimoto, Y., 2006. Effects of poly-L-arginine on the permeation of hydrophilic compounds through surface ocular tissues. Biol Pharm Bull 29, 155-160.

Nguyen, M.K., Lee, D.S., 2010. Injectable biodegradable hydrogels. Macromol Biosci 10, 563-579.

Packhaeuser, C.B., Kissel, T., 2007. On the design of in situ forming biodegradable parenteral depot systems based on insulin loaded dialkylaminoalkyl-amine-poly(vinyl alcohol)-g-poly(lactide-co-glycolide) nanoparticles. J Control Release 123, 131-140.

Peeters, A., Schouten, J.S., Severens, J.L., Hendrikse, F., Prins, M.H., Webers, C.A., Latanoprost versus timolol as first choice therapy in patients with ocular hypertensionA cost-effectiveness analysis. Acta Ophthalmol.

Peyman, G.A., Bok, D., 1972. Peroxidase diffusion in the normal and laser-coagulated primate retina. Invest Ophthalmol 11, 35-45.

Pfister, R.R., 1975. The normal surface of conjunctiva epithelium. A scanning electron microscopic study. Invest Ophthalmol 14, 267-279.

Pitkanen, L., Ranta, V.P., Moilanen, H., Urtti, A., 2005. Permeability of retinal pigment epithelium: effects of permeant molecular weight and lipophilicity. Invest Ophthalmol Vis Sci 46, 641-646.

Polak, M.B., Valamanesh, F., Felt, O., Torriglia, A., Jeanny, J.C., Bourges, J.L., Rat, P., Thomas-Doyle, A., BenEzra, D., Gurny, R., Behar-Cohen, F., 2008. Controlled delivery of 5-chlorouracil using poly(ortho esters) in filtering surgery for glaucoma. Invest Ophthalmol Vis Sci 49, 2993-3003.

Prausnitz, M.R., Noonan, J.S., 1998. Permeability of cornea, sclera, and conjunctiva: a literature analysis for drug delivery to the eye. J Pharm Sci 87, 1479-1488.
Pulapura, S., Kohn, J., 1992. Trends in the development of bioresorbable polymers for medical applications. J Biomater Appl 6, 216-250.

Qiao, M., Chen, D., Ma, X., Liu, Y., 2005. Injectable biodegradable temperature-responsive PLGA-PEG-PLGA copolymers: synthesis and effect of copolymer composition on the drug release from the copolymer-based hydrogels. Int J Pharm 294, 103-112.

Rait, J.L., 1999. Systemic effects of topical ophthalmic beta-adrenoceptor antagonists. Aust N Z J Ophthalmol 27, 57-64.

Reddy Ik, Aziz W, Sause RB, 1996. Artificial tear formulations, irrigating solutions and contact lens products, in: Reddy IK (Ed.), Ocular therapeutics and drug delivery: a multi-disciplinary aapproach. Technomic, Lancaster, pp. 171-212.

Rohner, D., Hutmacher, D.W., Cheng, T.K., Oberholzer, M., Hammer, B., 2003. In vivo efficacy of bone-marrow-coated polycaprolactone scaffolds for the reconstruction of orbital defects in the pig. J Biomed Mater Res B Appl Biomater 66, 574-580.

Rosenberg, L.F., Krupin, T., Tang, L.Q., Hong, P.H., Ruderman, J.M., 1998. Combination of systemic acetazolamide and topical dorzolamide in reducing intraocular pressure and aqueous humor formation. Ophthalmology 105, 88-92; discussion 92-83.

Ryu, J., Jeong, Y.I., Kim, I.S., Lee, J.H., Nah, J.W., Kim, S.H., 2000. Clonazepam release from core-shell type nanoparticles of poly(epsilon-caprolactone)/poly(ethylene glycol)/poly(epsilon-caprolactone) triblock copolymers. Int J Pharm 200, 231-242.

Saha, P., Yang, J.J., Lee, V.H., 1998. Existence of a p-glycoprotein drug efflux pump in cultured rabbit conjunctival epithelial cells. Invest Ophthalmol Vis Sci 39, 1221-1226.

Sethi, R.K., Neavyn, M.J., Rubash, H.E., Shanbhag, A.S., 2003. Macrophage response to cross-linked and conventional UHMWPE. Biomaterials 24, 2561-2573.

Sharma, R.K., Ehinger, B.E.J., 2003. Development and structure of retina, in: Kaufman, P.L., Alam, A., Adler, F.H. (Eds.), Adler's physiology of the eye: clinical application. Mosby, St. Louis, pp. 319-347.

Sheikh, F.A., Barakat, N.A., Kanjwal, M.A., Aryal, S., Khil, M.S., Kim, H.Y., 2009. Novel self-assembled amphiphilic poly(epsilon-caprolactone)-grafted-poly(vinyl alcohol) nanoparticles: hydrophobic and hydrophilic drugs carrier nanoparticles. J Mater Sci Mater Med 20, 821-831.

Sheng, Y., Yuan, Y., Liu, C., Tao, X., Shan, X., Xu, F., 2009. In vitro macrophage uptake and in vivo biodistribution of PLA-PEG nanoparticles loaded with hemoglobin as blood substitutes: effect of PEG content. J Mater Sci Mater Med 20, 1881-1891.
Shuai, X., Ai, H., Nasongkla, N., Kim, S., Gao, J., 2004. Micellar carriers based on block copolymers of poly(epsilon-caprolactone) and poly(ethylene glycol) for doxorubicin delivery. J Control Release 98, 415-426.

Siepmann, J., Gopferich, A., 2001. Mathematical modeling of bioerodible, polymeric drug delivery systems. Adv Drug Deliv Rev 48, 229-247.

Smith, R.S., Rudt, L.A., 1975. Ocular vascular and epithelial barriers to microperoxidase. Invest Ophthalmol 14, 556-560.

Soares, J.S., Zunino, P., 2010. A mixture model for water uptake, degradation, erosion and drug release from polydisperse polymeric networks. Biomaterials 31, 3032-3042.

Soppimath, K.S., Aminabhavi, T.M., Kulkarni, A.R., Rudzinski, W.E., 2001. Biodegradable polymeric nanoparticles as drug delivery devices. J Control Release 70, 1-20.

Stevenson, B.R., Anderson, J.M., Goodenough, D.A., Mooseker, M.S., 1988. Tight junction structure and ZO-1 content are identical in two strains of Madin-Darby canine kidney cells which differ in transepithelial resistance. J Cell Biol 107, 2401-2408.

Stjernschantz, J., Astin, M., 1993. Anatomy and physiology of the eye. Physiological aspects of ocular drug therapy, in: Edman, P. (Ed.), Biopharmaceutics of ocular drug delivery. CRC press, pp. 1-26.

Sun, K.H., Sohn, Y.S., Jeong, B., 2006. Thermogelling poly(ethylene oxide-b-propylene oxide-b-ethylene oxide) disulfide multiblock copolymer as a thiol-sensitive degradable polymer. Biomacromolecules 7, 2871-2877.

Tamargo, R.J., Epstein, J.I., Reinhard, C.S., Chasin, M., Brem, H., 1989. Brain biocompatibility of a biodegradable, controlled-release polymer in rats. J Biomed Mater Res 23, 253-266.

Tamboli, V., Mishra, G.P., Mitra, A.K., 2011. Polymeric vectors for ocular gene delivery. Ther Deliv 2, 523-536.

Tang, R., Palumbo, R.N., Ji, W., Wang, C., 2009. Poly(ortho ester amides): acid-labile temperature-responsive copolymers for potential biomedical applications. Biomacromolecules 10, 722-727.

Urtti, A., 2006. Challenges and obstacles of ocular pharmacokinetics and drug delivery. Adv Drug Deliv Rev 58, 1131-1135.

Urtti, A., Salminen, L., 1993. Minimizing systemic absorption of topically administered ophthalmic drugs. Surv Ophthalmol 37, 435-456.
Urtti, A., Salminen, L., Periviita, L., 1984. Ocular distribution of topically applied adrenaline in albino and pigmented rabbits. Acta Ophthalmol (Copenh) 62, 753-762.

van den Berg, A.A., 2004. An audit of peribulbar blockade using 15 mm, 25 mm and 37.5 mm needles, and sub-Tenon's injection. Anaesthesia 59, 775-780.

Wadhwa, S., Paliwal, R., Paliwal, S.R., Vyas, S.P., 2009. Nanocarriers in ocular drug delivery: an update review. Curr Pharm Des 15, 2724-2750.

Watsky, M.A., Jablonski, M.M., Edelhauser, H.F., 1988. Comparison of conjunctival and corneal surface areas in rabbit and human. Curr Eye Res 7, 483-486.

Wei, X., Gong, C., Gou, M., Fu, S., Guo, Q., Shi, S., Luo, F., Guo, G., Qiu, L., Qian, Z., 2009. Biodegradable poly(epsilon-caprolactone)-poly(ethylene glycol) copolymers as drug delivery system. Int J Pharm 381, 1-18.

Weijtens, O., Schoemaker, R.C., Lentjes, E.G., Romijn, F.P., Cohen, A.F., van Meurs, J.C., 2000. Dexamethasone concentration in the subretinal fluid after a subconjunctival injection, a peribulbar injection, or an oral dose. Ophthalmology 107, 1932-1938.

Wu, D.Q., Chu, C.C., 2008. Biodegradable hydrophobic-hydrophilic hybrid hydrogels: swelling behavior and controlled drug release. J Biomater Sci Polym Ed 19, 411-429.

Xiao, R.Z., Zeng, Z.W., Zhou, G.L., Wang, J.J., Li, F.Z., Wang, A.M., 2010. Recent advances in PEG-PLA block copolymer nanoparticles. Int J Nanomedicine 5, 1057-1065.

Yang, Y., Hua, C., Dong, C.M., 2009. Synthesis, self-assembly, and in vitro doxorubicin release behavior of dendron-like/linear/dendron-like poly(epsilon-caprolactone)-b-poly(ethylene glycol)-b-poly(epsilon-caprolactone) triblock copolymers. Biomacromolecules 10, 2310-2318.

Yenice, I., Mocan, M.C., Palaska, E., Bochot, A., Bilensoy, E., Vural, I., Irkec, M., Hincal, A.A., 2008. Hyaluronic acid coated poly-epsilon-caprolactone nanospheres deliver high concentrations of cyclosporine A into the cornea. Exp Eye Res 87, 162-167.

Yi, X., Wang, Y., Yu, F.S., 2000. Corneal epithelial tight junctions and their response to lipopolysaccharide challenge. Invest Ophthalmol Vis Sci 41, 4093-4100.

Yim, E.S., Zhao, B., Myung, D., Kourtis, L.C., Frank, C.W., Carter, D., Smith, R.L., Goodman, S.B., 2009. Biocompatibility of poly(ethylene glycol)/poly(acrylic acid) interpenetrating polymer network hydrogel particles in RAW 264.7 macrophage and MG-63 osteoblast cell lines. J Biomed Mater Res A 91, 894-902.

Yin, H., Gong, C., Shi, S., Liu, X., Wei, Y., Qian, Z., 2010. Toxicity evaluation of biodegradable and thermosensitive PEG-PCL-PEG hydrogel as a potential in situ sustained ophthalmic drug delivery system. J Biomed Mater Res B Appl Biomater 92, 129-137.

Yu, L., Ding, J., 2008. Injectable hydrogels as unique biomedical materials. Chem Soc Rev 37, 1473-1481.

Zhang, J., Men, K., Gu, Y., Wang, X., Gou, M., Guo, G., Luo, F., Qian, Z., 2011. Preparation of core cross-linked PCL-PEG-PCL micelles for doxorubicin delivery in vitro. J Nanosci Nanotechnol 11, 5054-5061.

Zhang, J.T., Bhat, R., Jandt, K.D., 2009. Temperature-sensitive PVA/PNIPAAm semi-IPN hydrogels with enhanced responsive properties. Acta Biomater 5, 488-497.

Zhang, Y., Wu, X., Han, Y., Mo, F., Duan, Y., Li, S., 2010. Novel thymopentin release systems prepared from bioresorbable PLA-PEG-PLA hydrogels. Int J Pharm 386, 15-22.

Zhao, S., Cao, M., Li, H., Li, L., Xu, W., 2010. Synthesis and characterization of thermo-sensitive semi-IPN hydrogels based on poly(ethylene glycol)-co-poly(epsilon-caprolactone) macromer, N-isopropylacrylamide, and sodium alginate. Carbohydr Res 345, 425-431.

Zimmerman, T.J., Kaufman, H.E., 1977a. Timolol, dose response and duration of action. Arch Ophthalmol 95, 605-607.

Zimmerman, T.J., Kaufman, H.E., 1977b. Timolol. A beta-adrenergic blocking agent for the treatment of glaucoma. Arch Ophthalmol 95, 601-604.

VITA

Gyan Prakash Mishra was born on March 23, 1981, in Kanpur, Uttar Pradesh, India. He completed his Bachelor of Pharmacy degree from Shri G.S. Institute of Technology and Science (SGSITS) in 2003 and then he received Master of Pharmacy with specialization in Medicinal and Pharmaceutical Chemistry from SGSITS in 2005. Following completion he joined Torrent Research Center, Gujarat, India, as a Research Scientist in Medicinal Chemistry division.

Gyan Mishra initiated his Doctoral studies at University of Missouri Kansas City in the Fall of 2006. He was awarded Chancellor's doctoral fellowship from school of graduate studies in the year 2010. He received travelship award by the American Association of Pharmaceutical Scientists (AAPS) to present his work in the annual meetings of 2008 and 2010. Gyan Mishra is interested in pursuing research in the polymeric drug delivery field. He has authored several publications in prestigious journals and books. and presented work in several annual meetings.